

Structural Characterization of UHPC Waffle Bridge Deck and Connections



Final Report
July 2014



IOWA STATE UNIVERSITY
Institute for Transportation

Sponsored by
Iowa Highway Research Board
(IHRB Project TR-614)
Iowa Department of Transportation
(InTrans Project 09-362)

About the Bridge Engineering Center

The mission of the Bridge Engineering Center (BEC) is to conduct research on bridge technologies to help bridge designers/owners design, build, and maintain long-lasting bridges.

About the Institute for Transportation

The mission of the Institute for Transportation (InTrans) at Iowa State University is to develop and implement innovative methods, materials, and technologies for improving transportation efficiency, safety, reliability, and sustainability while improving the learning environment of students, faculty, and staff in transportation-related fields.

Disclaimer Notice

The contents of this report reflect the views of the authors, who are responsible for the facts and the accuracy of the information presented herein. The opinions, findings and conclusions expressed in this publication are those of the authors and not necessarily those of the sponsors.

The sponsors assume no liability for the contents or use of the information contained in this document. This report does not constitute a standard, specification, or regulation.

The sponsors do not endorse products or manufacturers. Trademarks or manufacturers' names appear in this report only because they are considered essential to the objective of the document.

Non-Discrimination Statement

Iowa State University does not discriminate on the basis of race, color, age, religion, national origin, sexual orientation, gender identity, genetic information, sex, marital status, disability, or status as a U.S. veteran. Inquiries can be directed to the Director of Equal Opportunity and Compliance, 3280 Beardshear Hall, (515) 294-7612.

Iowa Department of Transportation Statements

Federal and state laws prohibit employment and/or public accommodation discrimination on the basis of age, color, creed, disability, gender identity, national origin, pregnancy, race, religion, sex, sexual orientation or veteran's status. If you believe you have been discriminated against, please contact the Iowa Civil Rights Commission at 800-457-4416 or the Iowa Department of Transportation affirmative action officer. If you need accommodations because of a disability to access the Iowa Department of Transportation's services, contact the agency's affirmative action officer at 800-262-0003.

The preparation of this document was financed in part through funds provided by the Iowa Department of Transportation through its "Second Revised Agreement for the Management of Research Conducted by Iowa State University for the Iowa Department of Transportation" and its amendments.

The opinions, findings, and conclusions expressed in this publication are those of the authors and not necessarily those of the Iowa Department of Transportation.

Technical Report Documentation Page

1. Report No. IHRB Project TR-614	2. Government Accession No.	3. Recipient's Catalog No.	
4. Title and Subtitle Structural Characterization of UHPC Waffle Bridge Deck and Connections		5. Report Date July 2014	
		6. Performing Organization Code	
7. Author(s) Sriram Aaleti, Ebadollah Honarvar, Sri Sritharan, Matt Rouse, and Terry Wipf		8. Performing Organization Report No. InTrans Project 09-362	
9. Performing Organization Name and Address Bridge Engineering Center Iowa State University 2711 South Loop Drive, Suite 4700 Ames, IA 50010-8664		10. Work Unit No. (TRAIS)	
		11. Contract or Grant No.	
12. Sponsoring Organization Name and Address Iowa Highway Research Board Iowa Department of Transportation 800 Lincoln Way Ames, IA 50010		13. Type of Report and Period Covered Final Report	
		14. Sponsoring Agency Code IHRB Project TR-614	
15. Supplementary Notes Visit www.intrans.iastate.edu for color pdfs of this and other research reports.			
16. Abstract <p>The AASHTO strategic plan in 2005 for bridge engineering identified extending the service life of bridges and accelerating bridge construction as two of the grand challenges in bridge engineering. These challenges have the objective of producing safer and more economical bridges at a faster rate with a minimum service life of 75 years and reduced maintenance cost to serve the country's infrastructure needs. Previous studies have shown that a prefabricated full-depth precast concrete deck system is an innovative technique that accelerates the rehabilitation process of a bridge deck, extending its service life with reduced user delays and community disruptions and lowering its life-cycle costs. Previous use of ultra-high performance concrete (UHPC) for bridge applications in the United States has been considered to be efficient and economical because of its superior structural characteristics and durability properties.</p> <p>Full-depth UHPC waffle deck panel systems have been developed over the past three years in Europe and the United States. Subsequently, a single span, 60-ft long and 33-ft wide prototype bridge with full-depth prefabricated UHPC waffle deck panels has been designed and built for a replacement bridge in Wapello County, Iowa. The structural performance characteristics and the constructability of the UHPC waffle deck system and its critical connections were studied through an experimental program at the structural laboratory of Iowa State University (ISU). Two prefabricated full-depth UHPC waffle deck (8 feet by 9 feet 9 inches by 8 inches) panels were connected to 24-ft long precast girders, and the system was tested under service, fatigue, overload, and ultimate loads. Three months after the completion of the bridge with waffle deck system, it was load tested under live loads in February 2012. The measured strain and deflection values were within the acceptable limits, validating the structural performance of the bridge deck. Based on the laboratory test results, observations, field testing of the prototype bridge, and experience gained from the sequence of construction events such as panel fabrication and casting of transverse and longitudinal joints, a prefabricated UHPC waffle deck system is found to be a viable option to achieve the goals of the AASHTO strategic plan.</p>			
17. Key Words accelerated bridge construction—bridge deck connections—Highways for LIFE—load testing—precast bridge sections—ultra-high-performance concrete—waffle deck—Wapello County Iowa		18. Distribution Statement No restrictions.	
19. Security Classification (of this report) Unclassified.	20. Security Classification (of this page) Unclassified.	21. No. of Pages 91	22. Price NA

STRUCTURAL CHARACTERIZATION OF UHPC WAFFLE BRIDGE DECK AND CONNECTIONS

**Final Report
July 2014**

Principal Investigator

Sri Sritharan, Jon “Matt” Rouse, and Terry Wipf
Department of Civil, Construction, and Environmental Engineering, Iowa State University

Postdoctoral Researcher

Sriram Aaleti, Research Assistant Professor
Department of Civil, Construction, and Environmental Engineering, Iowa State University

Authors

Sriram Aaleti, Ebadollah Honarvar, Sri Sritharan, Matt Rouse, and Terry Wipf

Sponsored by
the Iowa Highway Research Board and
the Iowa Department of Transportation
(IHRB Project TR-614)

Preparation of this report was financed in part
through funds provided by the Iowa Department of Transportation
through its Research Management Agreement with the
Institute for Transportation
(InTrans Project 09-362)

A report from
Institute for Transportation
Iowa State University
2711 South Loop Drive, Suite 4700
Ames, IA 50010-8664
Phone: 515-294-8103
Fax: 515-294-0467
www.intrans.iastate.edu

TABLE OF CONTENTS

ACKNOWLEDGEMENTS	xi
1. INTRODUCTION	1
1.1 Introduction.....	1
2. PROTOTYPE BRIDGE AND LABORATORY TESTING.....	3
2.1 Introduction.....	3
2.2 Bridge Description	3
2.3 Connection Details.....	4
2.4 Design of UHPC Waffle Deck Panel.....	5
2.5 Experimental Investigation	7
2.5.1 Panel Prefabrication	8
2.5.2 Test Setup.....	10
2.5.3 Instrumentation	13
2.5.4 Load Protocols	14
2.5.5 Test 1—Panel Service Load Test.....	16
2.5.6 Test 2—Joint Service Load Test.....	19
2.5.7 Test 3—Joint Fatigue Load Test.....	23
2.5.8 Test 4—Joint Overload Load Test.....	26
2.5.9 Test 5—Panel Fatigue Load Test.....	30
2.5.10 Test 6—Panel Overload Load Test.....	33
2.5.11 Test 7—Panel Ultimate Load Test.....	38
2.5.12 Test 8—Joint Ultimate Load Test.....	38
2.5.13 Test 9—Punching Shear Failure Test	39
2.6 Finite Element Modeling	40
2.7 Summary of Test Observations.....	42
2.8 Characterization of Deck Riding Surface Texture.....	45
3. CONSTRUCTION.....	48
3.1 Introduction.....	48
3.2 Bridge Deck Panel Details and Prefabrication.....	48
3.3 Field Installation	52
4. FIELD TESTING	57
4.1 Introduction.....	57
4.2 Instrumentation and Test Method	58
4.3 Results of Static Live Load Testing.....	61
4.3.1 Maximum Strains of the Mid-Span Deck Panel	61
4.3.2 Maximum Strains of the Deck Panel Adjacent to Abutment.....	63
4.3.3 Maximum Deflections at Mid-Span.....	65
4.3.4 Selected Data from the Static Live Load Test	65
4.4 Analytical Assessment.....	69
4.4.1 Global Bridge Behavior	70
4.4.2 Comparison of Live Load Strains for the Mid-Span Deck Panel	71
4.4.3 Comparison of Live Load Strains of Deck Panel Adjacent to Abutment.....	72

4.5	Girder Live Load Distribution Factor	73
4.6	Dynamic Amplification Effects	74
5.	CONCLUSIONS AND RECOMMENDATIONS.....	77
5.1	Conclusions.....	77
5.2	Recommendations for Future Research	78
REFERENCES.....		79

LIST OF FIGURES

Figure 2.1. Plan of the UHPC waffle deck bridge in Wapello County, Iowa-----	3
Figure 2.2. Cross-section of the UHPC waffle deck bridge designed for Wapello County Bridge in Iowa-----	4
Figure 2.3. Shear pocket connection details between girder and waffle deck panel-----	4
Figure 2.4. Connection details between the center girder and the waffle deck-----	5
Figure 2.5. Connection details between the waffle deck panels-----	5
Figure 2.6. Deck panel geometry and cross-section details-----	6
Figure 2.7. Reinforcement details of the UHPC waffle deck test panels-----	7
Figure 2.8 Cross-section details of the proposed UHPC waffle deck bridge in Wapello County ---	8
Figure 2.9. Construction sequence used for the UHPC waffle deck panels at the precast plant ----	9
Figure 2.10. Schematic of the setup used for testing of the UHPC waffle deck panel system-----	10
Figure 2.11. Details of the reinforcement provided in various joints-----	11
Figure 2.12. Construction of UHPC joints in the ISU laboratory-----	12
Figure 2.13. Schematic of the displacement transducers mounted to the test unit-----	13
Figure 2.14. Location of strain gauges used on the bottom deck reinforcing bars-----	14
Figure 2.15. Location of strain gauges on the top deck reinforcing bars and dowel bars-----	14
Figure 2.16. Measured force-displacement response and peak rebar strain from gauge B3 at the center of the transverse rib TR2 of panel UWP2-----	17
Figure 2.17. Measured strains along the bottom reinforcement of the transverse rib TR2 of panel UWP2-----	18
Figure 2.18. Measured strains along a bottom reinforcement of the panel-to-panel joint-----	18
Figure 2.19. A hairline crack in the UWP2 panel transverse rib TR2 at 21.3 kips-----	19
Figure 2.20. A relationship proposed for the UHPC tensile strength variation as a function of crack width (AFGC 2002)-----	19
Figure 2.21. Measured force-displacement response and peak rebar strain at the center of the joint at the service load-----	20
Figure 2.22. Measured strains along the bottom reinforcement of the joint during the service load test-----	21
Figure 2.23. Measured strains in the bottom reinforcement of the transverse rib (TR2) along the length of panel UWP2 at service load-----	21
Figure 2.24. Measured strains in the bottom reinforcement of the transverse rib (TR2) along the length of panel UWP1 at service load-----	22
Figure 2.25. Measured strains at the center of the panel across the transverse ribs of UWP1 at service load-----	22
Figure 2.26. A hairline crack formed at the center of underside of the transverse joint at 28 kips--	23
Figure 2.27. The variation of the peak displacement at the center of the joint during the joint fatigue test-----	24
Figure 2.28. The variation of the peak strain in the bottom joint transverse reinforcement during the joint fatigue test-----	25
Figure 2.29. The variation of the crack width in the transverse joint with number of load cycles --	25
Figure 2.30. Measured responses of the waffle deck system from the static service load tests conducted during the joint fatigue test-----	26
Figure 2.31. Measured force-displacement response and peak rebar strain at the center of the joint at the overload load of 48 kips-----	27

Figure 2.32. Measured strains in the bottom reinforcement of transverse rib TR2 along the length of panel UWP2 at the overload load -----	28
Figure 2.33. Measured strains in the bottom reinforcement of transverse rib TR2 along the length of panel UWP1 at the overload load -----	28
Figure 2.34. Measured strains at the center of the panel across the transverse ribs of panel UWP1 at joint overload load -----	29
Figure 2.35. Hairline cracks formed at the center of underside of the transverse joint at the overload load of 48 kips -----	29
Figure 2.36. The variation in the width of the most critical flexural crack in the transverse ribs forming the transverse joint -----	30
Figure 2.37. The peak displacement variation at the center of panel UWP1 during the joint fatigue test -----	31
Figure 2.38. The peak strain variation in bottom deck reinforcement in the transverse rib of UWP1 and the joint during panel fatigue test-----	31
Figure 2.39. The crack width variation in transverse rib TR2 of panel UWP1 during panel fatigue test-----	32
Figure 2.40. Measured responses of the waffle deck system for static service load tests conducted during the panel fatigue test -----	33
Figure 2.41. Measured force-displacement response and peak rebar strain at the center of the transverse rib of UWP1 at the overload load of 40 kips -----	34
Figure 2.42. Measured strains in the bottom reinforcement of the transverse rib along the length of UWP1 during the overload load test-----	34
Figure 2.43. Measured strains in the bottom reinforcement of the joint along the joint length during the overload load test -----	35
Figure 2.44. Hairline cracks developed on panel UWP1 at an overload load of 40 kips -----	36
Figure 2.45. Measured crack width in transverse rib TR2 of UWP1 during the overload load test-	37
Figure 2.46. Strain variations in a dowel bar placed in the panel-to-girder joint during the panel overload load test -----	37
Figure 2.47. Measured force-displacement response of waffle deck system -----	38
Figure 2.48. Measured force-displacement response and cracking at the center of the panel-to-panel joint under ultimate loads -----	39
Figure 2.49. Measured load-displacement behavior and failure surface during punching shear failure test of the waffle deck system -----	40
Figure 2.50. Test specimen discretization and material behavior of UHPC used in FEA software (ABAQUS) -----	41
Figure 2.51. Comparison of experimental and ABAQUS force-displacement responses -----	42
Figure 2.52. Test setup for characterization of skid resistance of textures using British Pendulum tester -----	46
Figure 3.1. Deck panel geometry and cross-section details -----	49
Figure 3.2. UHPC waffle deck panel reinforcement details-----	50
Figure 3.3. Formwork used for waffle deck panel construction at the precast plant -----	51
Figure 3.4. Construction of the UHPC waffle deck panel for the demonstration bridge -----	51
Figure 3.5. Placement of UHPC waffle deck panels on the prestressed girders -----	52
Figure 3.6. Water-tight seal at panel-to-girder connection after applying quick-setting spray -----	53
Figure 3.7. Transverse and longitudinal joints in the demonstration bridge in Wapello County ----	54
Figure 3.8. Batching of UHPC joint fill using IMER Mortarman 750 mixers at the bridge site ----	55

Figure 3.9. Filling of joints with in situ UHPC and completed joints -----	55
Figure 3.10. Finished transverse joints (panel-to-panel joint) covered with plywood -----	56
Figure 3.11. Close-up of the waffle panel deck after grinding along the joints -----	56
Figure 4.1. Dahlongega road bridge plan-----	57
Figure 4.2. Dahlongega road bridge cross section -----	57
Figure 4.3. Location of transducers at the mid-span panel: (a) Top and bottom of deck; (b) Cross-section view-----	60
Figure 4.4. Location of transducers at the panel adjacent to abutment: (a) Top and bottom of deck; (b) Cross-section view -----	60
Figure 4.5. Transducers under deck adjacent to abutment face-----	60
Figure 4.6. Loading: (a) Schematic layout of bridge loading paths; (b) Truck configuration and axle load; (c) Load paths marked on bridge deck -----	61
Figure 4.7. Measured transverse strains at the bottom of mid-span panel vs. time for MDTB1b5 transducer -----	66
Figure 4.8. Girder top and bottom longitudinal strain at mid-span for load path 2 -----	66
Figure 4.9. Girder top and bottom longitudinal strain near abutment for load path 2 -----	67
Figure 4.10. Longitudinal bottom strains at mid-span panel for load path 2 -----	67
Figure 4.11. Transverse bottom strains at mid-span panel for load path 2-----	67
Figure 4.12. Transverse top strains at mid-span panel for load path 2 -----	68
Figure 4.13. Longitudinal bottom strains at end panel for load path 2 -----	68
Figure 4.14. Longitudinal top strains at end panel for load path 2 -----	68
Figure 4.15. Transverse bottom strains at end panel for load path 2-----	69
Figure 4.16. Transverse top strains at end panel for load path 2 -----	69
Figure 4.17. Dynamic live load longitudinal strain at mid-span for load path 2 -----	75
Figure 4.18. Dynamic live load longitudinal strain at mid-span for load path 3 -----	75
Figure 4.19. Dynamic live load longitudinal strain at mid-span for load path 6 -----	75

LIST OF TABLES

Table 2.1. Strength Gain Reported for UHPC Used in the Laboratory Waffle Deck Panels-----	9
Table 2.2. Measured Flow Values for the UHPC Joint Fill -----	11
Table 2.3. Strength Gain of UHPC in the Joints -----	12
Table 2.4. Sequence and Details of the Tests Conducted on the Waffle Deck System -----	16
Table 2.5. Details of the Textures and Average Sand Patch Diameters -----	45
Table 2.6. Measured SRVs for Different Textured Surfaces Using British Pendulum Tester -----	46
Table 4.1. Transducer Nomenclature-----	59
Table 4.2. Maximum Transverse Strains at the Bottom of Mid-Span Panel-----	62
Table 4.3. Maximum Transverse Strains at the Top of Mid-Span Panel-----	62
Table 4.4. Maximum Longitudinal Strains at the Bottom of Mid-Span Panel -----	62
Table 4.5. Maximum Girder Top Longitudinal Strain at Mid-Span -----	63
Table 4.6. Maximum Girder Bottom Longitudinal Strain at Mid-Span -----	63
Table 4.7. Maximum Transverse Strains at the Bottom of the Panel near Abutment -----	63
Table 4.8. Maximum Transverse Strains at the Top of the Panel near Abutment -----	64
Table 4.9. Maximum Longitudinal Strains at the Bottom of the Panel near Abutment-----	64
Table 4.10. Maximum Longitudinal Strains at the Top of the Panel near Abutment-----	64
Table 4.11. Maximum Girder Top Longitudinal Strain near Abutment-----	64
Table 4.12. Maximum Girder Bottom Longitudinal Strain near Abutment -----	64
Table 4.13. Maximum Live Load Girder and Deck Deflections (in.) -----	65
Table 4.14. Maximum Live Load Girder Deflections-----	70
Table 4.15. Girder Top and Bottom Longitudinal Strains at Mid-Span -----	70
Table 4.16. Live Load Longitudinal Strains at the Bottom of the Mid-Span Deck Panel -----	71
Table 4.17. Live Load Transverse Strains at the Bottom of the Mid-Span Deck Panel-----	71
Table 4.18. Live Load Transverse Strains at the Top of the Mid-Span Deck Panel-----	71
Table 4.19. Live Load Longitudinal Strains at the Bottom of the Deck Panel Adjacent to the Abutment-----	72
Table 4.20. Live Load Transverse Strains at the Bottom of the Deck Panel Adjacent to the Abutment-----	72
Table 4.21. Live Load Transverse Strains at the Top of the Deck Panel Adjacent to the Abutment	73
Table 4.22. Live Load Distribution Factors for Bridge Girders -----	73
Table 4.23. Live Load Distribution Factors -----	74
Table 4.24. Summary of Static Live Load Strain ($\mu\epsilon$) for Bottom of Girders at Mid-Span -----	76
Table 4.25. Summary of Dynamic Live Load Strain ($\mu\epsilon$) for Bottom of Girders at Mid-Span -----	76
Table 4.26. Dynamic Amplification Factors -----	76

ACKNOWLEDGEMENTS

The authors would like to thank the Iowa Highway Research Board and the Iowa Department of Transportation for sponsoring this research project. The Federal Highway Administration, via Coreslab Structures, also provided support through Highways for LIFE (HfL) for work that is reflected in this final report.

The authors would also like to thank Kyle Nachuk from Lafarge North America for providing technical assistance with the UHPC mixing and help with casting of joints in the test specimen. We would like to thank Dean Bierwagen from the Iowa Department of Transportation for leading the design of the prototype bridge and John Heimann from the Coreslab Structures of Omaha for helping and organizing the fabrication of the waffle deck panels in a timely manner.

The authors want to acknowledge and thank all the help provided by undergraduate lab assistants Andrew Barone and Owen Steffens with the test setup and testing of the waffle deck system. The help and guidance provided by Doug Wood, structural lab manager at Iowa State University, in completing the tests and conducting the field test on a tight schedule is greatly appreciated.

The following individuals served on the Technical Advisory Committee of this research project: Ahmad Abu-Hawash, Dean Bierwagen, Kenneth Dunker, Mark Dunn, Ping Lu Norman McDonald, Brian Moore, and Wayne Sunday. Their guidance and feedback during the course of the project are also greatly appreciated.

1. INTRODUCTION

1.1 Introduction

Today there are more than 160,000 bridges in the United States that are structurally deficient or obsolete, with more than 3,000 new bridges added to this list each year (Bhide 2001). Many bridges are subjected to weights, loads, and traffic volumes exceeding limits of their original design, while current bridge inspection methods do not detect all structural problems encountered in the field. Deterioration of the bridge deck is a leading cause for the obsolete and/or deficient inspection rating of the bridges (Stantill-McMcillan and Hatfield 1994; Zellcomp Inc 2011). Federal, State and municipal bridge engineers are seeking alternative ways to build better bridges, reduce travel times, and improve repair techniques, thereby reducing maintenance costs of bridge infrastructure. Additionally, owners are challenged with replacing critical bridge components, particularly rapidly deteriorating bridge decks, during limited or overnight road closure periods. Therefore, there is an impending need to develop and use longer-lasting materials and innovative technologies to accomplish safe and fast construction of high-quality bridges and highways.

To address the Nation's aging bridge infrastructure requires development of cost-efficient, widely applicable, and long-lasting bridge elements and systems and accelerated bridge construction techniques. To increase longevity and reduce maintenance costs, the potential use of ultra-high performance concrete (UHPC) in bridges is gaining significant interest among several State Departments of Transportations (DOTs) and the Federal Highway Administration (FHWA). The use of full-depth precast deck panels in bridges is not new, nor is the use of UHPC as deck panel joint fill. Several U.S. State and Canadian Provincial DOTs have explored the use of full-depth precast deck panels in bridges. Ultra-high performance concrete has also been used as joint fill material by the Ontario Ministry of Transportation on full-depth solid deck panels made from high-performance concrete (Perry et al. 2007).

In support of reducing the aging bridge infrastructure stock in the United States, innovative use of UHPC in bridge applications has been under way for the past several years. The State of Iowa has been in the forefront of this effort with implementation of the first UHPC bulb-tee and Pi girders in bridges and development of an H-shaped UHPC precast pile for foundation application (Vande Voort et al. 2007; Keierleber et al. 2007, Sritharan 2009). The interest in using UHPC for highway bridge decks has been ongoing in the United States since the year 2000. Research and development (R&D) at the FHWA Turner Fairbanks facility commenced in 2000 and prototype bridge decks utilizing UHPC have been under development since that time. Various types of UHPC precast deck systems have been prototyped during this period. To date, however, there are no UHPC precast deck panels in service in our highway system.

Full-depth UHPC waffle deck panel systems have been developed over the past three years in Europe and the United States. The FHWA explored this system and published a Techbrief on this topic (FHWA 2007). Significant R&D, analysis, design, and prototyping of separate components of this innovation have also been explored (i.e., joints, shear keys, skid resistance, durability, etc.) (Perry et al. 2007). Nevertheless, these innovations have not been installed in the U.S.

highway system. State DOTs from Virginia, Florida, Iowa, and New York have expressed interest in utilizing a UHPC waffle deck panel system if the performance of the system is proven satisfactory through experimental testing. The main reason for the broad interest in the UHPC waffle deck panel is that this concept is applicable for new bridges as well as for rehabilitation of existing deteriorated bridge decks because of its relatively low self-weight.

The second chapter of this report describes the prototype bridge superstructure that was constructed using UHPC waffle deck panels and UHPC infill joints, experimental evaluation of structural characteristics of the UHPC waffle deck, critical connections, system performance, and rideability of the panel surface through large-scale testing at the structural laboratory of Iowa State University (ISU). The details about fabrication of full-depth UHPC waffle panels and construction of the field bridge are presented in Chapter 3. The fourth chapter presents the results of field testing performed on the field bridge, with conclusions and recommendations in the final chapter.

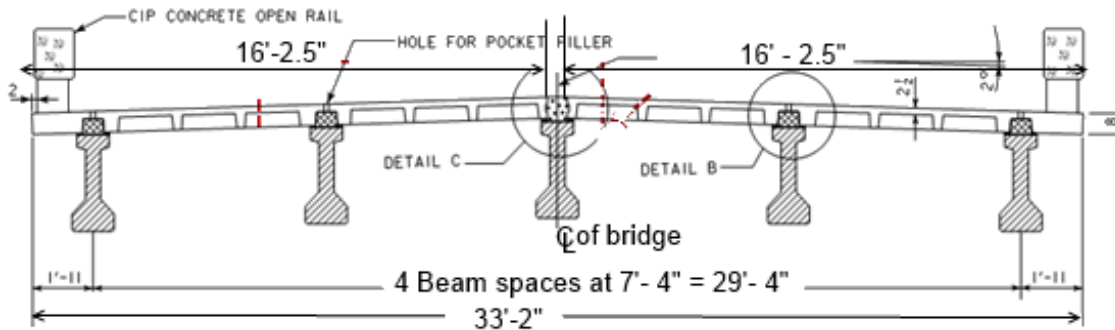


Figure 2.2. Cross-section of the UHPC waffle deck bridge designed for Wapello County Bridge in Iowa

2.3 Connection Details

The waffle deck panel system was designed to act fully composite with the prestressed concrete girders using the following three connection details:

1. **Shear Pocket Connection:** This connection is formed between the girder and the waffle deck panel using shear pockets. In this connection, a shear hook from the girder is extended into the shear pocket and the shear pockets in the waffle deck panel are filled with UHPC (see Figure 2.3). This will cause the girders and the waffle deck to act in a composite manner.

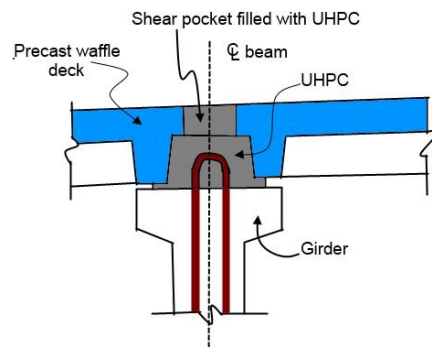


Figure 2.3. Shear pocket connection details between girder and waffle deck panel

2. **Waffle Panel to Girder Longitudinal Connection:** This connection is formed between the center girder and the waffle deck panel. In this connection, the dowel bars from the panels and the shear hook from the girder are tied together with additional reinforcement along the girder length and the gap between the panels is filled with in situ UHPC (Figure 2.4). This connection provides a positive moment connection between the girder and the panels.

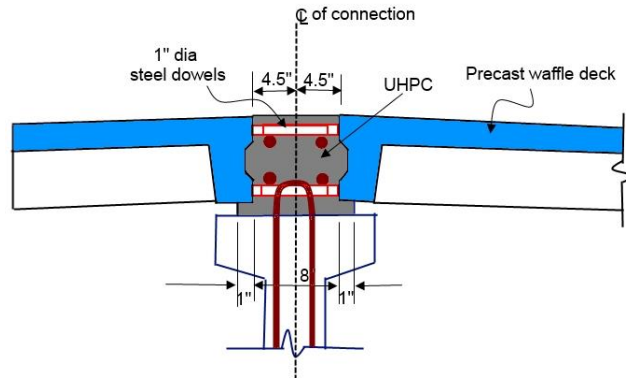


Figure 2.4. Connection details between the center girder and the waffle deck

3. **Panel-to-Panel Connection:** The bridge consists of waffle deck panels with dimensions of 16 feet 2.5 inches (length) by 8 feet (width) by 8 inches (thickness). These panels are connected across the width of the bridge using a transverse joint connection as shown in Figure 2.5. In this connection, the dowel bars from each panel are tied together with additional transverse reinforcement and the gap between the panels is filled with UHPC (see Figure 2.5). This connection will provide continuity and facilitate load transfer between the panels.

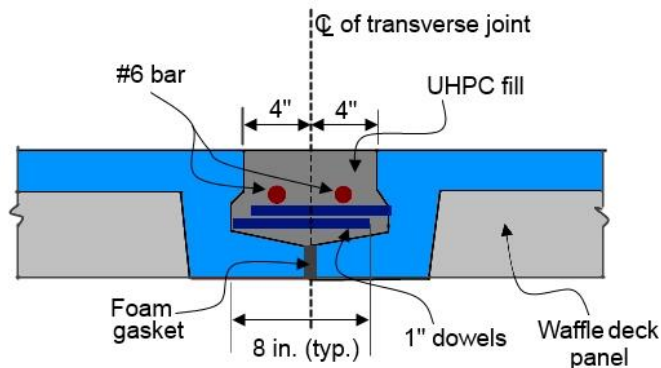


Figure 2.5. Connection details between the waffle deck panels

2.4 Design of UHPC Waffle Deck Panel

The UHPC waffle deck panel consists of a slab cast integrally with concrete ribs spanning in the transverse and longitudinal directions. Of the total thickness of 8 inches, the deck thickness is composed of a 2.5-inch thick uniform slab and 5.5-inch deep ribs in the transverse and longitudinal directions. Figure 2.6 shows the plan view of a typical waffle deck panel designed for the prototype bridge.

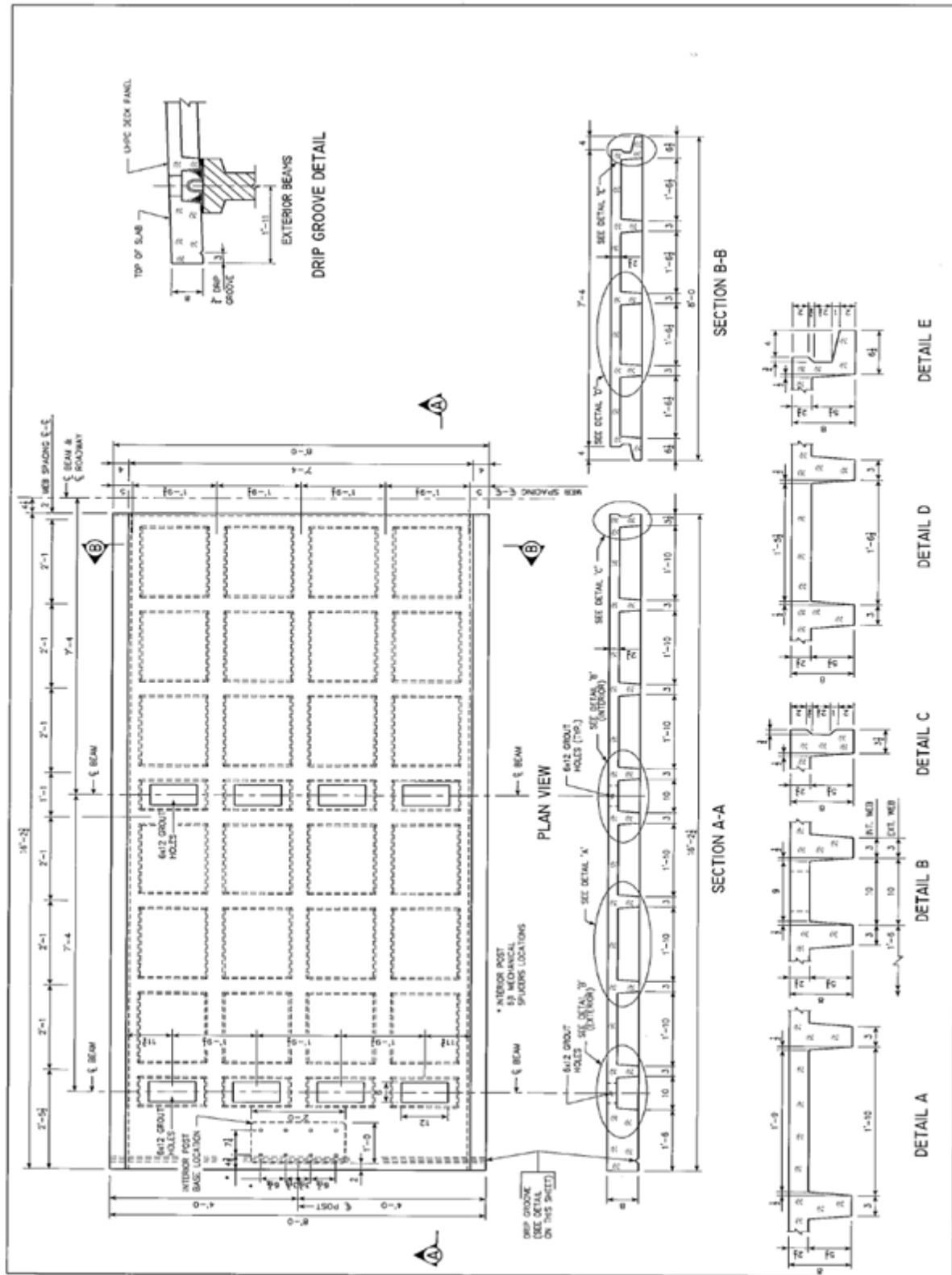


Figure 2.6. Deck panel geometry and cross-section details

The UHPC waffle panels were designed with conventional mild steel reinforcement primarily to resist the transverse flexural moments (i.e., for moments induced about the bridge longitudinal axis) in accordance with the current AASHTO slab deck design provisions (AASHTO 2007). This resulted in Grade 60, No. 7 ($d_b = 0.875$ inch, where d_b is the diameter of the bar) and No. 6 ($d_b = 0.75$ inch) mild steel reinforcement located at 1.25 inches from the bottom surface and at 1.625 inches from the top surface of the panel, respectively. In the longitudinal direction, the panels were detailed with Grade 60, No. 7 and No. 6 mild steel reinforcement at 2.125 inches from the bottom surface and at 2.375 inches from the top surface, respectively. All the reinforcement was provided along panel ribs in both directions. Figure 2.7 shows the cross-section and reinforcement details of a typical waffle deck panel designed for the prototype bridge.

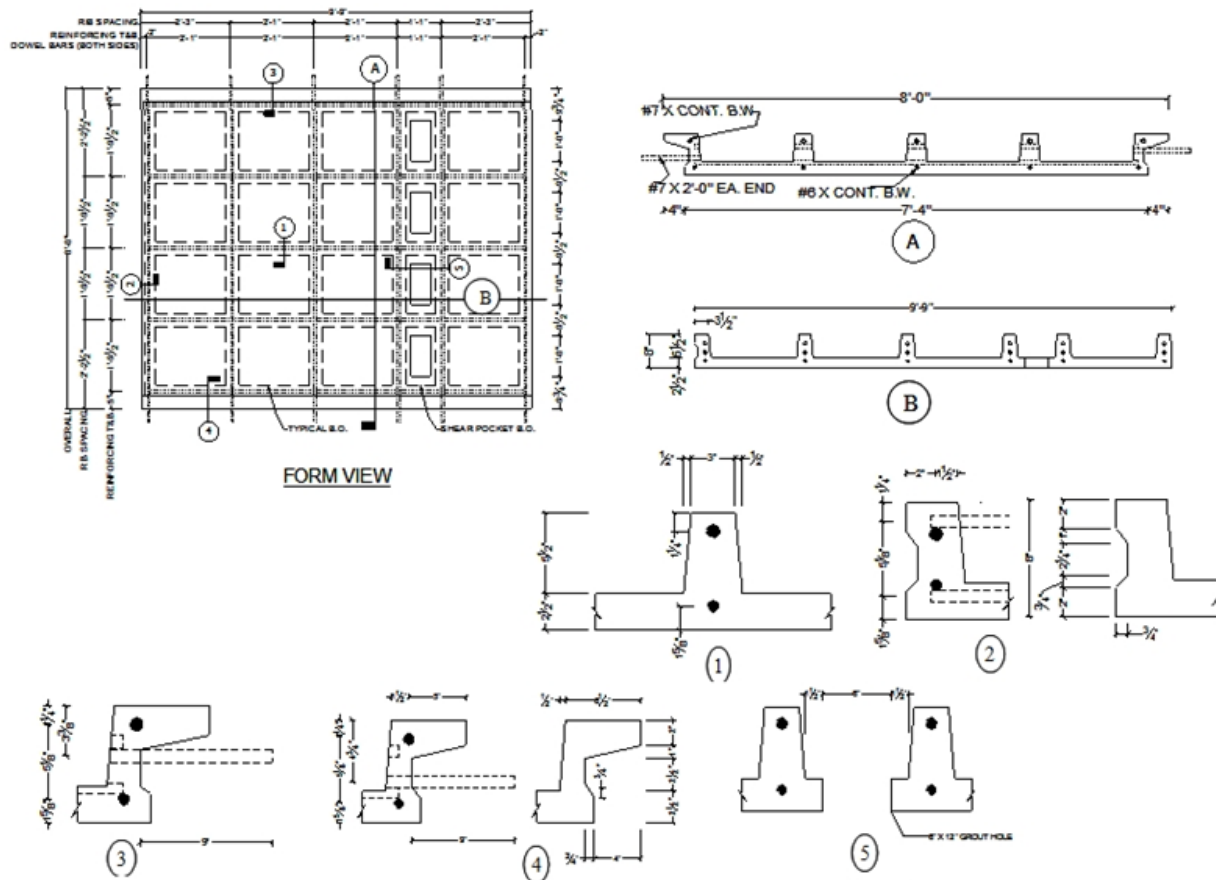


Figure 2.7. Reinforcement details of the UHPC waffle deck test panels

2.5 Experimental Investigation

Prior to finalizing the design of the full-depth UHPC waffle deck system for the planned replacement bridge in Wapello County, Iowa, its adequate design was verified through an experimental program. With the deck panels designed specifically for this project, the verifications of the assumed structural performance characteristics of the UHPC waffle deck, critical connections, system performance, and rideability of the panel surface were performed

through an experimental program at the structural laboratory of ISU. For this project, two prefabricated full-depth UHPC waffle deck (8 feet by 9 feet 9 inches by 8 inches) panels were connected to 24-foot long precast girders and the system was tested under service, fatigue, overload, and ultimate loads. For the experimental investigation of the performance of the waffle deck panel and its connections, a region between two adjacent girders as shown in Figure 2.8 was chosen. This section discusses the test panel fabrication, test setup, instrumentation, and loading protocols used for the experimental investigation of the UHPC waffle deck system as well as the test observations and results.

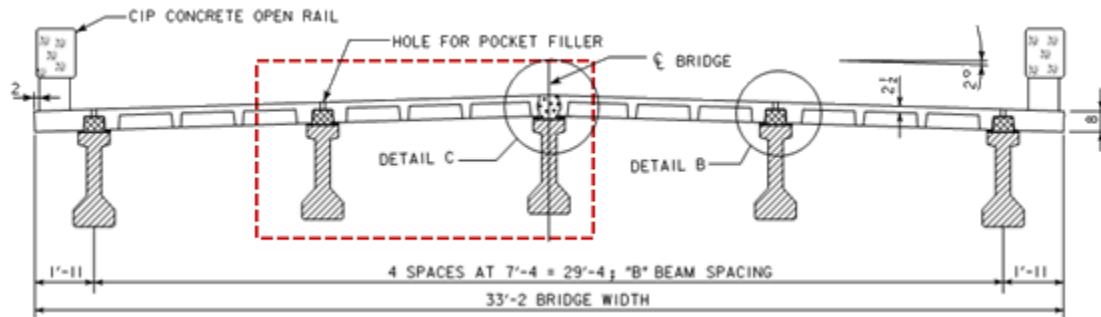


Figure 2.8 Cross-section details of the proposed UHPC waffle deck bridge in Wapello County

2.5.1 Panel Prefabrication

For the experimental investigation, a waffle deck region between two adjacent girders as identified in Figure 2.8 was chosen. Accordingly, two waffle deck panels with dimensions of 8 ft (length) by 9 ft 9 inches (width) were fabricated by Coreslab Structures (Omaha) Inc. in September 2009. Commercially available standard Ductal® mix produced by Lafarge North America was used as the UHPC. Figure 2.9 illustrates the sequence of steps used for casting the waffle-shaped deck panels. The formwork for the panels was designed and constructed by Coreslab Structures (Omaha) Inc. to cast them in an upside position in order to facilitate a flat finish for the driving surface and easy placement and removal of the voids (see Figure 2.9e). As shown in Figure 2.9b, a trough system with nearly the same width as the panel was filled with UHPC and was used to pour the UHPC in place. The formwork was first filled with UHPC up to three quarters of the panel height (see Figure 2.9d) and the voids were placed into it (see Figure 2.9e), displacing the UHPC to form the ribs.

Standard compression test cylinders (3 inches by 6 inches) and modulus beams were cast for every pour to establish the strength gain of the panel with time. A standard flow table was used to measure the flow ability of UHPC for each pour. After casting, the panels were covered with plastic tarp and subjected to cure at 110°F for two days using a torpedo-style propane heater. After 7 days, the slabs were heat treated at 190°F \pm 5°F for a period of 48 hours using steam to maintain 100% relative humidity. The test cylinders and modulus beams were also subjected to the same curing conditions as the panels and were tested by Coreslab Structures (Omaha) Inc. These tests were conducted through a subcontract by the precaster at regular intervals to monitor the strength gain with time. Table 2.1 shows the details of the UHPC strength gain with time.

The average 28-day compressive strength of the concrete was found to be 21,981 psi, which is below the expected value of about 26,000 psi. This noticeable discrepancy is attributed to inadequate quality control performed during the compression testing of the cylinders. While more improved compression tests should be conducted during construction of the prototype waffle panels, it is worth noting that the expected compression strength was achieved for similar compression cylinders produced by the same precaster in Omaha as part of an Iowa DOT-funded project on UHPC piles (Vande Voort et al. 2008). After curing, the panels were transported to ISU's structures laboratory. Both the deck panels exhibited a very smooth surface on all sides that were in contact with the formwork. Other surfaces, especially the underside of the panels, appeared somewhat rough.



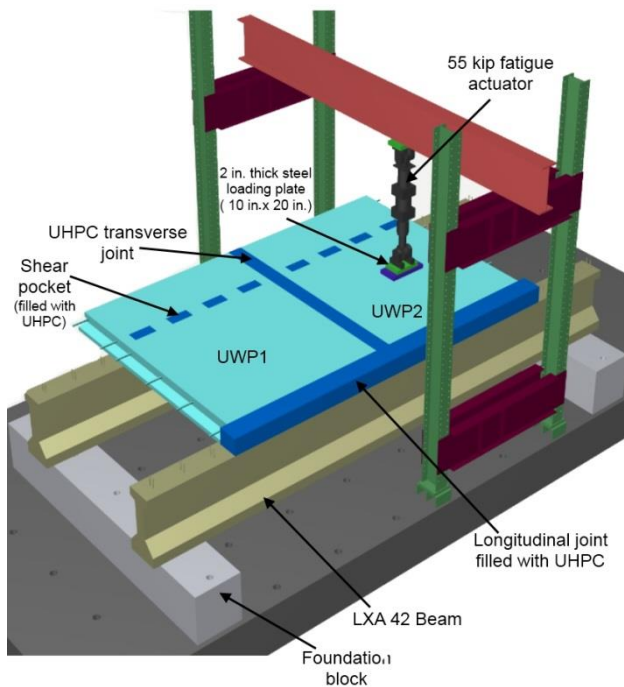
Figure 2.9. Construction sequence used for the UHPC waffle deck panels at the precast plant

Table 2.1. Strength Gain Reported for UHPC Used in the Laboratory Waffle Deck Panels

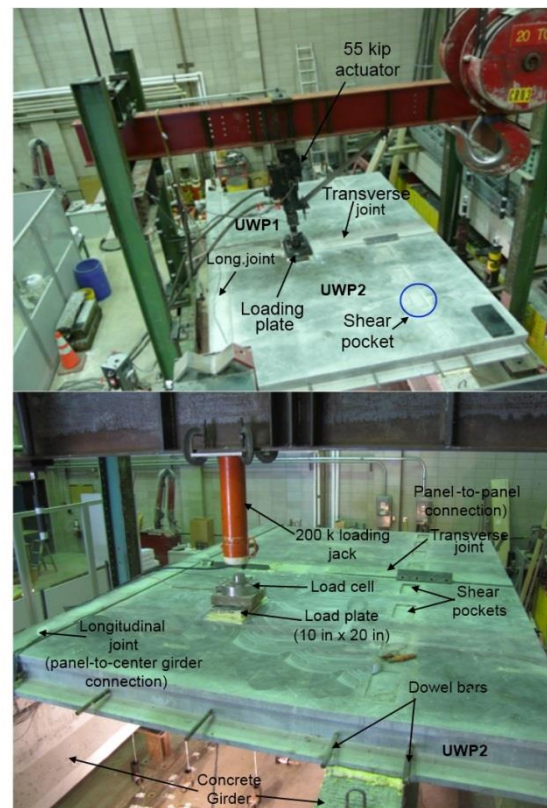
Panel-1 (UWP1)		Panel-2 (UWP2)	
Time (hours)	Strength (psi)	Time (hours)	Strength (psi)
22	1,800	20	850
24	4,500	26	5,000
26	6,250	44	10,650
44	11,650	52	13,800
52	13,400	-	-
28 days strength	21,843	28 days	22,120

2.5.2 Test Setup

A schematic of the test setup used for the UHPC waffle deck system is shown in Figure 2.10, which was established to closely replicate the critical regions of the field structure in the laboratory. As noted earlier, the setup represented an end section of the prototype bridge encompassing the center and intermediate girders, including the connections at those locations. The UHPC deck panels were supported on two 24-foot long prestressed concrete girders having cross sections of girder type LXA 42, which were simply supported at the ends on concrete foundation blocks as shown in Figure 2.10. The foundation blocks were posttensioned to the strong floor of the laboratory using a total of four 1-inch diameter high-strength threaded rod to prevent them from experiencing any lateral movement during testing. The girders were established by cutting a 48-foot long LXA 42 prestressed concrete girder, which was used by the Iowa DOT as a standard girder in the past. The girders were placed on the foundation blocks at a center-to-center distance of 7 feet 4 inches between them as expected in the prototype bridge. They were supported on rollers at one end and pinned at the other end. After the girders were set in place, the waffle deck panels were placed on the girders with 1.25 inches of the longitudinal ribs at the connection in contact with each girder as expected in the field.



a) Schematic of laboratory test setup



b) Completed view of UHPC joints and test setup for service and ultimate load tests

Figure 2.10. Schematic of the setup used for testing of the UHPC waffle deck panel system

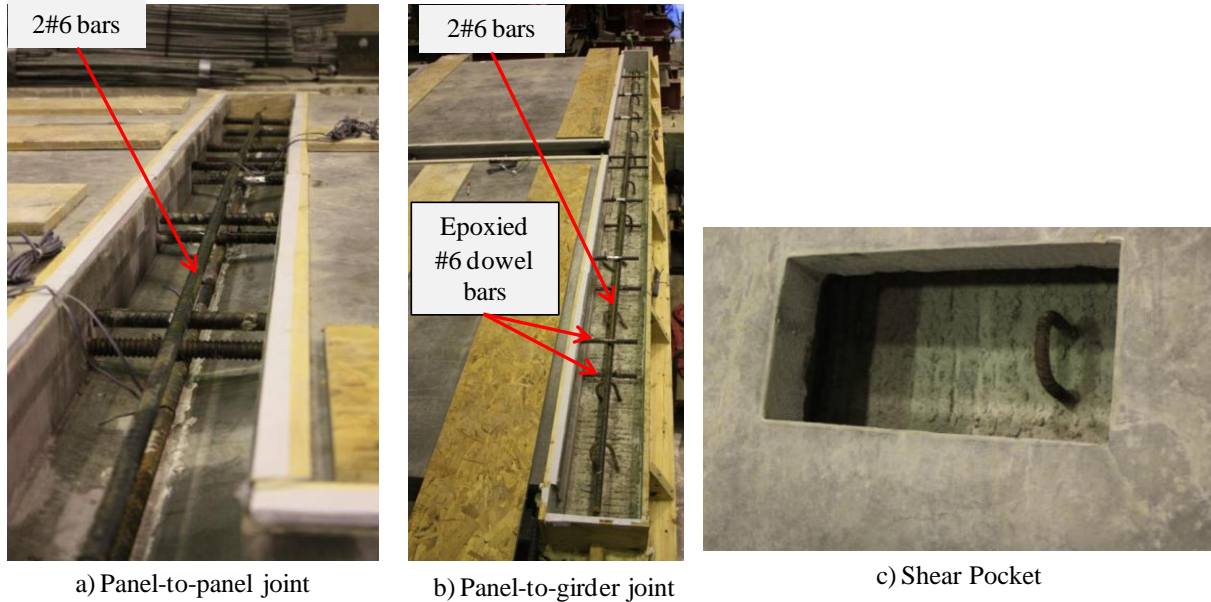


Figure 2.11. Details of the reinforcement provided in various joints

The test panels were constructed without dowel bars at the center girder-to-panel connection end. So, in order to establish a positive moment connection between the waffle deck and the center girder, 12-inch long Grade 60, No. 6 ($d_b = 0.75$ inch, where d_b is the diameter of the bar) mild steel dowel bars were embedded at the left end face of the panels using high-strength epoxy (see Figure 2.11b). In addition, two No. 6 bars were placed and tied to the dowel bars along the girder length to represent the effect of the continuous slab over the inner girder, which is expected in the prototype bridge. Two No. 6 bars were provided in the panel-to-panel joint (transverse joint) as the main reinforcement to resist the bending moment about the longitudinal axis (see Figure 2.11a). The connection between the exterior girder and the waffle deck was established using a shear pocket (see Figure 2.11c). Every shear pocket contained at least one shear hook extending from the girder.

Table 2.2. Measured Flow Values for the UHPC Joint Fill

Batch Number	Mix Temperature (°C)	Flow		Comments
		Static (in.)	Dynamic (in.)	
1	30	8.5	9.75	Longitudinal joint
2	29	9	10.125	Longitudinal joint
3	30	8.75	9.75	Transverse joint
4	26	9.5	Off table	Shear pockets
5	27	8.5	9.75	Shear pockets

The transverse joint between the two deck panels and the joints between the panels and the girders were cast using UHPC mixed in the laboratory at ISU. The UHPC required for the joint fill was prepared in a total of five batches using two Imer Mortarman 750 mixers. Every batch used nine bags of Ductal® premix and produced 5.3 feet³ of UHPC mix. Standard cylinders

(3 inches by 6 inches) were cast for every batch to establish the strength gain of the joint fill with time. A standard flow table was used to measure the flowability of every batch of UHPC, and measured values are presented in Table 2.2.

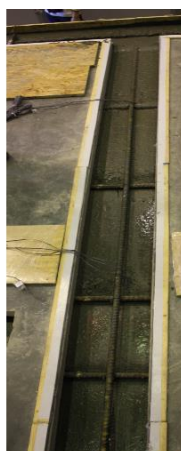
The UHPC was poured from one end of the longitudinal joint (panel-to-girder joint), and it was allowed to travel along the entire length of the joints (see Figure 2.12). After casting, all UHPC joints were covered with form plywood to minimize any moisture loss. The test cylinders were also subjected to the same curing conditions as the joints. They were tested in regular intervals to monitor the strength gain with time. Table 2.3 shows the details of the UHPC strength gain with time. The 28-day compressive strength of UHPC in the joints was less than typical strength of 26 ksi used in the deck panels but more than the required design strength of 15 ksi. This was expected because the UHPC in the joints was not subjected to any heat treatment. The test preparation work began immediately upon completion of the joints. The plywood was removed after 3 days, and the testing got under way 34 days after casting of the UHPC joints. A ± 55 kip capacity fatigue rated hydraulic actuator, mounted to a steel reaction frame as shown in Figure 2.10 was used to apply the load to the test unit. The frame was posttensioned to the strong floor of the laboratory using four 1.25-inch diameter high-strength bars. A 10 inch by 20 inch steel plate was used at the loading end of the actuator to simulate a truck wheel load on the panel for all testing.

Table 2.3. Strength Gain of UHPC in the Joints

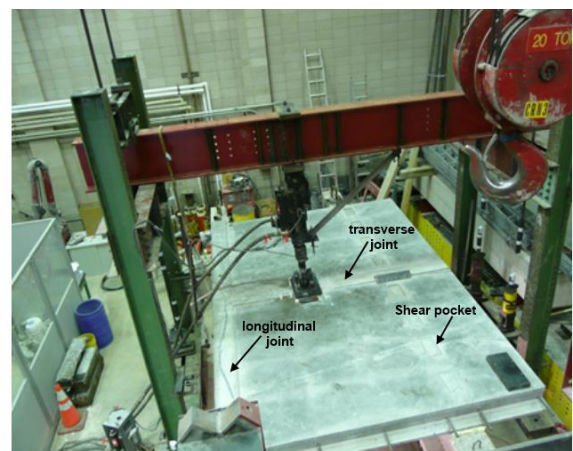
Time (days)	Strength (psi)
3	11,591
14	15,201
28	18,831



a) Pouring of UHPC at one end of the longitudinal joint



b) UHPC in the transverse joint



c) Finished UHPC joints

Figure 2.12. Construction of UHPC joints in the ISU laboratory

2.5.3 Instrumentation

This section presents the details of instrumentation used to monitor the performance of the waffle deck system during testing. Several different types of instruments were used for this study, including linear variable differential transducers (LVDTs), string potentiometers, and strain gauges. String potentiometers were used to measure the vertical displacements of the deck panels as well as the bridge girders. The locations and identifications used for these string potentiometers are shown in Figure 2.13.

The LVDTs were placed along the panel-to-panel joint region to capture any possible gap opening along the transverse joint during testing. They were also used down the depth of the panels to measure average strains and neutral axis depth during loading (see Figure 2.13). Also, the width of the flexural cracks along the transverse ribs was monitored during testing using LVDTs. A number of embedded strain gauges were used to measure the strain demands in the reinforcement along the transverse and longitudinal ribs of the panels and in the reinforcement placed within the joints. The No. 6 ($d_b = 0.75$ inch) dowel bars epoxied into the side face of the deck panels were also gauged to monitor the strain demands on these bars during testing. Figure 2.14 and Figure 2.15 show the locations of the strain gauges mounted on the bottom and top deck reinforcement, respectively. During the test, the data from all gauges and displacement devices were recorded using a computer-based data acquisition system.

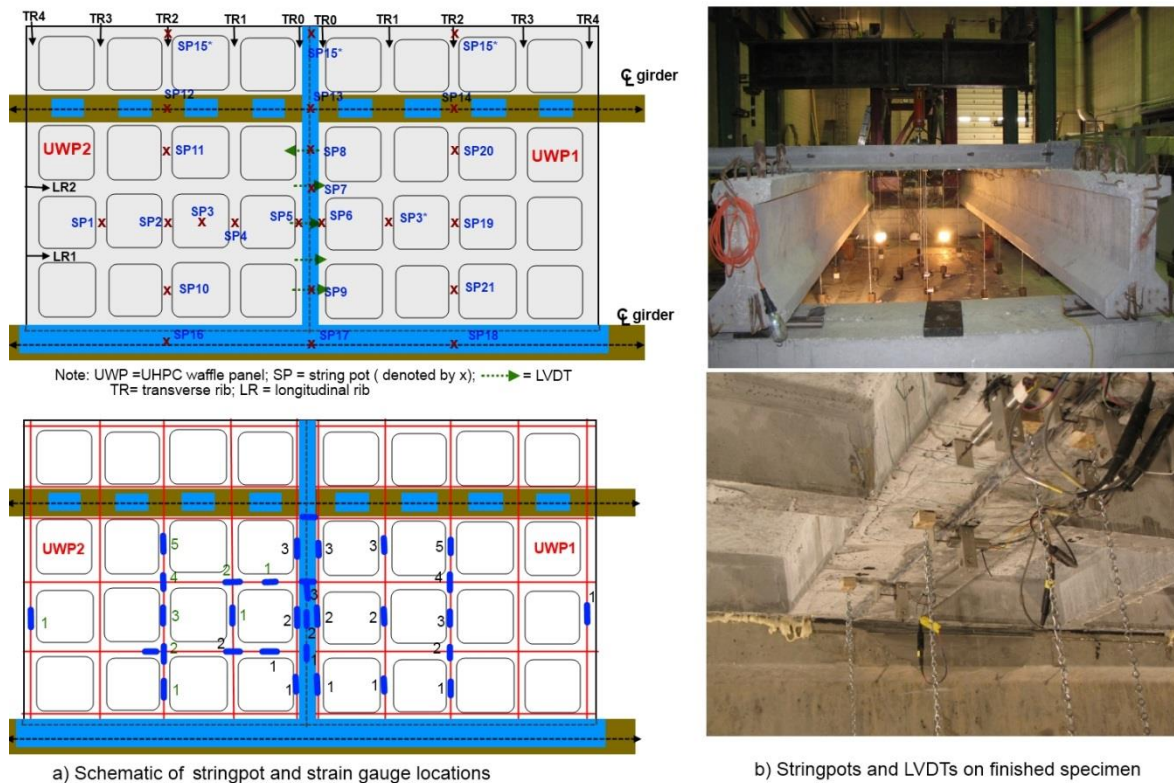


Figure 2.13. Schematic of the displacement transducers mounted to the test unit

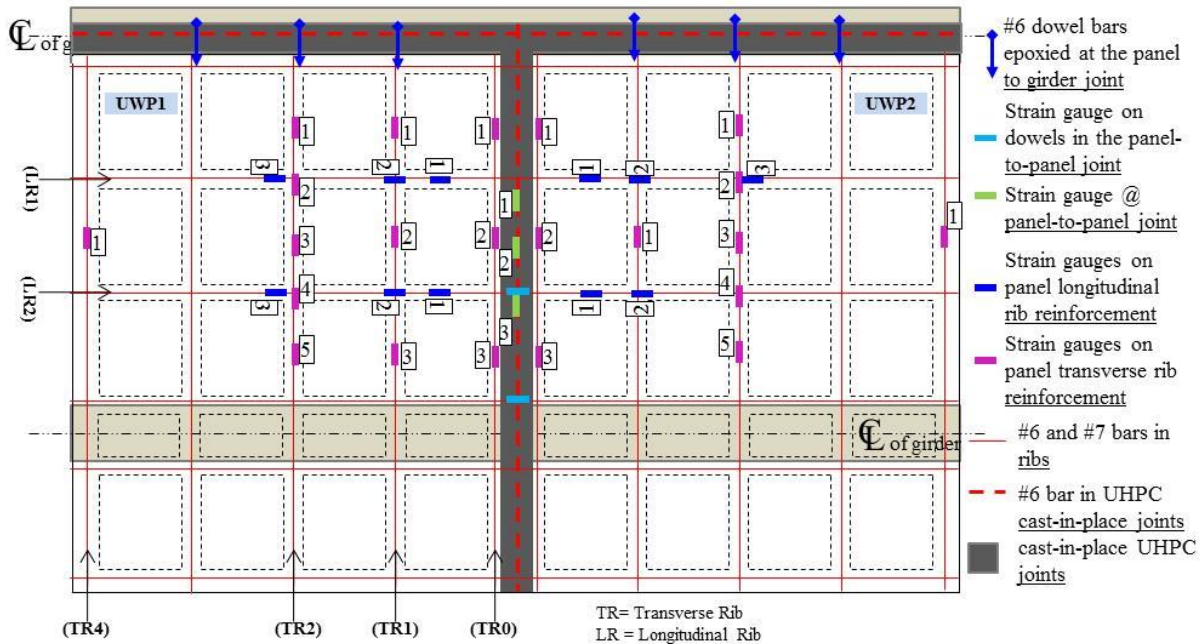


Figure 2.14. Location of strain gauges used on the bottom deck reinforcing bars

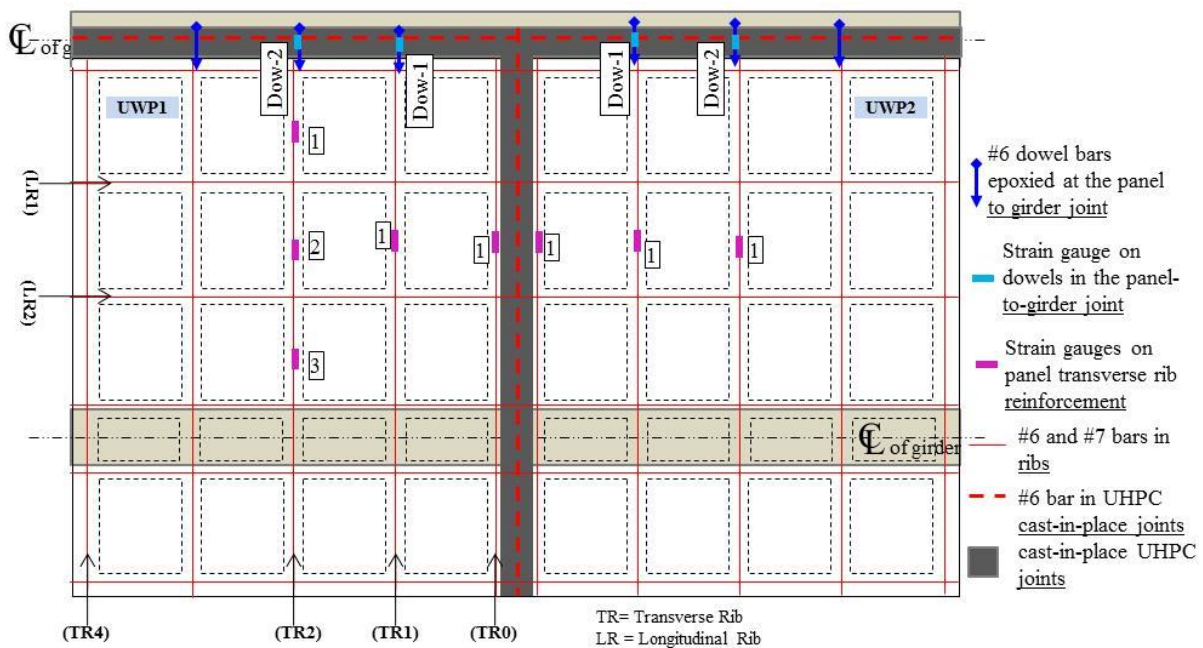


Figure 2.15. Location of strain gauges on the top deck reinforcing bars and dowel bars

2.5.4 Load Protocols

The performance of the UHPC waffle deck system, including the UHPC joints, was examined using nine different tests and a single wheel truck load. Two different locations were chosen to apply the load along the centerline between the two girders: one was at the center of the deck

panel and the other was at the center of the transverse joint between the deck panels (see Figure 2.10). The critical locations for the tests were determined using a 3-D finite element analysis model of the test specimen in ABAQUS software (ABAQUS 2008). For each test location, a service load test, a fatigue test, an overload test, an ultimate load test, and a punching failure test were conducted. The overload was defined as a factor of the service level load, which will cause very minimal damage to panel or joint. The ultimate load was defined as a factor of the service load, which will cause a significant cracking or failure of the panel and joints. All the service, overload, and ultimate load tests were performed using monotonic increments of loads, and these tests were paused during loading to the target values for visual inspection of any damage to the test system, including formation of cracks. The applied load values for service load tests were arrived at based on the current AASHTO standard truck wheel load. For the fatigue load test, the system was subjected to 1,000,000 cycles at a constant frequency of 2 Hz. This test was paused twice during the tests, and the same maximum load was applied in a quasi-static manner to evaluate any progressive damage to the system.

The specimen was load tested in the following order: (1) service load test of deck panel UWP2; (2) service load test of the panel-to-panel joint (transverse joint); (3) fatigue test of the panel-to-panel joint; (4) overload test of the panel-to-panel joint; (5) fatigue test of panel UWP1; (6) overload load test of panel UWP1; (7) ultimate load test of panel UWP1; (8) ultimate load test on panel-to-panel joint; and (9) punching shear failure test on panel UWP1. More details of each test and expected damage established from the finite element analysis are summarized in Table 2.4.

Table 2.4. Sequence and Details of the Tests Conducted on the Waffle Deck System

Test Number	Test Description	Location	Maximum Load	Expected Damage
1	Service load test panel-2 (UWP2)	Center of the panel	$1.33^a \times 16$ kips = 21.3 kips	Microcracking in ribs
2	Service load test on transverse joint	Center of the joint	$1.75^b \times 16$ kips = 28 kips	Microcracking in joint
3	Fatigue test on the transverse joint	Center of the joint	28 kips (1 million cycles)	No prediction was made
4	Overload test of transverse joint	Center of the joint	48 kips	Visible flexural cracks (more than one) along the joint and transverse ribs
5	Fatigue test on the panel-1 (UWP1)	Center of the panel	21.3 kips (1 million cycles)	No prediction was made
6	Overload test of the panel	Center of the panel	40 kips	Several visible flexural cracks along transverse ribs
7	Ultimate load test on panel UWP1	Center of the panel	160 kips	Significant cracking
8	Ultimate load test on the transverse joint	Center of the joint	155 kips	Significant cracking
9	Punching shear failure test on UWP1	Between transverse ribs	155 kips	Punching shear failure

^{a, b}Dynamic load allowance factors from AASHTO Table 3.6.2.1-1

2.5.5 Test 1—Panel Service Load Test

As noted earlier in Section 0, a 10 inch by 20 inch plate represented the dimensions of a wheel when a maximum load of 21.3 kips was applied at the center of panel UWP2 to simulate the service load condition. This load was established using the AASHTO service truck wheel load of 16 kips with a 1.33 factor to account for the 33% load increase suggested to account for the wheel load impact from the moving loads. A 3-D finite element model of the test setup developed in ABAQUS was used to confirm the most critical location as being one wheel at the center of the panel rather than placing two wheels at off-centered positions. The details of the model are presented in Section 0. To ensure no strength or stiffness degradation would take place due to repeated loading, the panel was subjected to three load cycles at this load level. The load-deflection curve established at the center of the panel for this test is shown in Figure 2.16a. As seen in this figure, a nearly linear relationship was observed between the load and deflection, with the maximum recorded deflection during the first cycle being 0.02 inch. This deflection corresponds to $L/4400$ (L = the span length between the girder), which is significantly less than the specified AASHTO limit of $L/800$ recommended for the serviceability condition (see Section 9.5.2 in AASHTO [2007]) of continuous span bridges with pedestrian traffic. The

AASHTO allowable serviceability displacement of $L/800$ would lead to 0.11 inch for the tested system.

The peak recorded strain in the bottom reinforcement of the center rib running in the transverse direction is shown in Figure 2.16b, which reached a maximum strain of only $375 \mu\epsilon$, or 18% of the yield strain. The strain variations along the length of the bottom reinforcement in the transverse rib TR2 of panel UWP2 and the panel-to-panel joint are shown in Figure 2.17 and Figure 2.18, respectively. The maximum tensile strain in the joint reinforcement was $40 \mu\epsilon$, indicating no damage to the joint region. A single crack having a width less than 0.002 inch was observed on the transverse rib under the load and is identified in Figure 2.19. In comparison to traditional normal concrete, it is important to realize that the material behavior of UHPC is quite dependent on the crack width. Hence, it may not be appropriate to use the AASHTO crack width provisions to qualify the serviceability and durability considerations for the behavior of UHPC structural members. Because of the lack of any specific UHPC bridge design serviceability criteria available in the literature, the crack width limits suggested for UHPC to control the fiber pullout criteria are used to comment on the implication of the crack developed in this test. Based on the AFGC 2002 recommendations, the fiber pullout and strength degradation in UHPC initiate when a crack width reaches 0.0118 in. (0.3 mm) (see Figure 2.20). This limit is nearly more than six times the observed crack width during the service test, confirming that the overall behavior of the precast waffle deck system was outstanding. In addition, it is noted that the test results also confirmed that the system performance satisfied the deflection and crack width requirements recommended for the serviceability condition by AASHTO (AASHTO 2007).

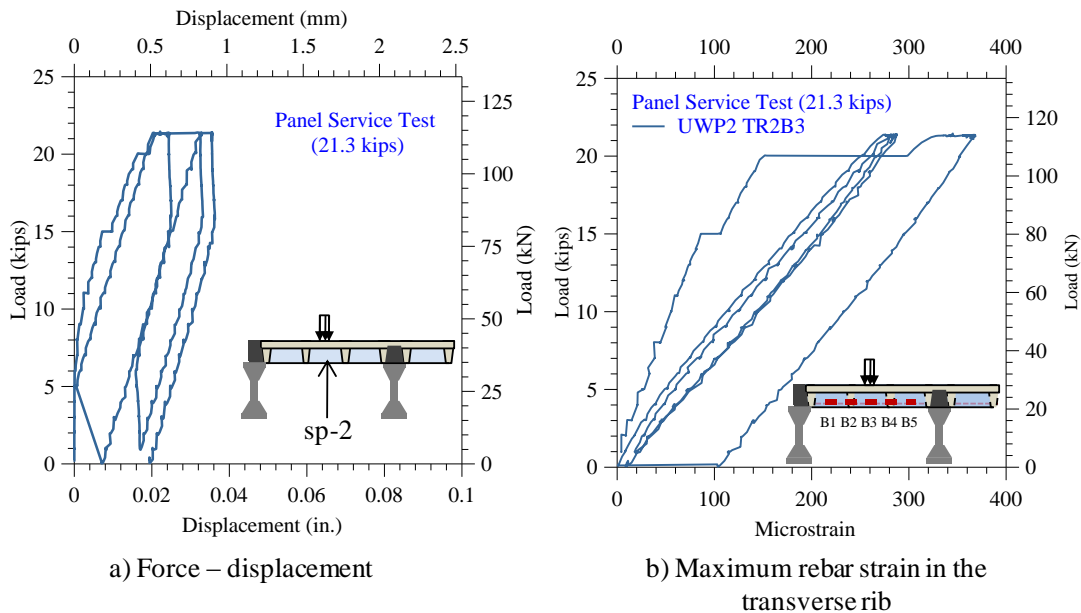


Figure 2.16. Measured force-displacement response and peak rebar strain from gauge B3 at the center of the transverse rib TR2 of panel UWP2

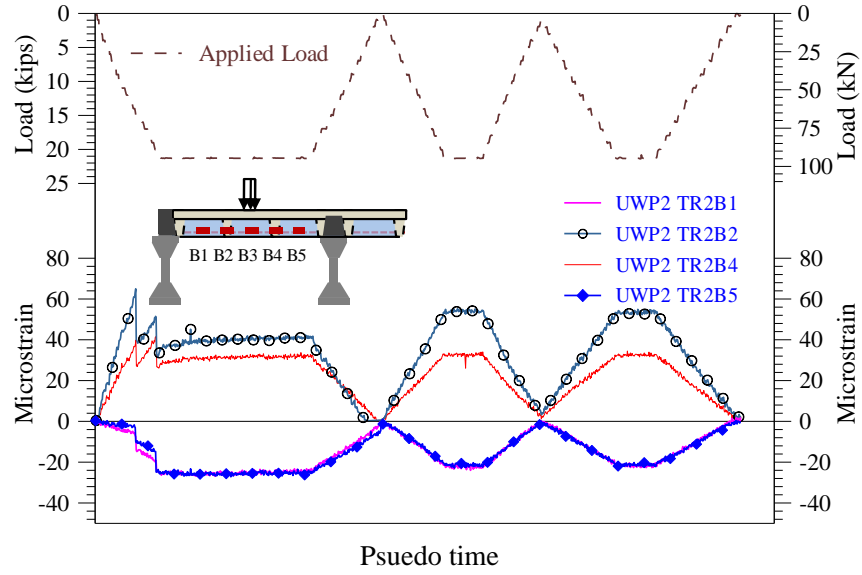


Figure 2.17. Measured strains along the bottom reinforcement of the transverse rib TR2 of panel UWP2

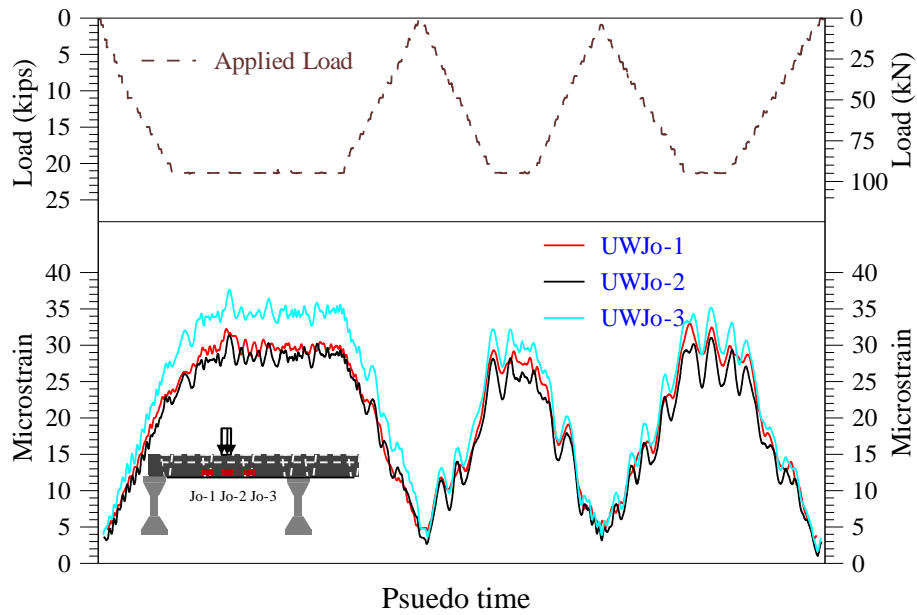


Figure 2.18. Measured strains along a bottom reinforcement of the panel-to-panel joint

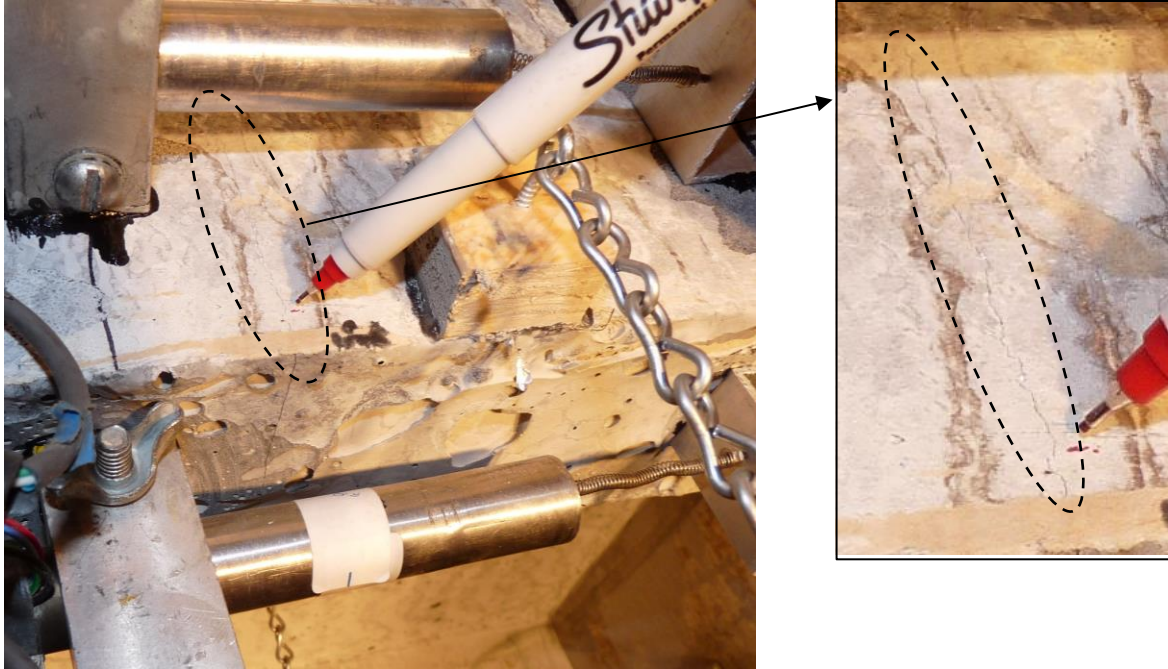


Figure 2.19. A hairline crack in the UWP2 panel transverse rib TR2 at 21.3 kips

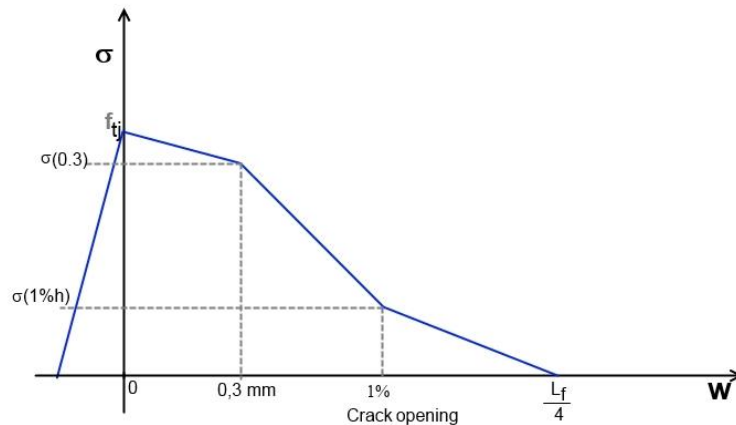


Figure 2.20. A relationship proposed for the UHPC tensile strength variation as a function of crack width (AFGC 2002)

2.5.6 Test 2—Joint Service Load Test

Similar to the panel service load test, the transverse panel-to-panel joint test was then conducted under the service loading condition. In this case, the maximum load of 28 kips was used, which represented the AASHTO service load of 16 kips for one wheel times the 1.75 factor, which accounted for 75% increase in load to account for the wheel load impact on joints due to moving loads. Similar to the previous service load test, the critical location of the load was determined from the finite element analysis and the load was repeated three times to ensure the stability of the force-displacement response of the system. The applied load vs. the measured deflection at

the center of the joint is shown in Figure 2.21a. Again, a linear response was obtained with a maximum deflection reaching only 0.022 inch during the first load cycle. This deflection corresponds to $L/4000$, which is 20% of the specified AASHTO limit of $L/800$ (see Section 9.5.2 in AASHTO [2007]) for continuous spans with pedestrian traffic under the serviceability condition.

The load vs. strain plot for the gauge recorded for the maximum strains and the strain variation along a bottom reinforcement in the joint are shown in Figure 2.21b and Figure 2.22, respectively. The peak recorded strain in the joint bottom reinforcement was $17 \mu\epsilon$, indicating significant reserve capacity of the joint. The strain variations obtained for the bottom reinforcement in the transverse rib TR2 of panels UWP2 and UWP1 are shown in Figure 2.23 and Figure 2.24, respectively. Both figures show comparable strain demands, indicating that the applied joint load was evenly distributed to both panels. Figure 2.25 shows the variation of strains at the center of the rib across the transverse ribs of panel 1, indicating their relative contribution. No cracking was observed at 21.3 kips load. At the peak load of 28 kips, however, a single hairline crack having width less than 0.002 inch was observed on the transverse ribs forming the joint (see Figure 2.26). Given that this crack is significantly smaller than 0.0118 in. (0.3 mm) (see Figure 2.20) corresponding to initiation of fiber pullout and strength degradation of UHPC in tension, it was concluded that the overall behavior of the transverse joint subjected to service load was outstanding. The test results also indicated that the system performance satisfied the deflection and crack width requirements recommended for the serviceability condition by AASHTO (AASHTO 2007).

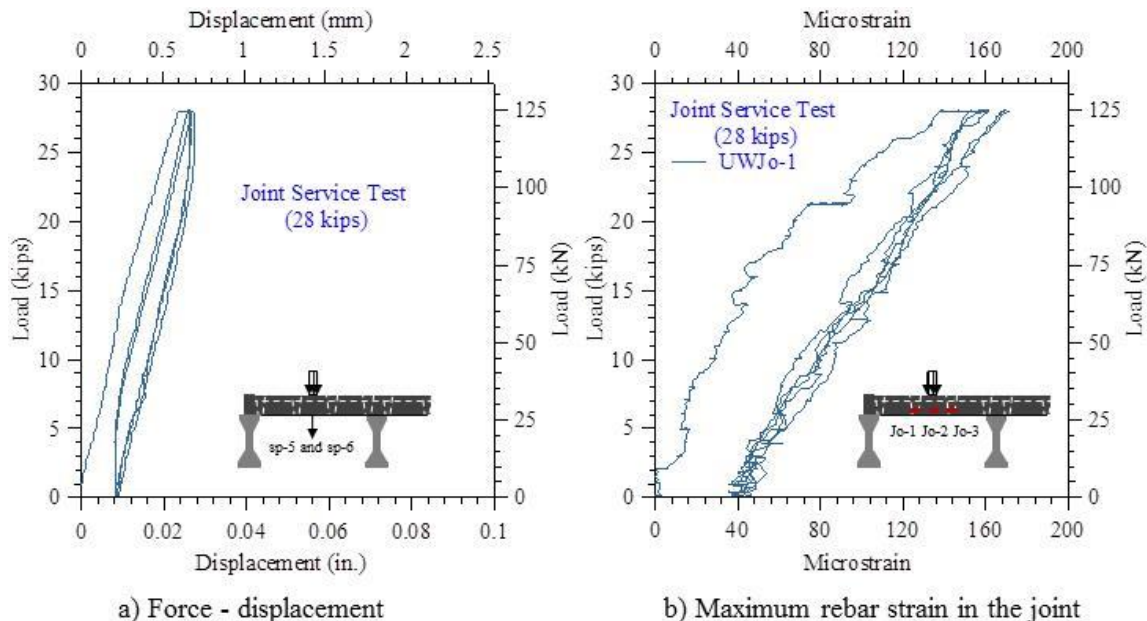


Figure 2.21. Measured force-displacement response and peak rebar strain at the center of the joint at the service load

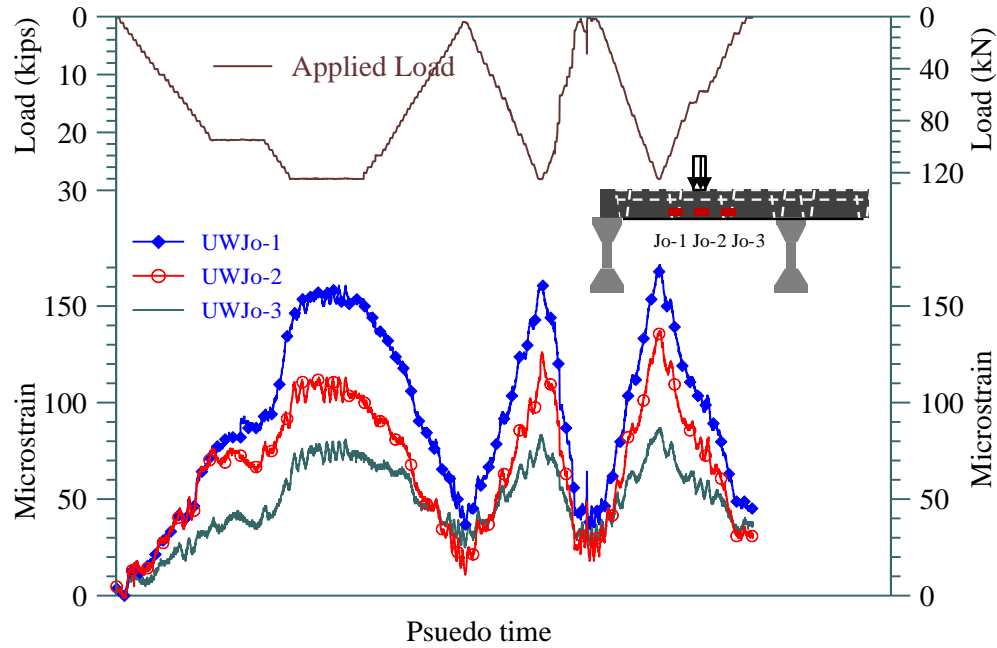


Figure 2.22. Measured strains along the bottom reinforcement of the joint during the service load test

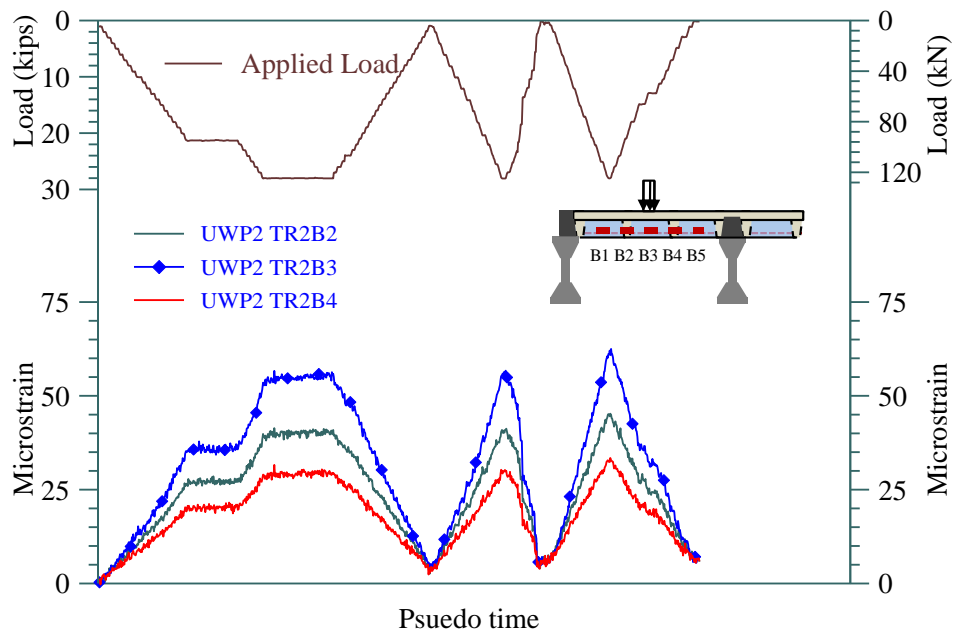


Figure 2.23. Measured strains in the bottom reinforcement of the transverse rib (TR2) along the length of panel UWP2 at service load

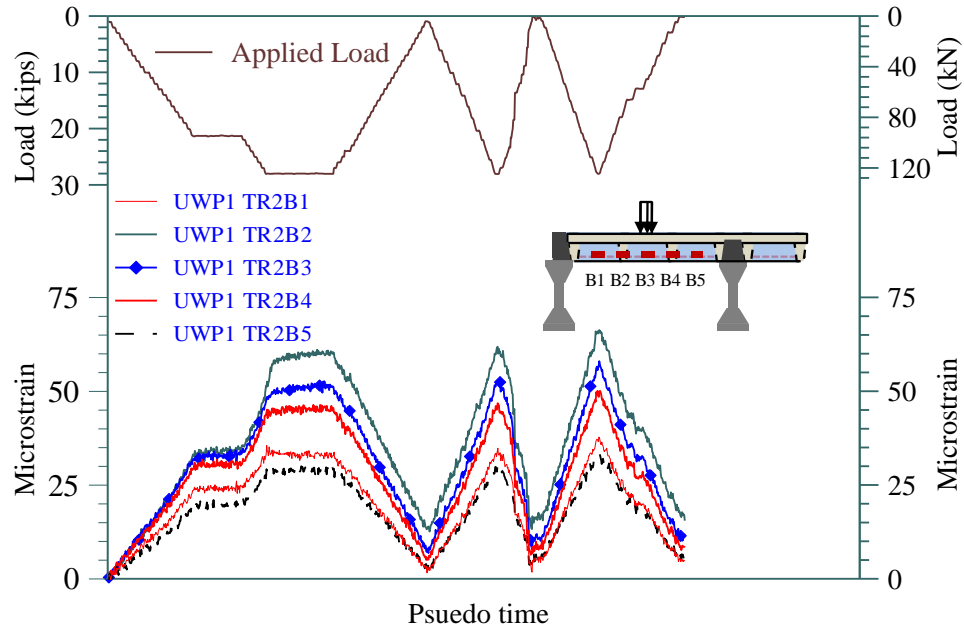


Figure 2.24. Measured strains in the bottom reinforcement of the transverse rib (TR2) along the length of panel UWP1 at service load

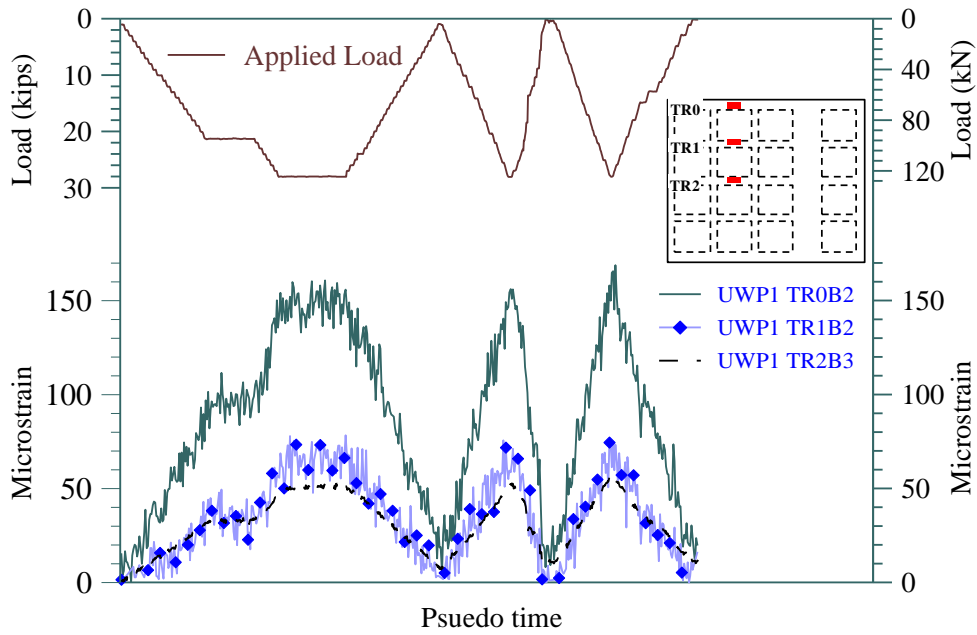


Figure 2.25. Measured strains at the center of the panel across the transverse ribs of UWP1 at service load

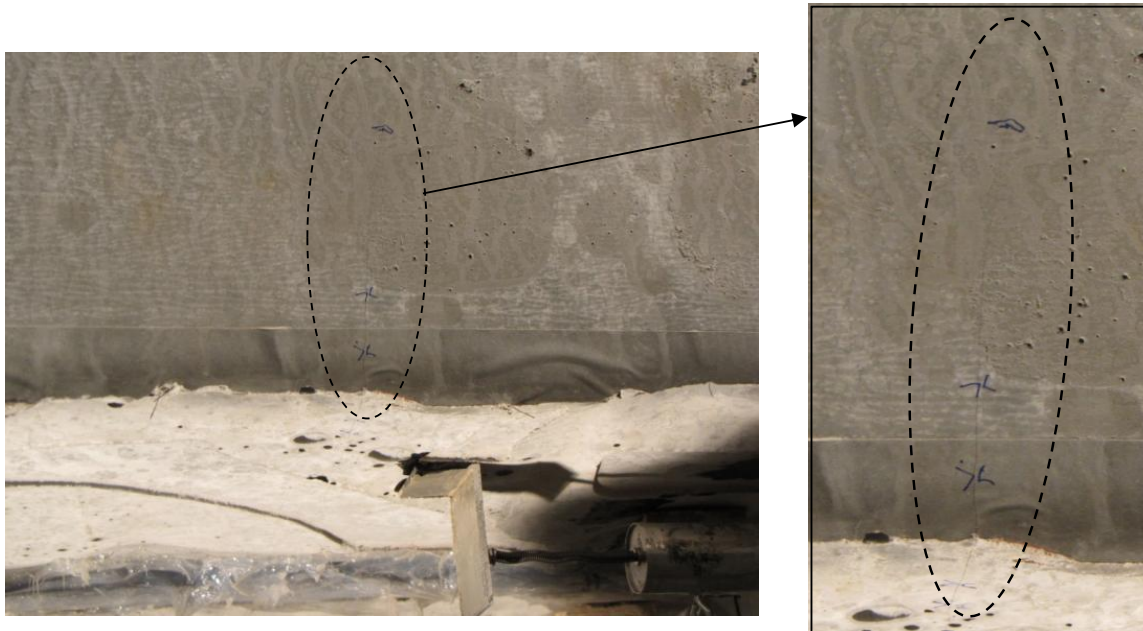


Figure 2.26. A hairline crack formed at the center of underside of the transverse joint at 28 kips

2.5.7 Test 3—Joint Fatigue Load Test

The transverse joint between the waffle deck panels was subjected to 1,000,000 load cycles to test the joint for potential low amplitude fatigue damage. The load variation was computer controlled in a sinusoidal manner between 1 kip and 28 kips at a frequency of 2 Hz. In other words, the peak load of 28 kips was reached twice within a one-second interval. The load, displacements, and strain data obtained from selected gauges from the test were recorded continuously for 5 seconds at 20-Hz frequency at the end of every 1,800 cycles (i.e., at every 15 minutes). In addition, the fatigue test was paused and static joint load tests were conducted at the end of 168,000, 333,875, and 1,000,000 cycles to determine the influence of fatigue damage on the joint and the entire system. During the test that lasted for several days as well as at the end of the fatigue test, the deck panels and the joint were monitored for formation of any new cracks. Except for those formed during the joint service load test, no further cracks developed during the joint fatigue test.

Based on the recorded data, the displacements recorded at the center of the joint at 28 kips and 1 kip are plotted as a function of the load cycle during the fatigue loading in Figure 2.27. It is apparent that the gauge data experienced drift due to ambient condition and other reasons during the test. When the displacement corresponding to the load increment of 27 kips (i.e., 28 kips–1 kip) was examined, however, it was clear that this displacement remained almost constant throughout the test and the change in the displacement reading is largely due to noise observed at 1 kip. With the variation of the displacement being very small and limitations with the sensitivity of the string potentiometers occurring, it is concluded that the UHPC did not experience any fatigue damage.

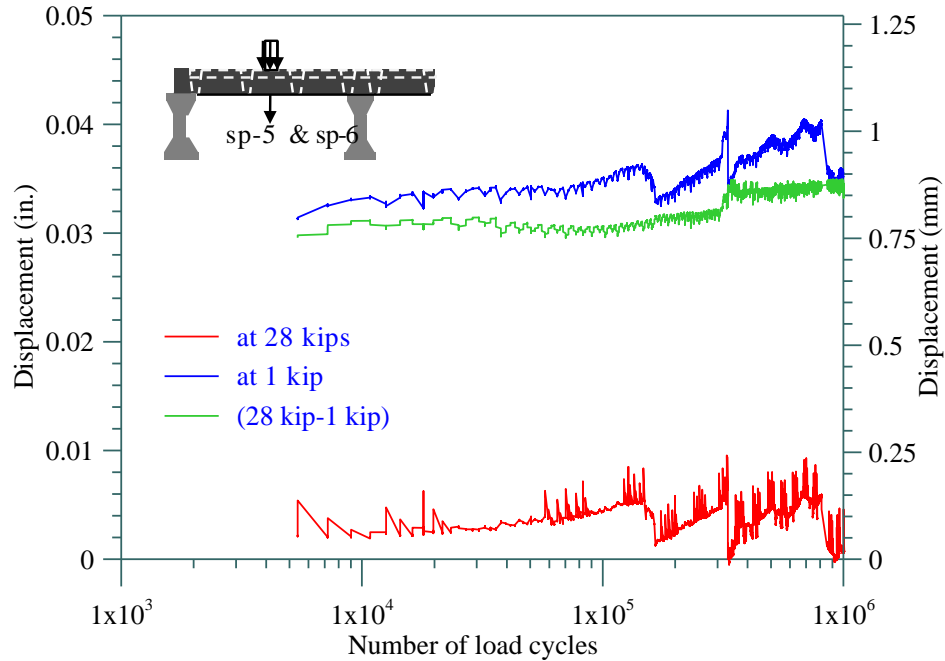


Figure 2.27. The variation of the peak displacement at the center of the joint during the joint fatigue test

Figure 2.28 shows the strains recorded by the gauge mounted to the joint transverse reinforcement located at the center of the joint as a function of the load cycle. Although the drifts in measured data are apparent, the change in strain remained almost constant at a value of $135 \mu\epsilon$ as the load increased from 1 to 28 kips. This variation is comparable to the peak strain of $170 \mu\epsilon$ recorded during the service load test. Except for the noise in the data, the crack width in the transverse joint was nearly constant over the entire fatigue test and is shown in Figure 2.29.

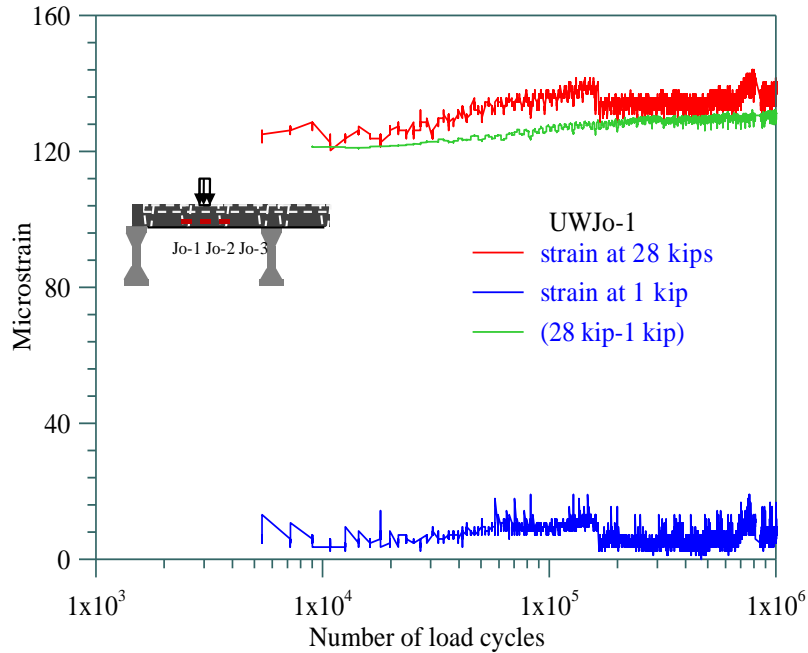


Figure 2.28. The variation of the peak strain in the bottom joint transverse reinforcement during the joint fatigue test

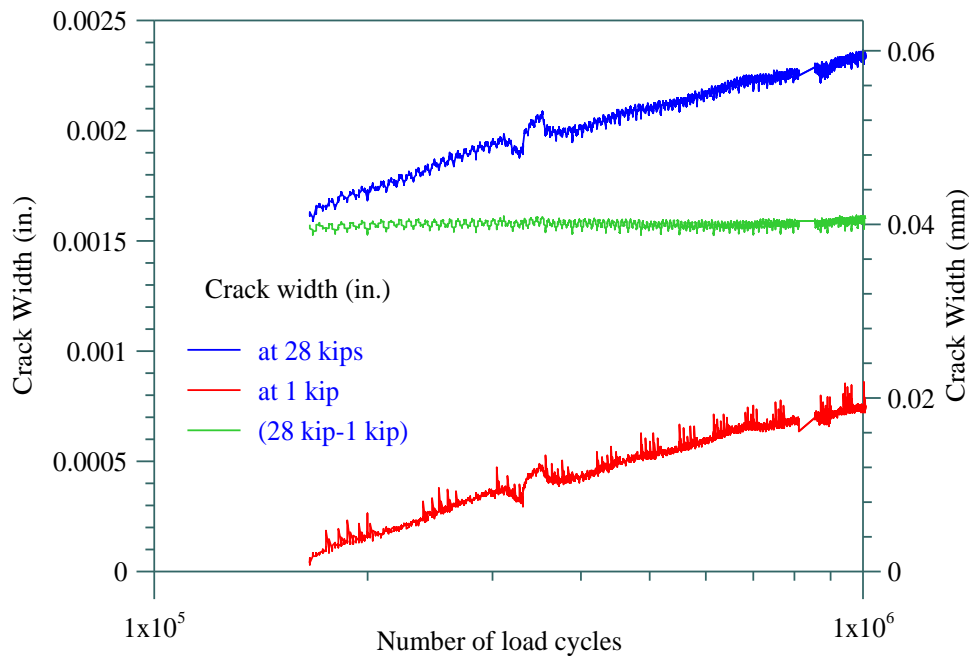


Figure 2.29. The variation of the crack width in the transverse joint with number of load cycles

For the static load tests performed at the end of 168,000, 333,875 and 1,000,000 cycles, the load-displacement, peak strain in the bottom reinforcement in the joint, and crack width in transverse ribs forming the joint during the intermediate static load tests are presented in Figure 2.30. The

initial secant stiffness at the peak load of panel-to-panel joint at the end of 168,000, 333,875 and 1,000,000 cycles of loading is 1,166.7 kip/inch, 1,135.6 kip/inch, and 1,139.2 kip/inch, respectively, which compares closely with the stiffness of 1,105.5 kip/inch established during the service load test and shows a variation of less than 5%. It can be seen from these figures that the joint or the UHPC waffle deck system did not experience any significant fatigue damage after subjected to 1,000,000 cycles of amplified service load.

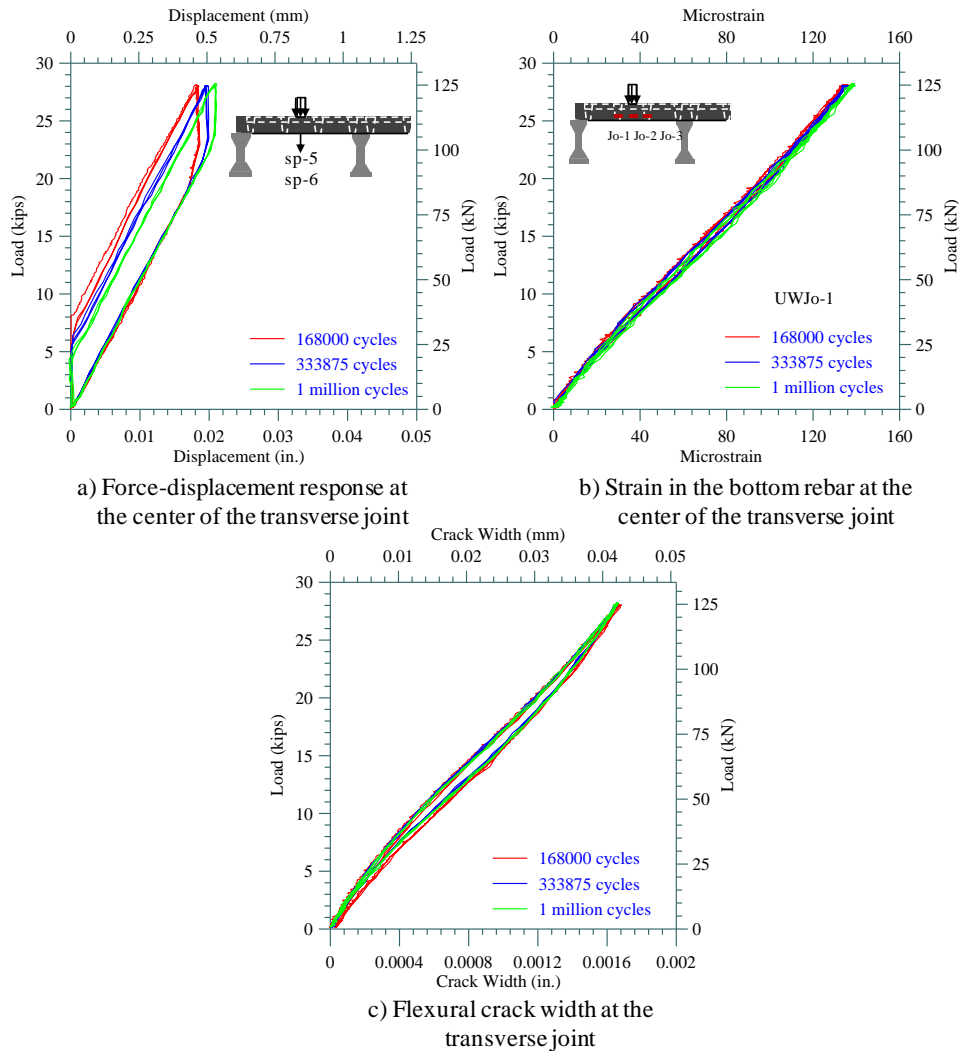


Figure 2.30. Measured responses of the waffle deck system from the static service load tests conducted during the joint fatigue test

2.5.8 Test 4—Joint Overload Load Test

The overload test was carried out to investigate the adequacy of the transverse joint at the overload limit state. The load corresponding to this limit state was defined as a factor of the service wheel load of 16 kips without causing any significant damage to the joint so that the waffle deck system could be used to conduct the fatigue and overload load tests at the center of a panel. Using a load factor of three, the maximum load suitable for conducting the overload load

test was defined as 48 kips. Similar to the service load test, the joint was subjected to three load cycles at this load level to ensure the stability of the force-displacement response of the system. The load-deflection curve established at the center of the joint for this test is shown in Figure 2.31a. The transverse joint exhibited a linear force-displacement response even for this test, with insignificant damage and a maximum deflection of 0.05 inch. This deflection corresponds to $L/1760$, which is 46% of the AASHTO serviceability limit of $L/800$ (see Section 9.5.2 in AASHTO [2007]) for continuous span bridges with pedestrian traffic.

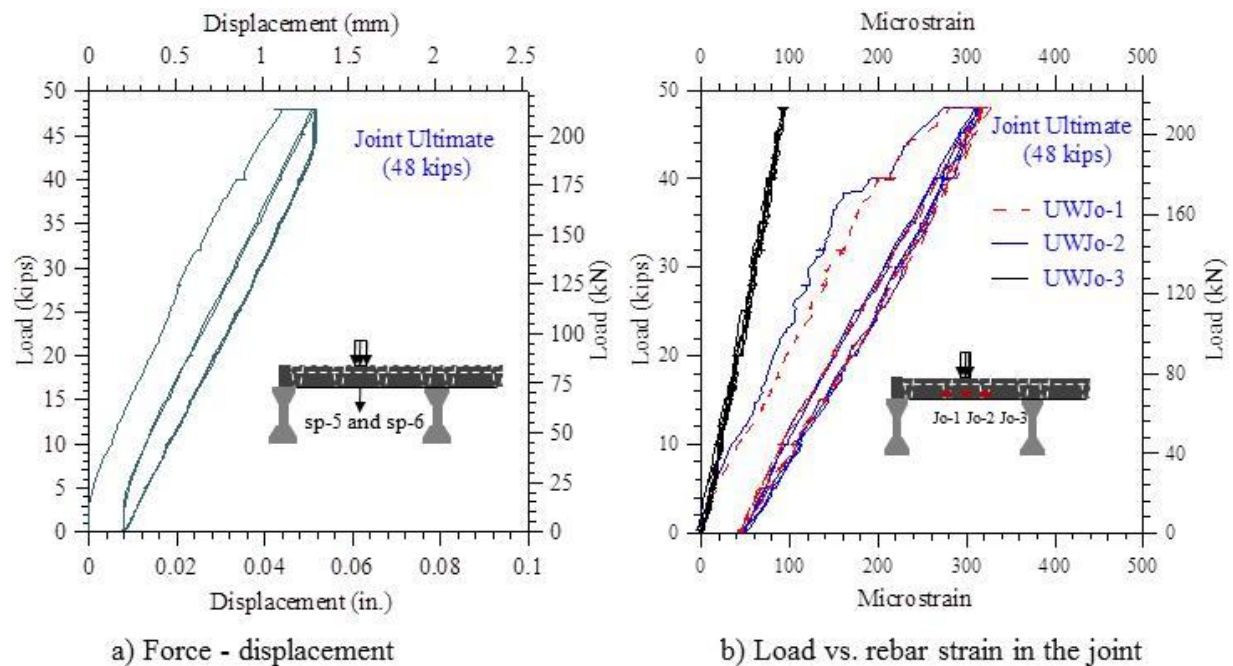


Figure 2.31. Measured force-displacement response and peak rebar strain at the center of the joint at the overload load of 48 kips

The strain variations along the bottom reinforcement in the joint as a function of the applied load are shown in Figure 2.31b. The peak strain in the joint region bottom reinforcement was $330 \mu\epsilon$, which is only about 15% of the yield strain of the reinforcement. The strain variations in the bottom reinforcement in the transverse rib TR2 of the panels UWP2 and UWP1 are shown in Figure 2.32 and Figure 2.33, respectively. Figure 2.34 shows the variation of the strain at the center of the rib across the transverse ribs of panel UWP1, indicating their relative participation in resisting the load. A series of hairline cracks were observed in the central region of the joint and are shown in Figure 2.35. The maximum crack width measured along the transverse ribs forming the joint was 0.003 inch, which can be seen in Figure 2.36.

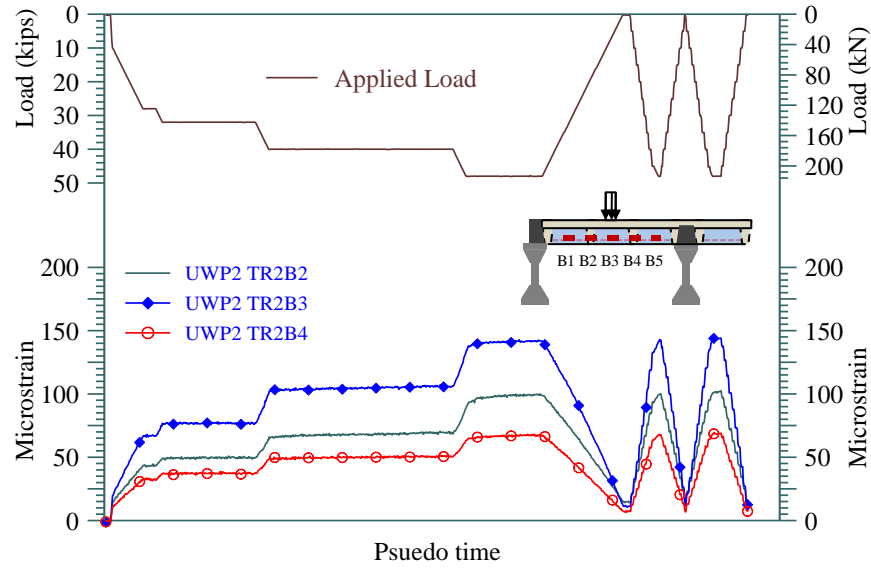


Figure 2.32. Measured strains in the bottom reinforcement of transverse rib TR2 along the length of panel UWP2 at the overload load

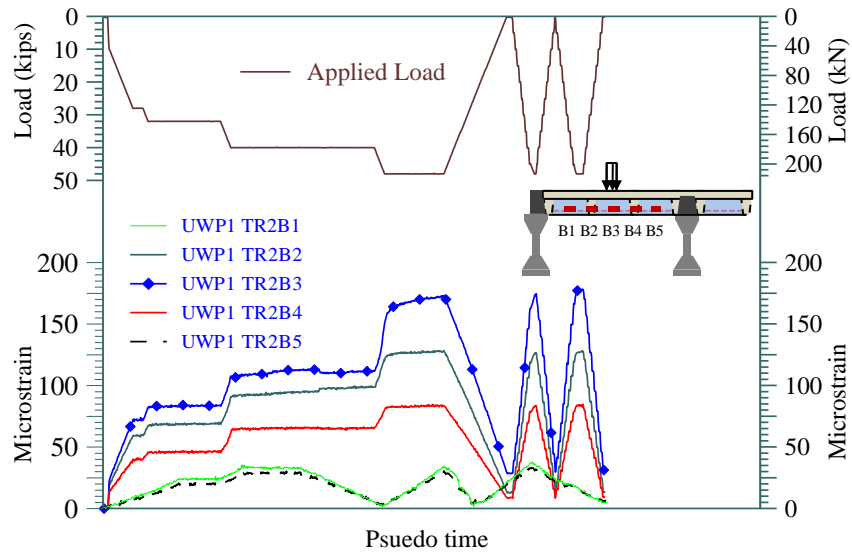


Figure 2.33. Measured strains in the bottom reinforcement of transverse rib TR2 along the length of panel UWP1 at the overload load

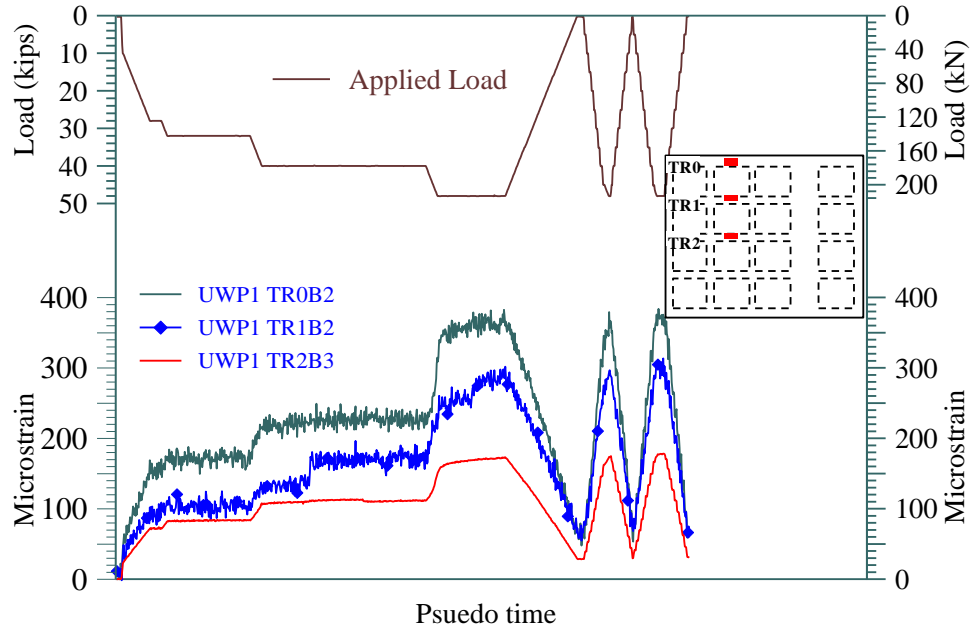


Figure 2.34. Measured strains at the center of the panel across the transverse ribs of panel UWP1 at joint overload load

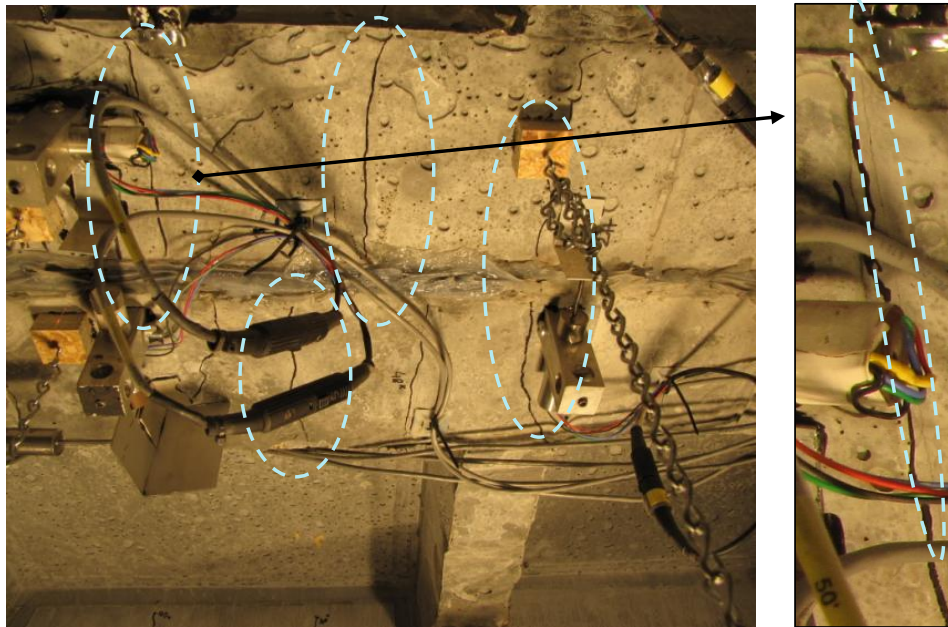


Figure 2.35. Hairline cracks formed at the center of underside of the transverse joint at the overload load of 48 kips

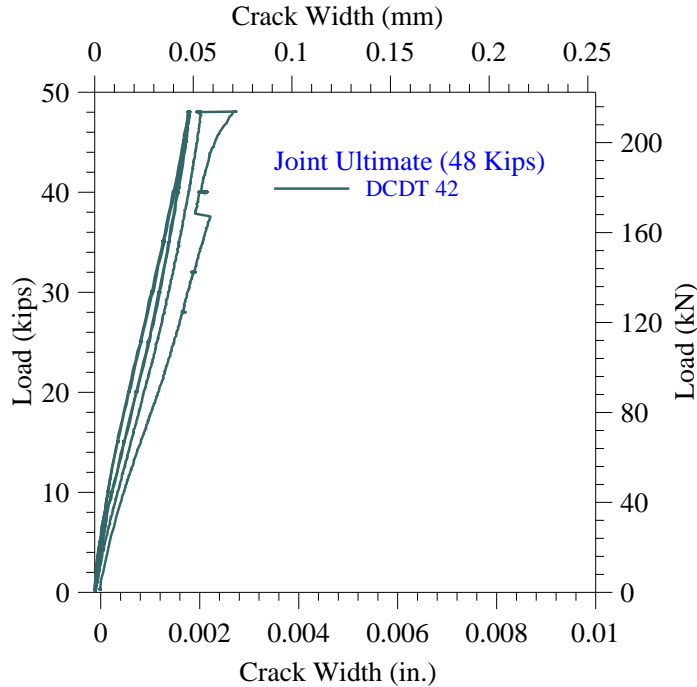


Figure 2.36. The variation in the width of the most critical flexural crack in the transverse ribs forming the transverse joint

2.5.9 Test 5—Panel Fatigue Load Test

As with the joint test, the waffle deck panel UWP1 was subjected to 1,000,000 cycles to test this panel for potential low amplitude fatigue damage. The load variation was again computer controlled in a sinusoidal manner between 2 kips and 21.3 kips at a frequency of 2 Hz. During the test, the load, displacements, and strain data from selected gauges were recorded continuously for 5 seconds at 20 Hz frequency at the end of every 1,800 cycles (i.e., at every 15 minutes). In addition, the fatigue test was paused and static load tests were conducted at the end of 135,000, 670,000 and 1,000,000 cycles with a maximum load of 21.3 kips to determine the influence of any fatigue damage on the panel and system behavior.

Based on the recorded data, the displacements recorded at the center of the panel UWP1 at 21.3 kips and 2 kips are plotted as a function of the load cycle in Figure 2.37. It is apparent again that the gauges experienced drifts due to ambient variations and that the data was influenced by high-frequency noise. When the displacement corresponding to the load increment of 19.3 kips (i.e., 21.3 kips–2 kips) was examined, however, it was clear that this displacement remained nearly constant throughout the test. Based on these observations, it is concluded that the UHPC panel did not experience any fatigue damage.

Figure 2.38a shows the strains recorded by the gauge mounted to the transverse rib reinforcement located at the center of rib TR2 of panel UWP1 as a function of the load cycle. Although the drifts in measured data are apparent, the change in strain remained almost constant at a value of $360 \mu\epsilon$ as the load increased from 2 to 21.3 kips. This variation is comparable to a

strain of $375\ \mu\epsilon$ recorded during the service load test of panel UWP2. Figure 2.38b shows the strains recorded by the gauge mounted to the joint transverse reinforcement located at the center of the joint as a function of the load cycle.

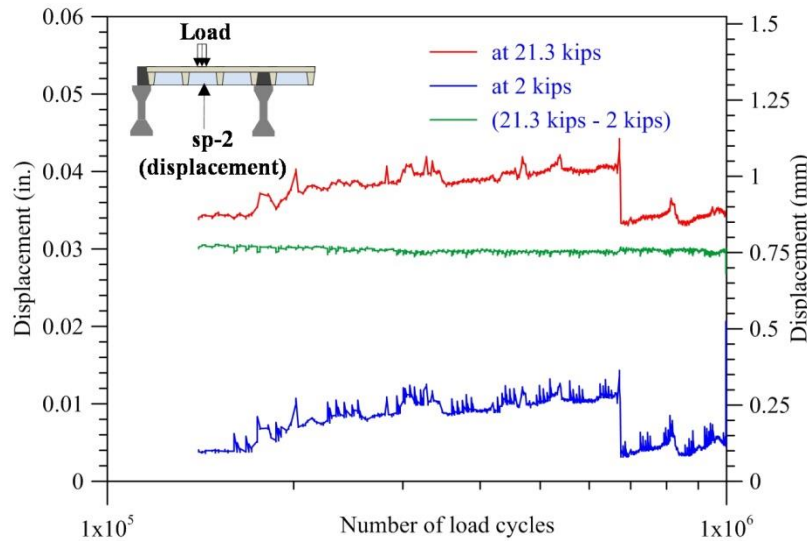
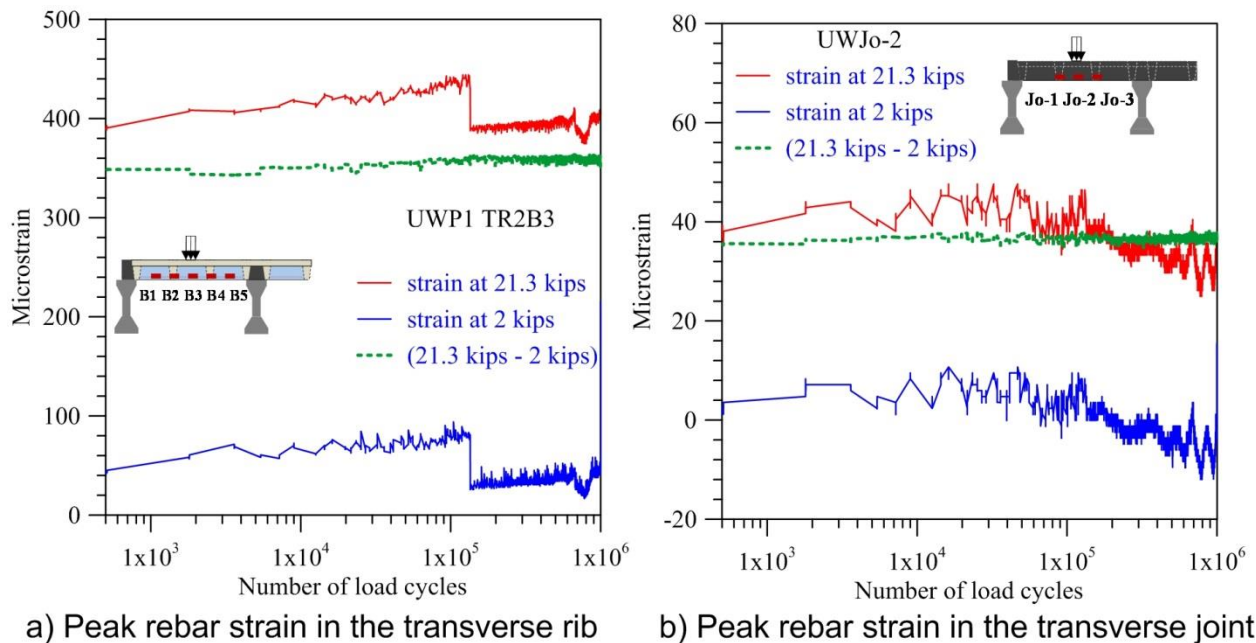


Figure 2.37. The peak displacement variation at the center of panel UWP1 during the joint fatigue test



a) Peak rebar strain in the transverse rib

b) Peak rebar strain in the transverse joint

Figure 2.38. The peak strain variation in bottom deck reinforcement in the transverse rib of UWP1 and the joint during panel fatigue test

During the test, the deck panels and the joint were examined periodically for formation of any new cracks. No additional cracking in the panel was observed besides those cracks formed during the service load test. The crack width at the bottom of the transverse rib was nearly

constant over the entire fatigue test and is shown in Figure 2.39. This data varied between 0.0018 inch and 0.0023 inch or within a range of 0.0005 inch, which is close to the sensitivity of the LVDTs used to measure the crack width. For the static load tests performed at the end of 135,000, 670,000 and 1,000,000 cycles, the load displacement, peak strain in the bottom reinforcement in the transverse joint, and crack width in transverse rib TR2 of panel UWP1 during the intermediate static load tests are presented in Figure 2.40. The initial secant stiffness of the panel at the peak load after 200, 135,000, 670,000, and 1,000,000 cycles of loading was 708.05 kip/inch, 667.71 kip/inch, 637.72 kip/inch, and 653.34 kip/inch, respectively. These values compare closely to each other and show variations of within 8% of the average stiffness value. From these observations and Figure 2.40, it is clear that the joint or the UHPC waffle deck system did not experience any significant fatigue damage even after subjected to 1,000,000 cycles at an amplified level of the service load.

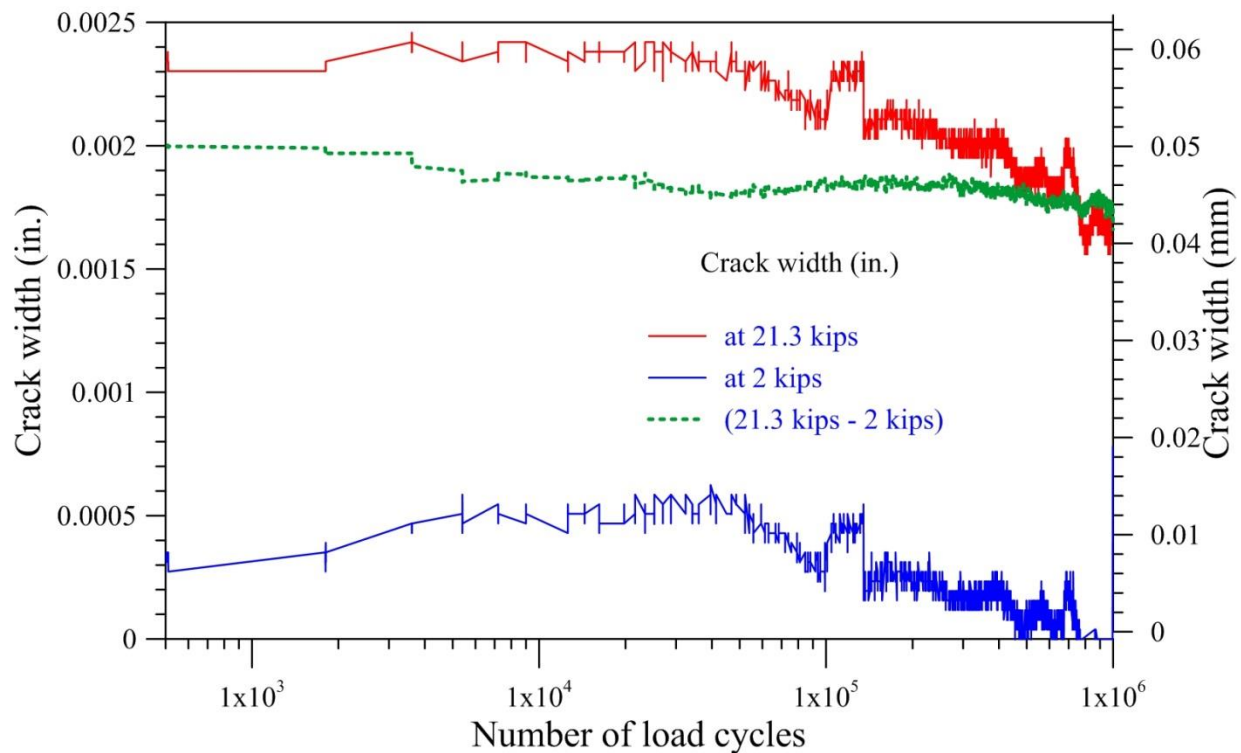


Figure 2.39. The crack width variation in transverse rib TR2 of panel UWP1 during panel fatigue test

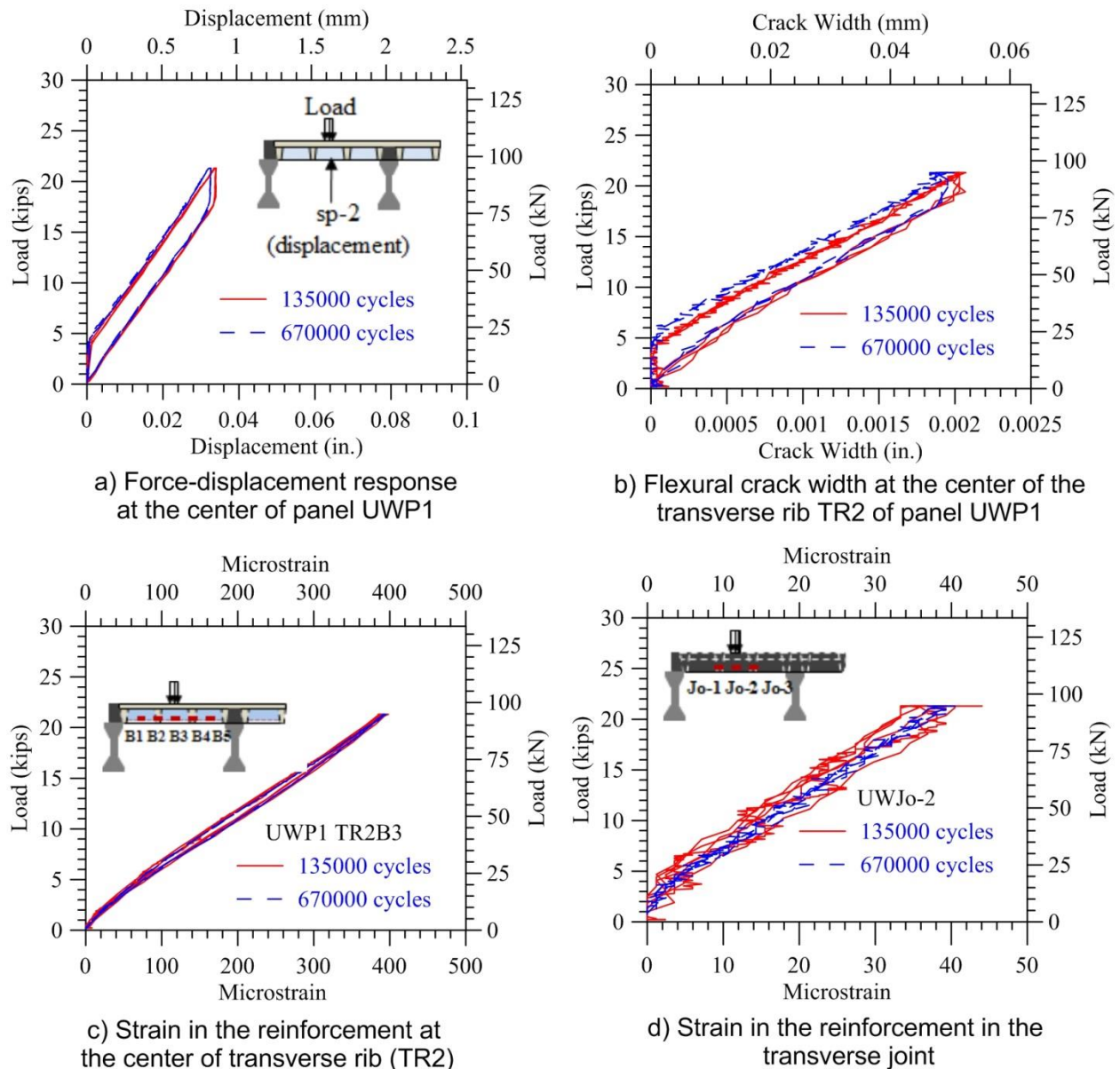


Figure 2.40. Measured responses of the waffle deck system for static service load tests conducted during the panel fatigue test

2.5.10 Test 6—Panel Overload Load Test

The overload test was carried out to investigate the adequacy of the waffle deck panel at the overload limit state. Similar to the joint overload load test, this limit state was defined as a factor of the service wheel load of 16 kips without causing any significant damage to panel UWP1. A maximum load of 40 kips, equivalent to 2.5 times the service wheel load of 16 kips, was applied at the center of panel UWP1.

Similar to the previous service load tests, three load cycles at this load level were conducted to ensure the stability of the force-displacement response of the system. The load-deflection curve

established at the center of panel UWP1 for this test is shown in Figure 2.41a. The panel exhibited a linear force-displacement behavior response with insignificant damage. A maximum deflection of 0.08 inch was measured at the center of panel UWP1. This deflection corresponds to $L/1100$, which is 73% of the AASHTO-specified serviceability limit of $L/800$ for continuous spans with pedestrian traffic.

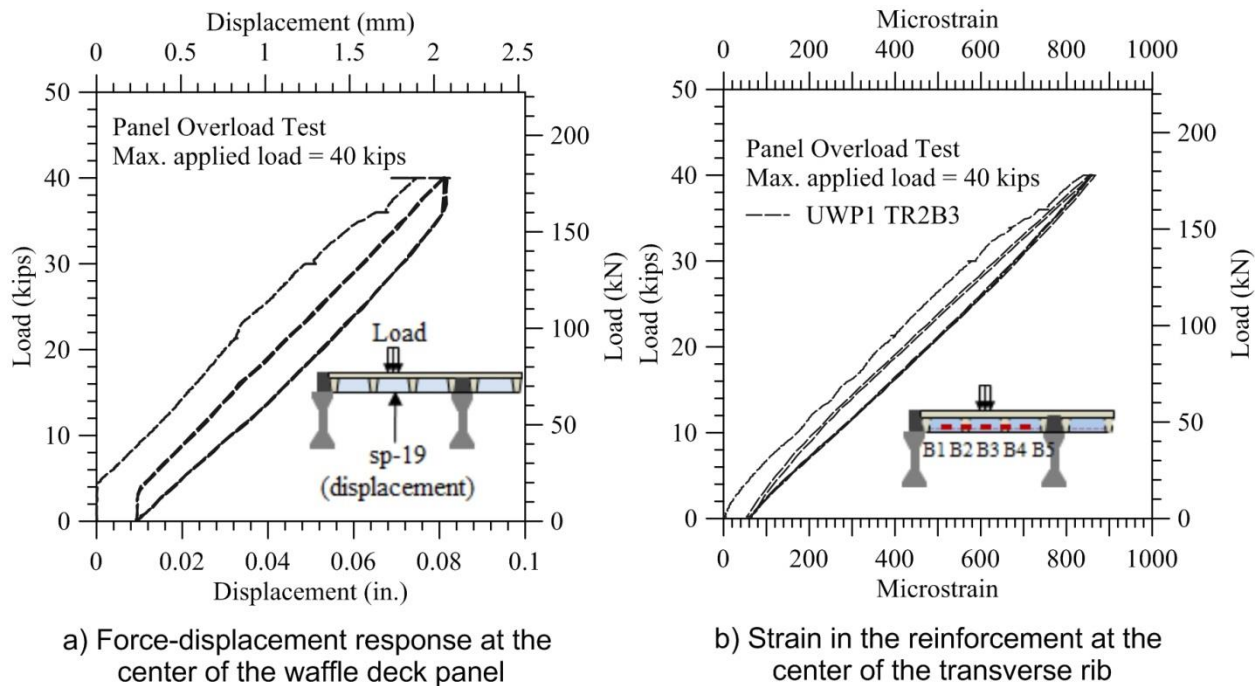


Figure 2.41. Measured force-displacement response and peak rebar strain at the center of the transverse rib of UWP1 at the overload load of 40 kips

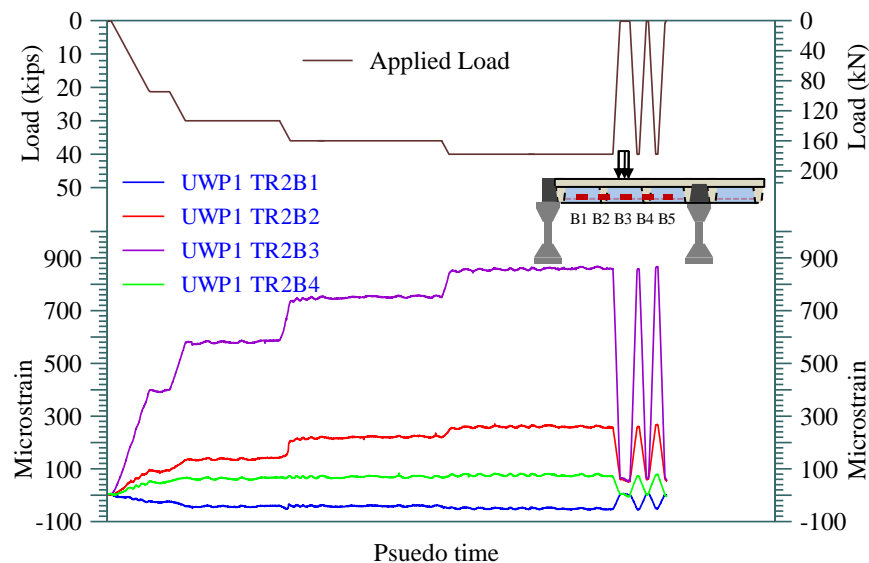


Figure 2.42. Measured strains in the bottom reinforcement of the transverse rib along the length of UWP1 during the overload load test

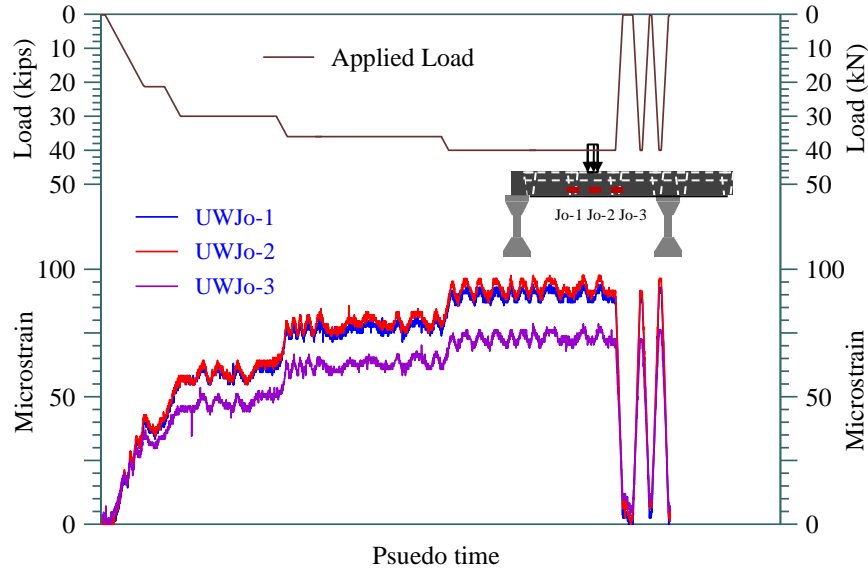
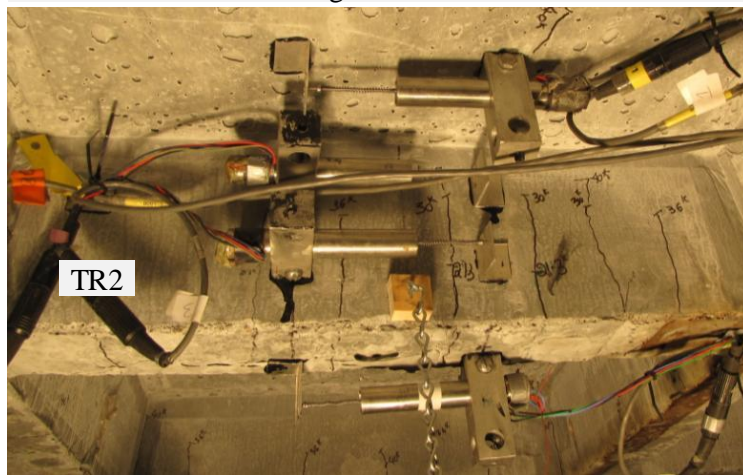


Figure 2.43. Measured strains in the bottom reinforcement of the joint along the joint length during the overload load test

The variation of the most critical strain in the bottom reinforcement of the transverse rib TR2 of panel UWP1 as a function of the applied load is shown in Figure 2.41b. The peak strain in the bottom reinforcement of transverse rib TR2 was only 880 $\mu\epsilon$, which is only about 43% of the yield strain of the reinforcement. The strain variations in the bottom reinforcement placed in the transverse rib TR2 of panel UWP1 and the joint are shown in Figure 2.42 and Figure 2.43, respectively. Three to four hairline cracks were observed on both transverse ribs (TR1, TR2, and TR3) and longitudinal ribs (LR1 and LR2) of panel UWP1 (see Figure 2.44). A hairline crack was seen on the bottom surface of UWP1 (between ribs TR2 and TR3) at the peak load (see Figure 2.44a). The maximum crack width measured along the transverse rib TR2 in UWP1 was 0.008 inch, and its variation with the applied load is shown in Figure 2.45. Figure 2.46 shows the strain demand on the dowel bar in the panel-to-girder joint during the panel overload load test. It is clear that the dowel bars were engaged in load transfer when the 35-kips load was applied at the center of the panel.



a) Cracking on the bottom surface of the slab and on a longitudinal rib



b) Cracking along transverse rib TR2 of UWP1

Figure 2.44. Hairline cracks developed on panel UWP1 at an overload load of 40 kips

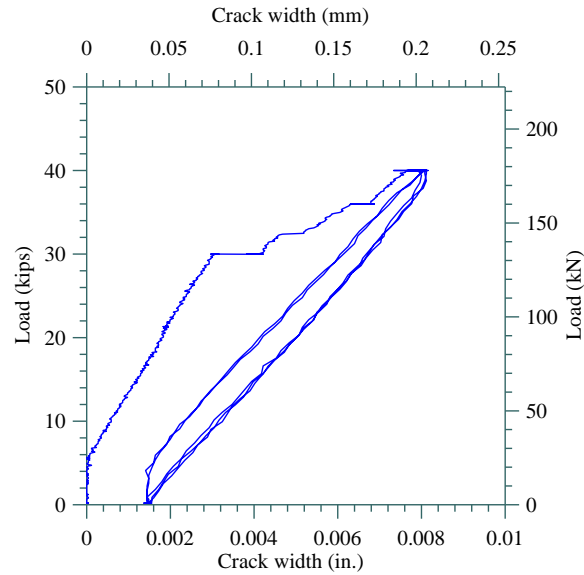
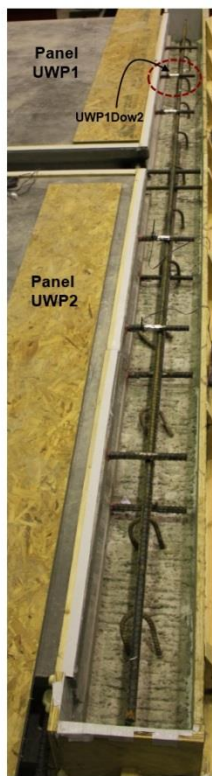
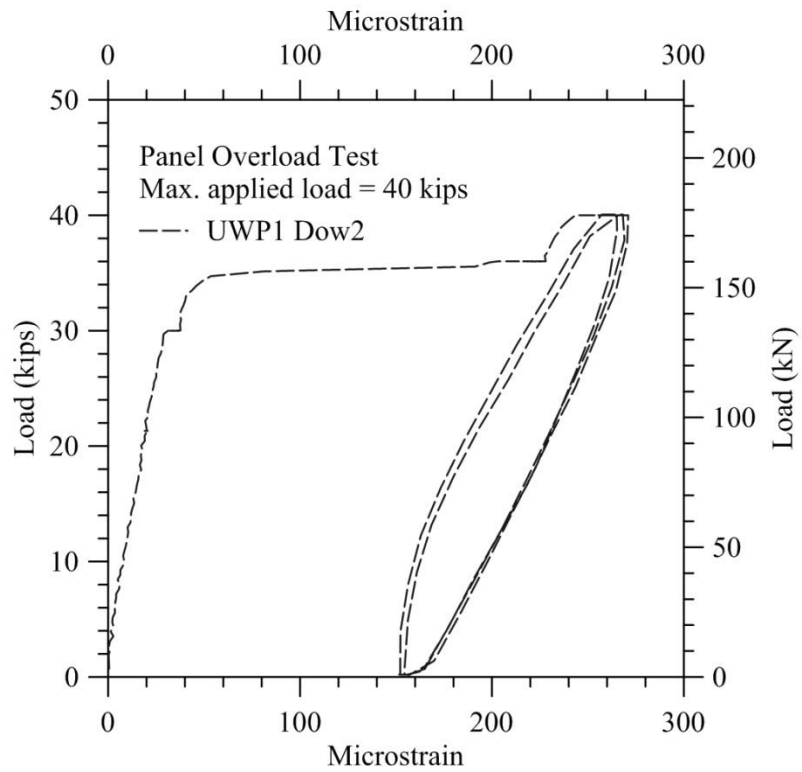


Figure 2.45. Measured crack width in transverse rib TR2 of UWP1 during the overload load test



a) Strain gauges on the dowel bars in Panel-to-girder joint



b) Strain in the dowel bar (shown in Figure a) in the panel-to-girder joint

Figure 2.46. Strain variations in a dowel bar placed in the panel-to-girder joint during the panel overload load test

2.5.11 Test 7—Panel Ultimate Load Test

The ultimate load test was carried out to investigate the adequacy of the precast deck system and its connections under ultimate load conditions. The ultimate load referred to in this study was arrived at based on the recommendations from the Iowa DOT personnel. A total load of 160 kips, equivalent to 10 times the AASHTO truck service load, was applied at the center of panel UWP1. The load-deflection curve established at the center of this panel during testing is shown in Figure 2.47.

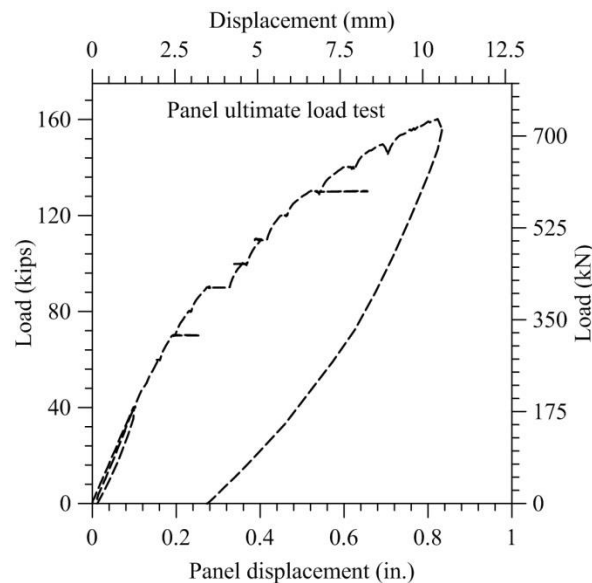
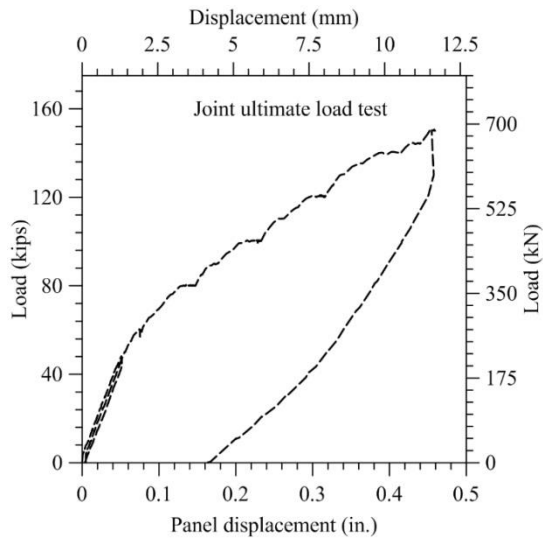


Figure 2.47. Measured force-displacement response of waffle deck system

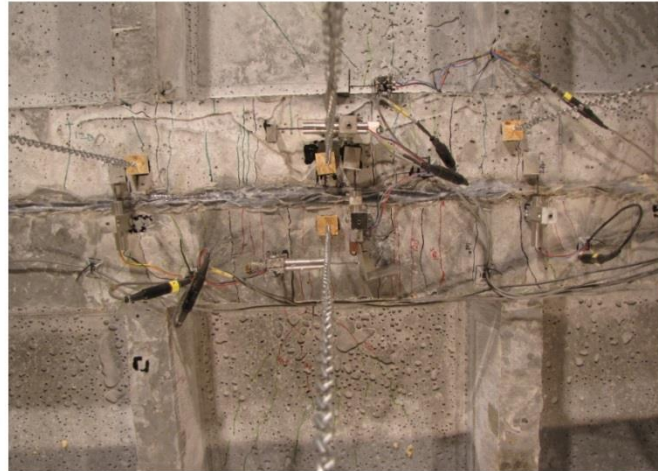
The panel exhibited a linear force-displacement behavior response up to about 80 kips. A maximum deflection of 0.82 inch was measured at the center of panel UWP1 (center of transverse rib TR2) as the load was increased to 160 kips. The peak strain measured in the bottom reinforcement of transverse rib TR2 at the maximum load was around $1,600 \mu\epsilon$, which is about 76% of the yield strain of the reinforcement. A significant amount of cracking was observed on both the transverse ribs (TR1, TR2, and TR3) and longitudinal ribs (LR1 and LR2) of panel UWP1. The maximum crack width measured along the transverse rib TR2 in UWP1 was 0.08 inch. When the load was removed, the deck panel had a residual displacement of 0.28 inch.

2.5.12 Test 8—Joint Ultimate Load Test

A total load of 160 kips, equivalent to 10 times the AASHTO truck service load, was applied at the center of the transverse joint. The load-deflection curve established at the center of the panel-to-panel joint is shown in Figure 2.48a. The peak strain measured in the bottom reinforcement of transverse rib TR2 was around $1,475 \mu\epsilon$, which is about 70% of the yield strain of the reinforcement. At the end of the test, numerous cracks were formed in transverse ribs of the joint (see Figure 2.48b). The maximum load applied was controlled by the shear cracking initiation in the prestressed girders.



a) Force-displacement response



b) Cracks in the transverse joint at 150 kip load

Figure 2.48. Measured force-displacement response and cracking at the center of the panel-to-panel joint under ultimate loads

2.5.13 Test 9—Punching Shear Failure Test

In this test, a wheel load was applied at the center of the waffle deck cell bounded by transverse and longitudinal ribs TR2, TR3, LR1, and LR2. Load was applied at increments of 5 kips on the waffle deck panel, using a 200-kip actuator. The 10-inch by 20-inch plate at the loading end of the actuator was replaced with a 6-inch by 8-inch steel plate to cause the punching shear failure in the panel between the ribs. A possible punching shear failure with a 10-inch by 20-inch plate was not expected to develop within the capacity of the system. As the loading increased, numerous radial cracks on the bottom surface of the panel between the ribs, along with flexural cracks in both transverse and longitudinal ribs, were formed. The measured load-displacement response at the center of the cell is shown in Figure 2.49a. The crack pattern on the bottom surface of the waffle deck was as expected for a typical punching shear failure mode, and it is shown in Figure 2.49b. The waffle deck failed suddenly at a maximum load of 154.6 kips, leaving behind a well-defined 6-inch by 8-inch hole (i.e., the same size as the steel plate placed at the top of the deck) at the center of the cell. The punching shear failure surface had approximately a 45-degree slope down the depth of the panel, as shown in Figure 2.49c. The measured average punching shear strength was around 1.068 ksi, which is equivalent to $6.62\sqrt{f'_c}$ (psi). This punching shear failure capacity is nearly 2.3 times the estimated value using the American Concrete Institute (ACI) equation recommended by Harris and Wollmann (2005).

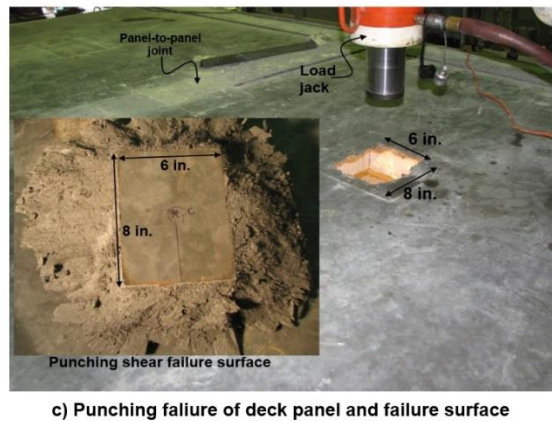
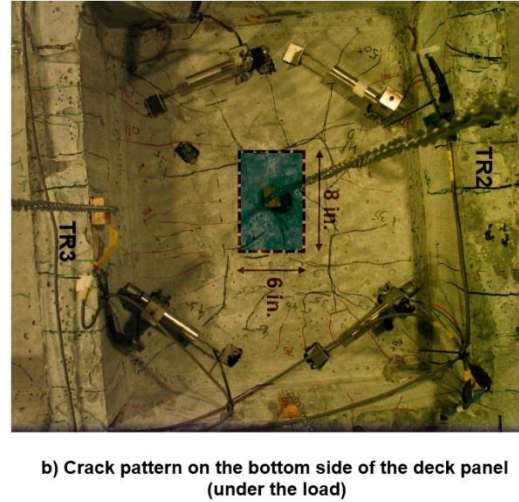
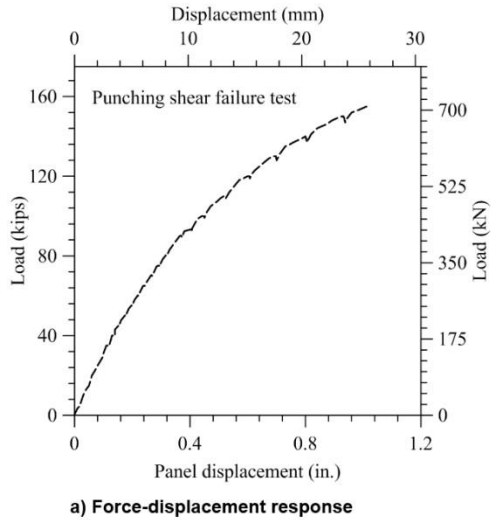


Figure 2.49. Measured load-displacement behavior and failure surface during punching shear failure test of the waffle deck system

2.6 Finite Element Modeling

Nonlinear finite element analysis (FEA) was carried out to model the system using ABAQUS software, Version 6.10. In this paper, selected results of the FEA are presented to support the experimental results and extent of damage. The exact geometric and reinforcement details, as well as the nonlinear material properties for UHPC and mild steel reinforcement of the system components, were employed in the FEA. The finite element model (FEM) was constructed using 3-D deformable elements. Meshing of the waffle deck panel and the prestressed concrete girders was completed using linear 3-D stress elements (i.e., C3D8R in ABAQUS), with 8 nodes and 1 integration point per element. A mesh size between 1 and 2 inches was chosen for the deck panels to provide more realistic stress and strain predictions in the critical regions. The panels were appropriately partitioned to allow structured meshing to be used, resulting in rectangular dominated elements. The mild steel reinforcement was modeled as wire beam elements with an appropriate cross-sectional area, with perfect bond between the steel reinforcement and concrete. The longitudinal and shear pocket connections between the UHPC waffle deck panels and the

girders were modeled using kinematic constraints. The meshed assembly of the test specimen FEM is shown in Figure 2.50a.

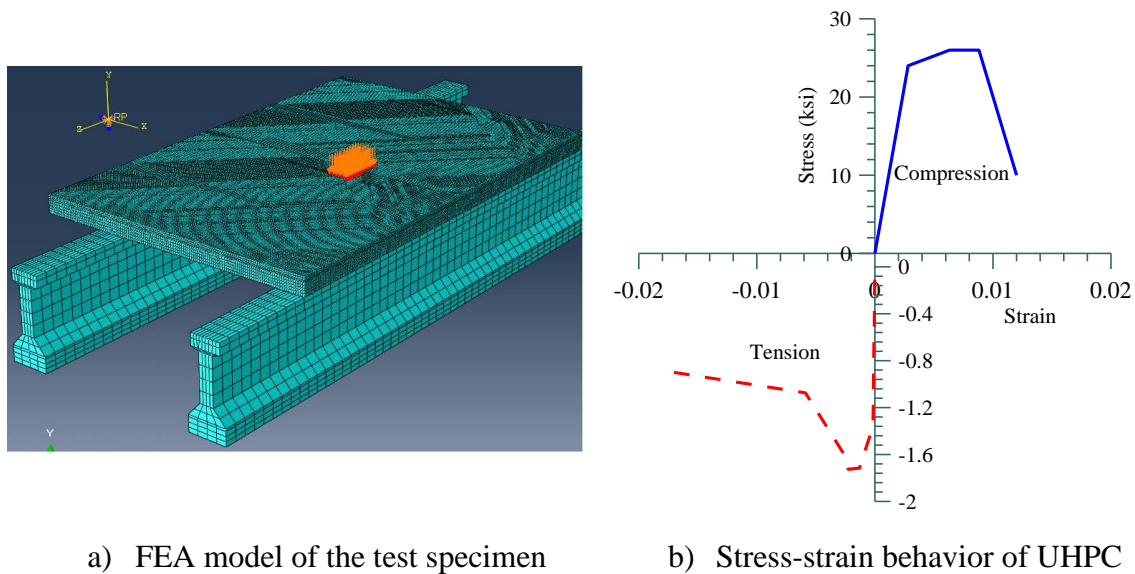


Figure 2.50. Test specimen discretization and material behavior of UHPC used in FEA software (ABAQUS)

The UHPC in the deck panels and joints was defined using the “concrete damaged plasticity” model available in FEA software (ABAQUS). The stress-strain definition for UHPC was derived for an assumed 26-ksi compressive strength for deck panels and 18.5 ksi for the connection regions. The tensile stress-strain behavior of the UHPC was adopted from results of a direct tension test on dog bone-shaped UHPC coupons. A steel material model was defined to simulate the mild steel reinforcement properties, with an idealized bilinear stress-strain material model used, based on an elastic modulus of 29,000 ksi, a yield stress of 60 ksi, an ultimate stress of 90 ksi, and an ultimate strain of 0.12. The UHPC stress-strain definition input into the FEM is shown in Figure 2.50b. The load was applied as a pressure load on the UHPC panel. The static-risks solver in ABAQUS was used for the analysis. Comparisons of the force-displacement responses from the FEM, with the measured response for service and overload cases, are presented in Figure 2.51. From this figure, it is evident that the FEM was able to accurately capture the force-displacement response at the transverse joint. The FEM underestimated the load-displacement response at the center of the panel, however, by 30% in the overload case.

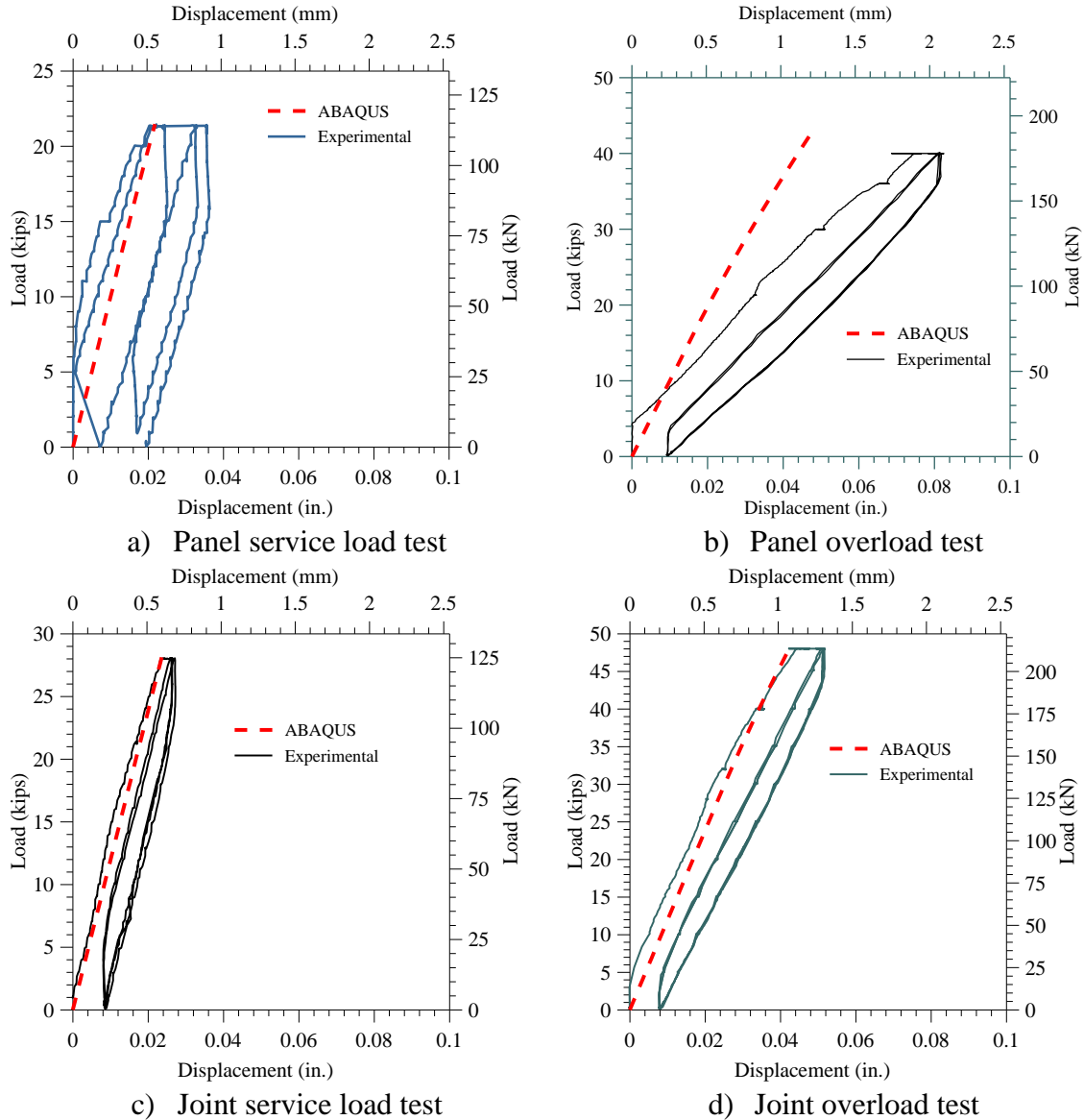


Figure 2.51. Comparison of experimental and ABAQUS force-displacement responses

2.7 Summary of Test Observations

Nine tests were conducted on a UHPC waffle deck panel system consisting of two panels at Iowa State University. The key results obtained from the different tests, indicating that the overall performance of the system was satisfactory under the service, fatigue, overload, and ultimate load conditions, are summarized below.

Panel Service Test (Test 1)

- Load applied: 16 kips x 1.33 (33% is the IM factor) = 21.3 kips
- Maximum measured panel displacement: 0.03 inch (<0.11 inch of allowable deck displacement at the service load specified by AASHTO, Section 9.5.2)
- Maximum measured strain in panel bottom reinforcement: 375×10^{-6}
- Maximum measured strain in joint bottom transverse reinforcement: 40×10^{-6}
- Measured crack width in the transverse rib: <0.002 inch (≤ 0.017 inch, the allowable crack width by AASHTO [2007]; ≤ 0.0118 inch of crack width expected for the fiber pullout [AFGC 2002])
- No cracks developed in the joint region

Joint Service Test (Test 2)

- Load applied: 16 kips x 1.75 (75% IM factor) = 28 kips
- Maximum measured panel displacement: 0.022 inch (<0.11 inch, allowable deck displacement at service load by AASHTO, Section 9.5.2)
- Maximum measured strain in panel bottom reinforcement: 160×10^{-6}
- Maximum measured strain in joint bottom transverse reinforcement: 175×10^{-6}
- Measured crack width in the transverse ribs forming the joint: <0.002 inch (≤ 0.017 inch, the allowable crack width by AASHTO [2007]; ≤ 0.0118 inch of crack width expected for the fiber pullout [AFGC 2002])

Joint Fatigue Test (Test 3)

- Load applied: 16 kips x 1.75 (75% IM factor) = 28 kips
- Number of load cycles: 1,000,000 cycles at 2 Hz frequency
- Maximum measured panel displacement: 0.024 inch (<0.11 inch, allowable deck displacement at service load by AASHTO, Section 9.5.2)
- Maximum measured strain in panel bottom reinforcement: “not measured”
- Maximum measured strain in joint bottom transverse reinforcement: 150×10^{-6}
- Measured crack width in the transverse ribs forming the joint: 0.0017 inch (≤ 0.017 inch, the allowable crack width by AASHTO [2007]; ≤ 0.0118 inch of crack width expected for the fiber pullout [AFGC 2002])
- No fatigue damage occurred to the joint or the panels

Joint Overload Test (Test 4)

- Load applied: 3.0 x 16 kips = 48 kips
- Maximum measured panel displacement: 0.052 inch (<0.11 inch, allowable deck displacement at service load by AASHTO, Section 9.5.2)
- Maximum measured strain in panel bottom reinforcement: 360×10^{-6}
- Maximum measured strain in joint bottom transverse reinforcement: 325×10^{-6}
- Crack width in the transverse ribs forming the joint: 0.003 inch (≤ 0.017 inch, the allowable crack width by AASHTO [2007]; ≤ 0.0118 inch of crack width expected for the fiber pullout [AFGC 2002])
- Multiple cracks were observed in the transverse and longitudinal ribs adjacent the joint

Panel Fatigue Test (Test 5)

- Load applied: 16 kips x 1.33 (33% IM factor) = 21.3 kips
- Number of load cycles: 1,000,000 cycles at 2 Hz frequency
- Maximum measured panel displacement: 0.039 inch (<0.11 inch, allowable deck displacement at service load by AASHTO, Section 9.5.2)
- Maximum measured strain in panel bottom reinforcement: 450×10^{-6}
- Maximum measured strain in joint bottom transverse reinforcement: 150×10^{-6}
- Measured crack width in the transverse ribs of the panel: <0.0023 inch (≤ 0.017 inch, the allowable crack width by AASHTO [2007]; ≤ 0.0118 inch of crack width expected for the fiber pullout [AFGC 2002])
- No fatigue loading damage observed to the panel and joint

Panel Overload Test (Test 6)

- Load applied: 2.5×16 kips = 40 kips
- Maximum measured panel displacement: 0.08 inch (<0.11 inch, allowable deck displacement at service load by AASHTO, Section 9.5.2)
- Maximum measured strain in panel bottom reinforcement: 880×10^{-6}
- Maximum measured strain in joint bottom transverse reinforcement: 100×10^{-6}
- Crack width in the transverse ribs forming the joint: 0.008 inch (≤ 0.017 inch, the allowable crack width by AASHTO [2007]; ≤ 0.0118 inch of crack width expected for the fiber pullout [AFGC 2002])
- Multiple cracks in the transverse and longitudinal ribs of the panel

Panel Ultimate Load Test (Test 7)

- Load applied: 10×16 kips = 160 kips
- Maximum measured panel displacement: 0.82 inch
- Maximum measured strain in panel bottom reinforcement: $1,600 \times 10^{-6}$
- A large number of cracks in the transverse and longitudinal ribs of the panel

Joint Ultimate Load Test (Test 8)

- Load applied: 10×16 kips = 160 kips
- Maximum measured panel displacement: 0.46 inch
- Maximum measured strain in panel bottom reinforcement: $1,475 \times 10^{-6}$
- A large number of cracks in the transverse and longitudinal ribs of the panel

Panel Punching Shear Failure Test (Test 9)

- Load applied: 155 kips
- Maximum measured panel displacement: 1 inch
- Measured average punching shear strength: 1.068 ksi ($= 6.62\sqrt{f'_c}$ [psi])
- A large number of cracks in the transverse and longitudinal ribs of the panel

2.8 Characterization of Deck Riding Surface Texture

The need for overlay on the UHPC precast deck panels was eliminated completely by providing an acceptable riding surface and grinding off any excess in situ UHPC poured in the joint region to make a smooth transition between the panels and joints. The suitability of different riding surfaces was investigated as part of this study. The rideability and surface characterizations of six different waffle deck surface finishes were investigated by measuring the skid resistance values (SRVs) and surface texture depth. Five of the textured surfaces were characterized using the standard sand patch test. The details of the textures investigated are presented in Table 2.5 along with average values of measured sand patch diameter and texture classification.

Table 2.5. Details of the Textures and Average Sand Patch Diameters

Serial No	Texture (brand)	Sand Patch Diameter (mm)	Average Sand Patch diameter (d) (mm)	Texture Depth (mm) = $\frac{4V}{\pi d^2} \times 10^3$ *
1	2/61 Thames (Rekli)	240, 220, 215, 225	225	1.26
2	Broom finish (Architectural Polymers)	255, 235, 245, 230	241.25	1.09
3	2/102 Parana (Rekli)	200, 195, 200, 205	200	1.59
4	Heavy broom finish (Architectural Polymers)	160, 160, 155, 150	156.25	2.61
5	Anti-skid (Fitzgerald Form liners)	220, 225, 230, 230	226.25	1.24

*V = volume of sand used (= 50 cm³); 1 inch = 25.4 mm

Skid resistance values for different surface finishes were measured with the British Pendulum tester using the ASTM E-303 standard method for measuring the surface friction properties. The skid-resistant test was performed on all six different texture surfaces with four tests per sample. In all tests, a minimum 12-inch by 12 inch sample size was used. The details of the test setup are shown in Figure 2.52. The details of the different textures tested and their mean SRV values are provided in Table 2.6. Based on the suggested minimum values of skid resistance by the Transport and Road Research Laboratory (TRRL 1969), all the tested texture surfaces surpass the minimum required SRV value of 65, satisfying the rideability criteria except for carpet finish in direction 1. So, if the carpet finish is used for riding surface, appropriate care should be taken to orient the texture.

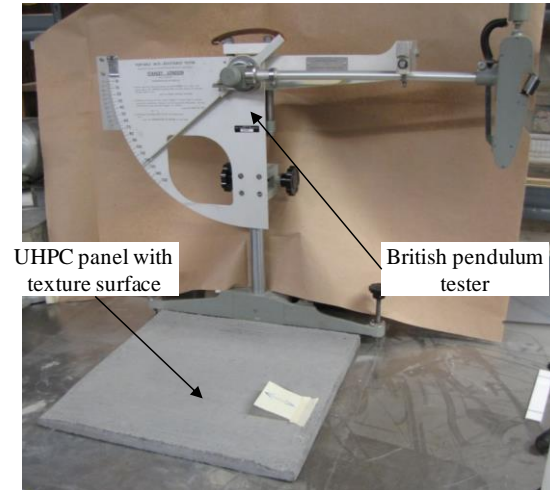

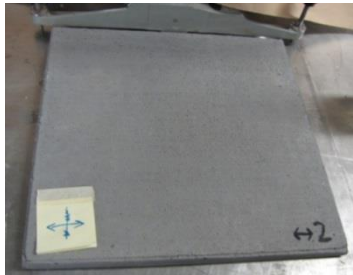





Figure 2.52. Test setup for characterization of skid resistance of textures using British Pendulum tester

Table 2.6. Measured SRVs for Different Textured Surfaces Using British Pendulum Tester

S. No	Texture/(Manufacturer's Brand)	Texture	SRVs (BPN*)		Average SRV
1	2/61 Thames / (Reckli)		87,88,88,88		87.75
2	Broom finish/(Architectural Polymers)		72,70,70,70		70.5
3	2/102 Parana/(Reckli)		Direction-1	96,96,96,96	96

S. No	Texture/(Manufacturer's Brand)	Texture	SRVs (BPN*)		Average SRV
			Direction-2	90,90,90,90	90
4	Heavy broom finish/(Architectural Polymers)		Direction-1	72,75,75,75	74.25
			Direction-2	80,81,80,81	80.5
5	Anti Skid/(Fitzgerald Form liners)		80,80,80,81		80.25
6	Carpet/(Fitzgerald Form liners)		Direction-1	62,65,65,65	64.25
			Direction-2	76,75,78,80	76.625

*BPN = British Pendulum number

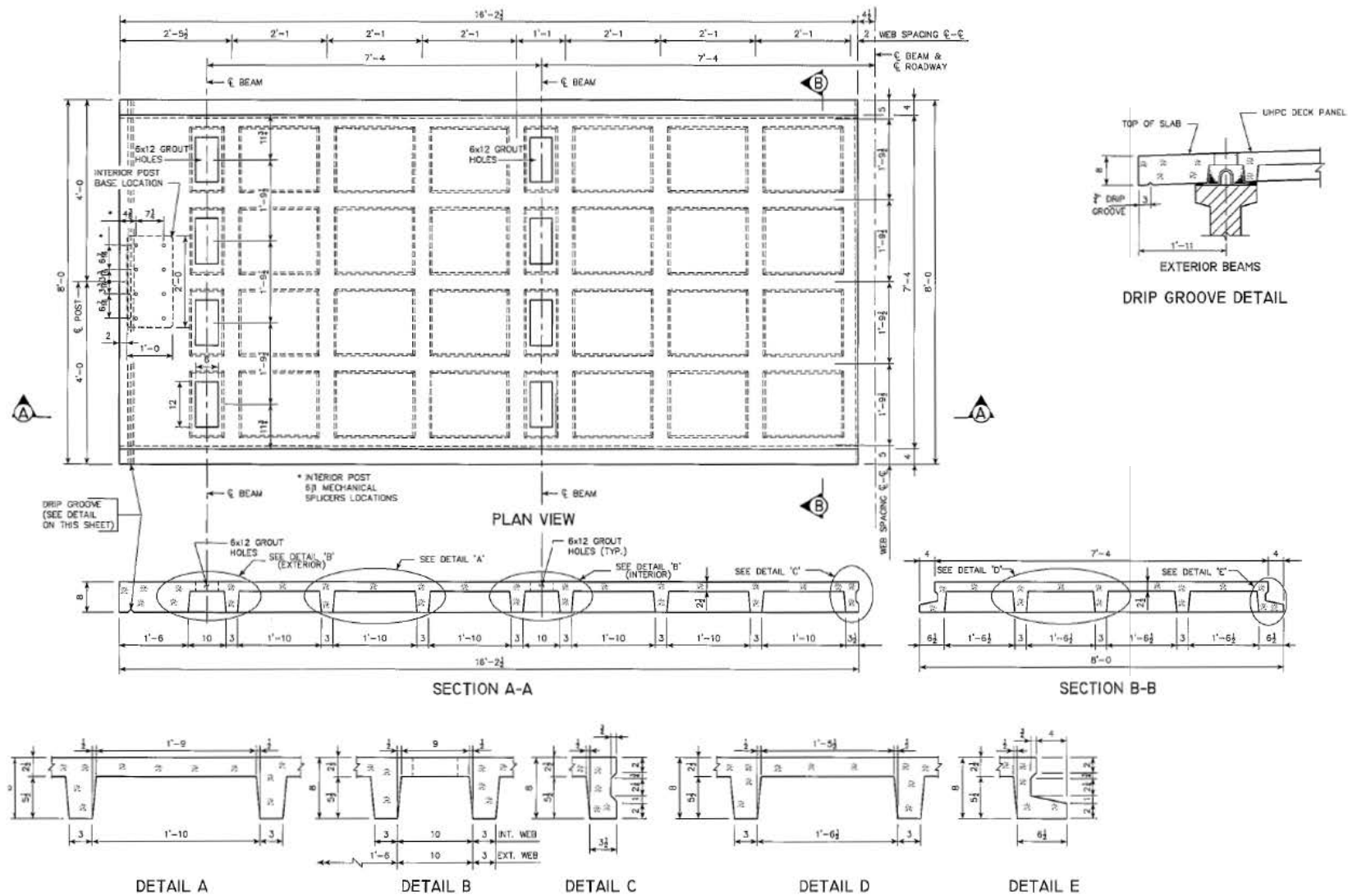
3. CONSTRUCTION

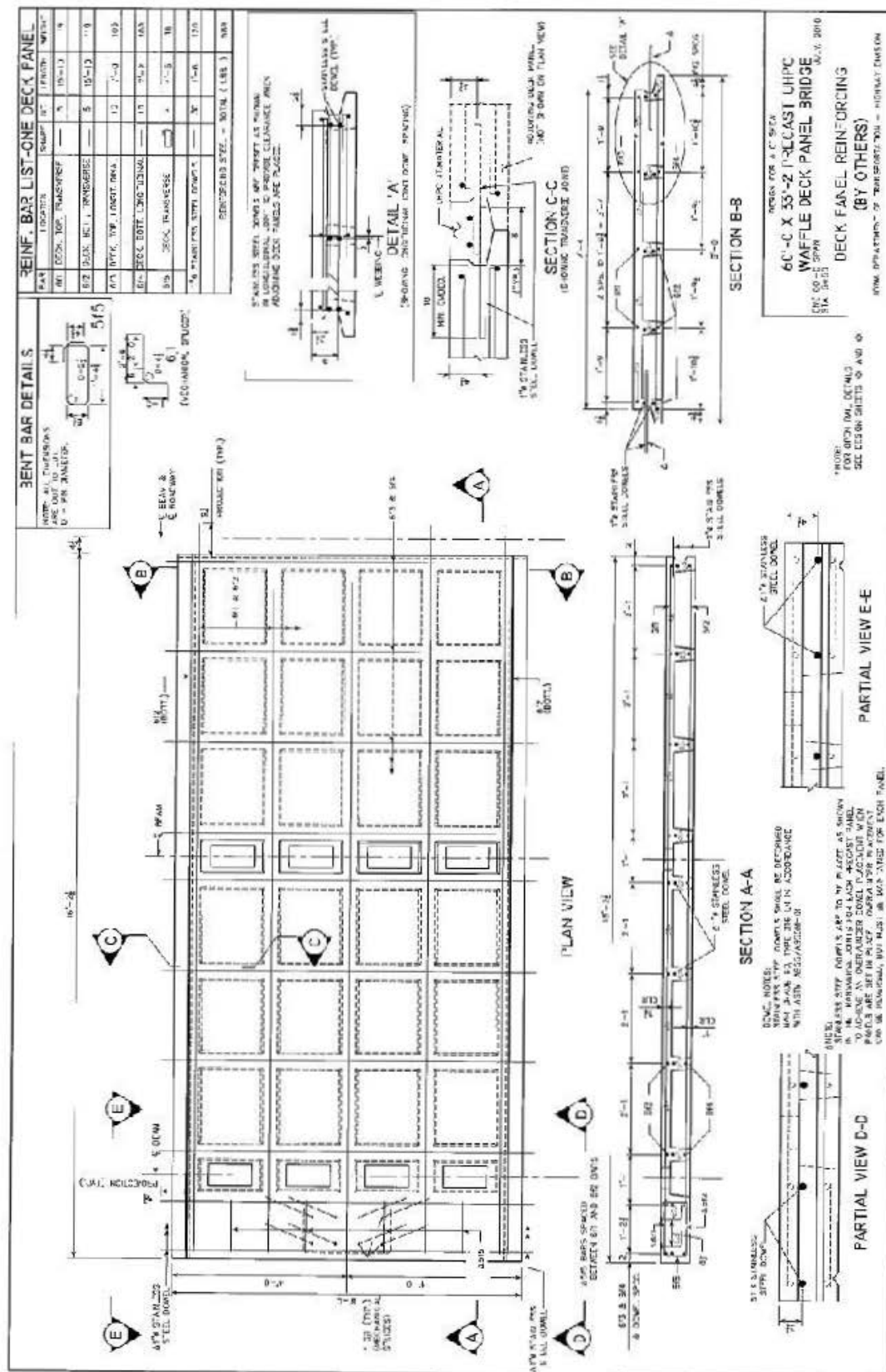
3.1 Introduction

Following the successful laboratory testing to characterize the structural performance of the UHPC waffle deck panel system and its connections, the experimental results and observations were used to finalize the design of a demonstration bridge on Dahlonge Road in Wapello County, Iowa. This bridge replacement project was used to demonstrate the deployment of the UHPC waffle slab technology from fabrication through construction and to evaluate the performance of the UHPC waffle slab deck under true service conditions. This chapter presents the details of the prefabrication of the deck panels and construction of the bridge.

3.2 Bridge Deck Panel Details and Prefabrication

The UHPC bridge deck panel was designed for the 33-foot wide and 60-foot long Dahlonge Road Bridge in Wapello County, Iowa. It consisted of five standard Iowa “B” girders placed at a center-to-center distance of 7 feet 4 inches. To meet the bridge geometry and have integer number of deck panels, the deck panels were chosen to be 16 feet 2.5 inches long and 8 feet wide. This resulted in a total of 14 panels for the entire bridge. Similar to the experimental waffle deck, the final bridge deck panel consisted of a 2.5-inch thick uniform slab and 5.5-inch deep transverse and longitudinal ribs. The transverse and longitudinal ribs were tapered with 3 inches at the bottom to 4 inches at the top. The chosen dimensions of the panel resulted in a transverse and longitudinal rib spacing of 21.5 inches and 25 inches, respectively. Figure 3.1 shows the plan view of a typical waffle deck panel designed for the demonstration bridge. The transverse reinforcement in the deck panel consisted of Grade 60, No. 6 ($d_b = 0.75$ inch, where d_b is diameter of the bar) mild steel reinforcement located at 1.25 inches from the bottom surface and at 1.625 inches from the top surface of the panel, respectively. In the longitudinal direction, the panels were detailed with Grade 60, No. 6 mild steel reinforcement at 2.1250 inches from the bottom surface and at 2.3750 inches from the top surface. All the reinforcement was provided along panel ribs in both directions. Figure 3.2 shows the cross section and reinforcement details of a typical waffle deck panel designed for the prototype bridge. It should be noted that the preliminary design of the deck panel included the Grade 60, No. 7 ($d_b = 0.875$ inch, where d_b is diameter of the bar) mild steel reinforcement as longitudinal and transverse deck bottom reinforcement, while the No. 6 reinforcement was used for the top deck reinforcement. The minimal difference in the bar sizes, however, caused confusion in distinguishing between No. 6 and No. 7 bars during the rebar placement for the test panel construction. Also, the test panel results have shown that the strains in the bottom reinforcement were well below the yield strains under design loads. Hence, by taking these observations into consideration, the Iowa DOT decided to replace the No. 7 bar with a No. 6 bar as longitudinal and transverse bottom deck reinforcement in the final design of the deck panel.





Similar to the test panels, the UHPC waffle deck panels were prefabricated at the Coreslab Structure's precast plant in Omaha, Nebraska. All the deck panels were cast in an upside-down position using a displacement casting method and a specially designed formwork made of steel sections (see Figure 3.3) with adjustable rib spacing. This formwork is different from the formwork used typically for full-depth solid precast deck panels made of normal concrete and helps in maintaining the desired tight tolerances due to thin UHPC sections in the waffle deck panels. Based on the texture characterization study, Parana 2/102 architectural liner was chosen and placed in the bottom form to create an acceptable riding surface texture for the deck panels. Then, longitudinal and transverse reinforcement was placed in the bottom form, before it was filled with UHPC (see Figure 3.4a–c). The high bond strength and excellent durability properties of UHPC eliminate the need for using standard hooks and epoxy-coated special reinforcement. As per the Iowa DOT design, however, the dowel bars were made of stainless steel to provide additional safety against the possible corrosion.

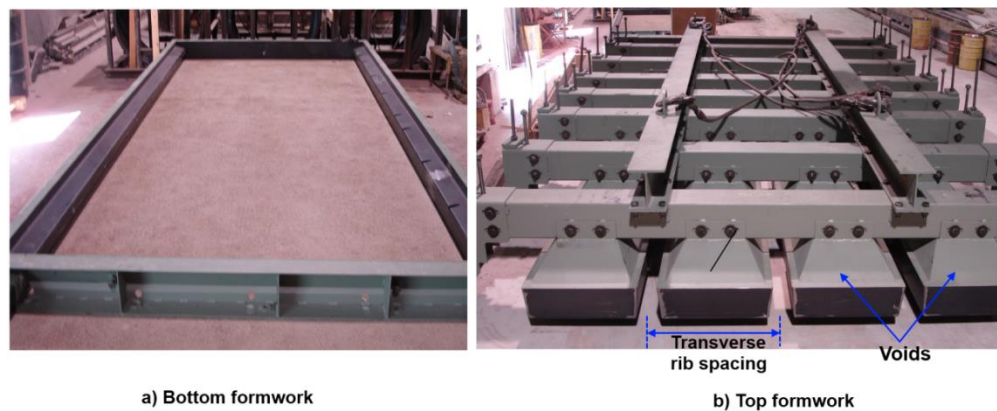


Figure 3.3. Formwork used for waffle deck panel construction at the precast plant

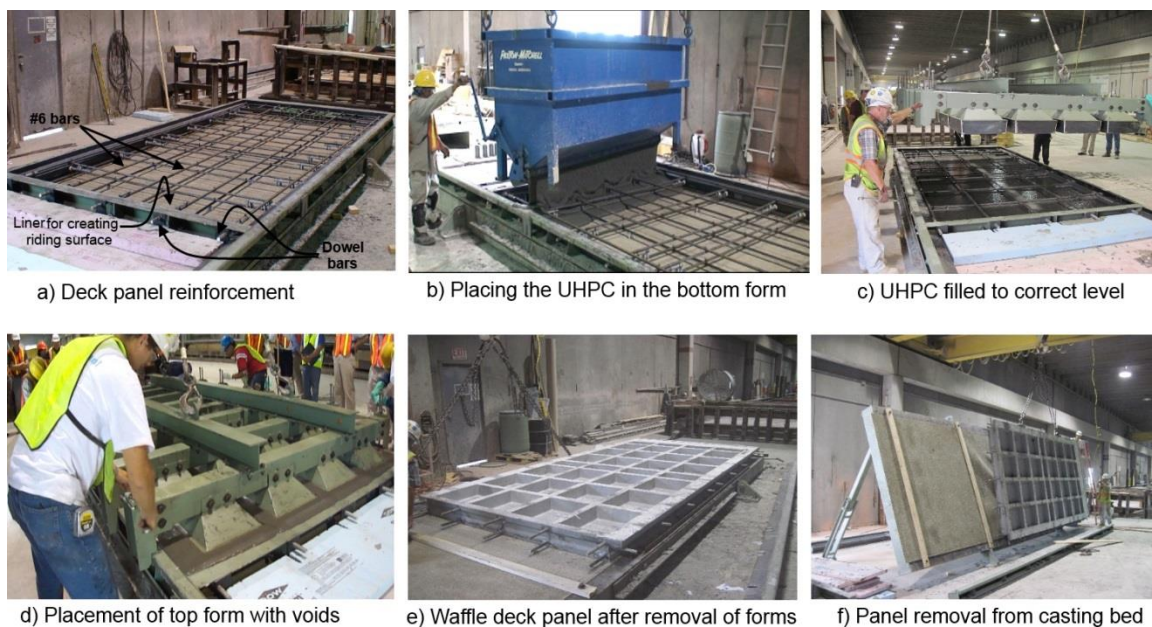


Figure 3.4. Construction of the UHPC waffle deck panel for the demonstration bridge

The bottom form was first filled up to approximately 4.5 inches with UHPC (for an 8-inch deep waffle panel), and the top formwork was then pushed into the UHPC causing it to displace and form the ribs. The voids were then removed once the UHPC initial set was achieved, which is typically after 12 to 14 hours from pouring (see Figure 3.4e). This allowed shrinkage to take place without any restraint and prevented cracking of deck panels. The panels were removed from the casting bed after approximately 40 hours from pouring, when the UHPC in the panels reached a minimum compressive strength of 14 ksi (see Figure 3.4f). The panels were then moved to a curing area and subjected to a controlled steam cure at 195°F with 100% relative humidity for 2 days as recommended by the UHPC material manufacturer. This helps with the rapid strength gain of UHPC and reaching a minimum design compressive strength of 24 ksi at the end of the curing process. The average compressive strength of the waffle panels after the steam curing was found to be 33.7 ksi.

3.3 Field Installation

The existing bridge on the Dahlonga Road in Wapello County, Iowa, was removed during the week of August 15, 2011, and new substructure and abutments were completed by September 5, 2011. The precast beams were then placed in position, ready for the placement of the UHPC deck panels. After completion of abutments and seating of standard prestressed concrete girders, 14 UHPC waffle deck panels were placed on the girders using a crane (see Figure 3.5). This work was started during the week of September 12, 2011.



Figure 3.5. Placement of UHPC waffle deck panels on the prestressed girders

The half-width precast deck panels were set to grade, spanning between the concrete girders and leveled to the needed elevation by placing shims. At the panel bearings on the beams, an Evazote foam strip was installed to provide a good contact and water-tight seal between the precast panels and prestressed concrete girder (see Figure 3.6). Once all panels were installed and tested for moderate water tightness, quick-setting spray foam was used to patch any gaps and create the water-tight seal between panels and girders (see Figure 3.6).

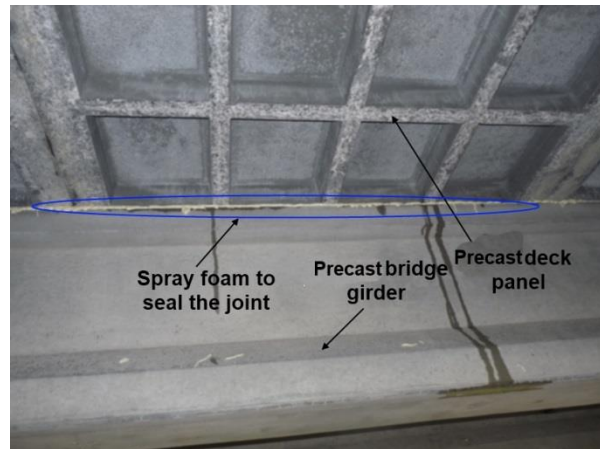
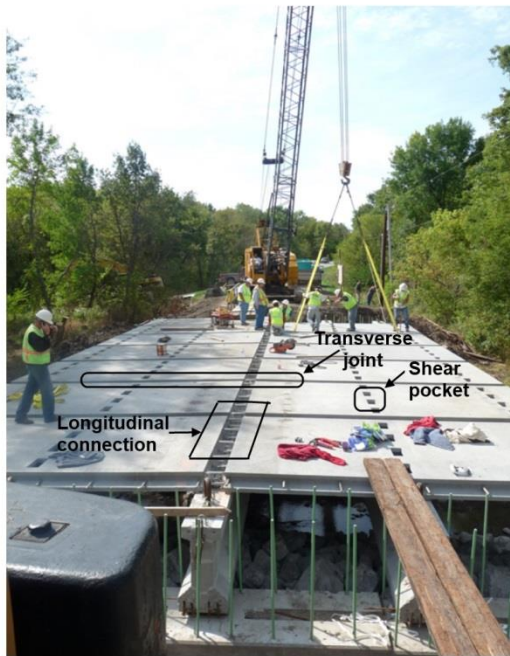


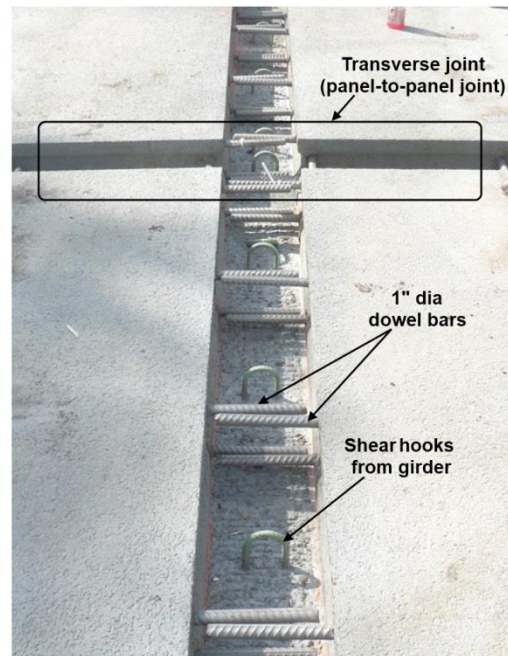
Figure 3.6. Water-tight seal at panel-to-girder connection after applying quick-setting spray

Prior to shipping to the site, the faces of the precast panels, which are part of the transverse and longitudinal joints, were sandblasted at the precast plant to create a roughened surface to enhance the bond between the precast panel and the joint fill, leading to water tightness of the transverse joint (panel-to-panel joint). In addition, the surface of each precast panel was dampened to saturate surface-dry prior to casting the joint fill. A close-up view of the transverse and longitudinal joints in the Wapello County bridge is shown in Figure 3.7.

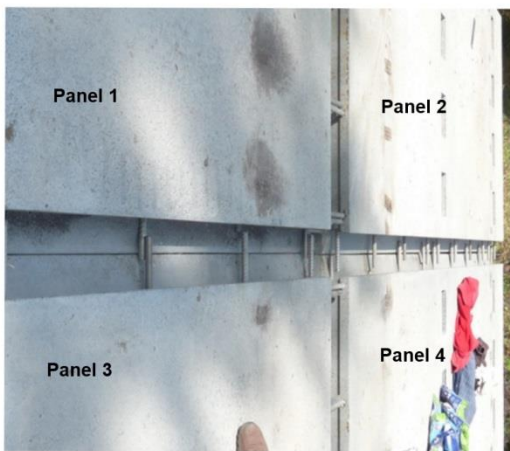
The field cast UHPC joints were poured on September 27 and 28, 2011. The in situ UHPC joint fill materials were batched using two IMER Mortarman 750 mixers (see Figure 3.8). These mixers were set up at the end of the bridge to provide a continuous supply of material for the joint-filling operation and provide direct access to the bridge deck. The UHPC joint material was transported to the joints by a wheelbarrow and then placed directly into the joints and shear pockets. The placement of UHPC began with the shear pocket connections (see Figure 3.9a). The transverse joints and longitudinal center joint were cast together. Placement of the UHPC for these joints began at the lowest (i.e., outer) edges of the transverse joints and proceeded to the center longitudinal joint at the crown. As the transverse joints were filled, plywood top forms were applied to allow hydrostatic head to fully fill the joints and ensure adequate curing (see Figure 3.10). The sequence was completed by filling the longitudinal center joint (see Figure 3.9c) and applying plywood top forms as shown in Figure 3.10. The top forms were used to prevent any moisture loss from the UHPC during curing. Following the field cure process, four days after pouring, the UHPC material in the joints was ground smooth in the areas of any high spots. The final surface of the bridge deck after grinding is shown in Figure 3.11. The bridge was opened to the traffic in November 2011.



a) Wapello County bridge with UHPC waffle deck panels



b) Close up of longitudinal joint at the center girder (panel-to-panel-to-girder connection)



c) Close up of transverse joint (panel-to-panel connection)



d) Shear pocket (panel-to-girder connection)

Figure 3.7. Transverse and longitudinal joints in the demonstration bridge in Wapello County



Figure 3.8. Batching of UHPC joint fill using IMER Mortarman 750 mixers at the bridge site



Figure 3.9. Filling of joints with in situ UHPC and completed joints



Figure 3.10. Finished transverse joints (panel-to-panel joint) covered with plywood

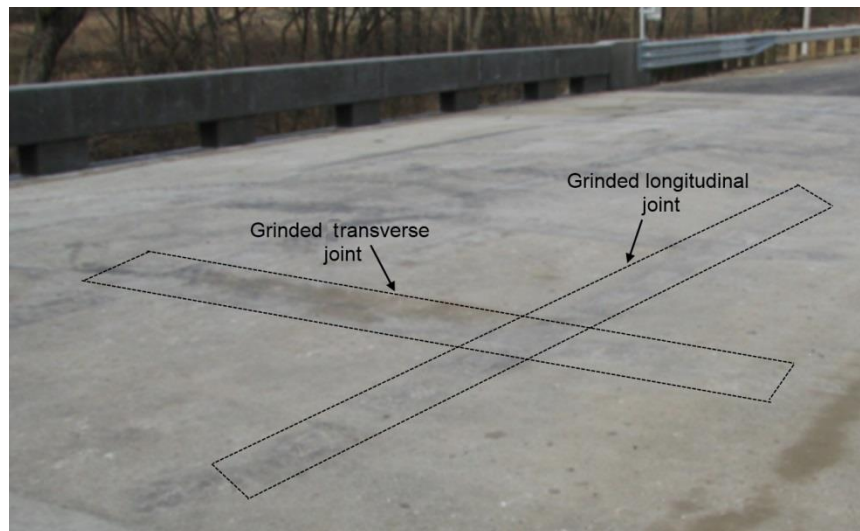


Figure 3.11. Close-up of the waffle panel deck after grinding along the joints

4. FIELD TESTING

4.1 Introduction

The Dahlonge Road Bridge over Little Cedar Creek in Wapello County, Iowa, was opened to traffic in November of 2011. The field testing of the bridge was performed in February of 2012 by the Iowa State University researchers. As part of the field testing, live load vertical deflections and strains at discrete, critical locations on the bridge superstructure were monitored as the bridge was subjected to static and dynamic truck loads. Figure 4.1 and Figure 4.2 show the locations of instrumented panels on the bridge plan and cross section, respectively.

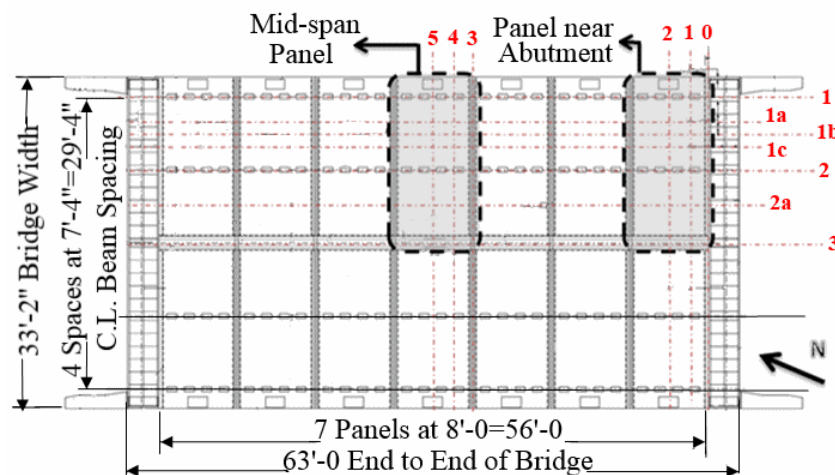


Figure 4.1. Dahlonge road bridge plan

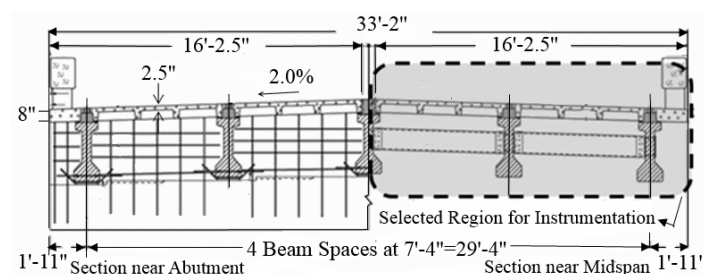


Figure 4.2. Dahlonge road bridge cross section

A 3-D finite element model, as detailed as the test unit model in Section 2.6, was developed for the bridge using ABAQUS software, Version 6-12, which was to help interpret the results of live load testing, including estimation of strains due to dead load, and live load distribution. During the field test, strains and deflections were measured as a function of time using surface-mounted BDI strain gages and string potentiometers, respectively. It is important to note that the data recorded during the field test captured only the incremental strain and deflection due to live loads. Therefore, to estimate the total strains in the deck panels, the measured live load strains were superimposed with the dead load strains computed with the FEM. Throughout this report,

negative values represent compressive strains and downward deflections, whereas positive values represent tensile strains and upward deflections.

4.2 Instrumentation and Test Method

Taking advantage of the bridge's symmetry about its longitudinal and transverse axes, two UHPC waffle deck panels along the length of the bridge were selected for instrumentation. One of these panels was located near the mid-span and the other was located adjacent to the south abutment as shown in Figure 4.1. Surface-mounted strain gages were used on each panel and their adjacent UHPC deck joints to quantify deformations and identify the likelihood of cracking under service loads. The locations of these strain gages were carefully selected to coincide with critical locations on the panels and deck joints where stress and strain would likely be extreme.

Fifteen strain gages were placed on the mid-span panel and surrounding UHPC joints. The locations of these gages and their orientations are shown in plan and cross section in Figure 4.3. Eight of these strain gages were located on the bottom of the deck at regions of maximum positive moment, and seven were located on the top of the deck at regions of maximum negative moment. Of these 15 gages, seven are located either on the UHPC infill deck joint or spanning the interface between the joint and the UHPC precast panel to identify distress in the joint regions or opening of the interface between joint and panel.

Similar to the mid-span panel, 10 gages were placed on the panel adjacent to the abutment and surrounding UHPC joints. The locations of these gages and their orientations are shown in plan and cross-section view in Figure 4.4. Six strain gages were located on the bottom of the deck at regions of maximum positive moment, and four were located on the top of the deck in regions of maximum negative moment. Of these 10 gages, 2 are located to span the interface between the UHPC infill joint and UHPC precast panel to identify the opening at this interface.

In addition to the strain gages on the deck panels, 13 surface-mounted strain gages and five string potentiometers were attached to the girders to characterize the global bridge behavior, measure mid-span deflections, and quantify the lateral live load distribution factors. Using two additional string potentiometers, deflections were also measured at the mid-spans of the deck panel located near the center of the bridge. Top and bottom girder strains were monitored for three of the girders at mid-span and at a section 2 feet from the south abutment.

Each transducer was assigned a name based on its location and orientation. The location was defined by whether it was located near the mid-span or near the abutment, whether it was attached to the girder or deck, and whether it was located on top or bottom of the deck. The orientation of each transducer was specified relative to the longitudinal or transverse axes of the bridge. The nomenclature for transducers is further explained in Table 4.1. Strain gage and string potentiometer locations are illustrated in Figure 4.3 and Figure 4.4 to show exactly where they were placed for the load testing. A photograph of several of the surface-mounted strain gages on the bottom of the panel adjacent to the abutment is shown in Figure 4.5.

Table 4.1. Transducer Nomenclature

Convention		
First Character	Span Location	
	M	Mid-Span
	A	Near Abutment
Second Character	Deck/Girder	
	G	Girder
	D	Deck
Third Character	Direction	
	L	Longitudinal
	T	Transverse
Fourth Character	Top/Bottom	
	T	Top
	B	Bottom
Fifth Character	Longitudinal Grid Number*	
Sixth Character	Transverse Grid Number*	

* See bridge plan in Figure 4.1 for grid locations.

Example: MDTT13 corresponds to mid-span deck panel, oriented transversely on top along longitudinal grid line 1 and transverse grid line 3

Live load was applied by driving a loaded dump truck across the bridge along predetermined paths. The total weight of the truck was 60,200 pounds with a front axle weight of 18,150 pounds and two rear axles weighing roughly 21,000 pounds each. The truck configuration with axle loads is shown in Figure 4.6.

Seven load paths were used for this test, as shown in Figure 4.6. Load paths 1 and 7 were 2 feet from each barrier rail for the outer edge of the truck. Load paths 2 and 6 were along the centerline of each respective traffic lane. Load paths 4 and 5 were 2 feet to either side of the bridge centerline for the outer edge of the truck, and load path 3 straddled the centerline of the bridge. To guide the truck driver, lines were painted on the bridge deck along the load paths as shown in Figure 4.6.

For static tests, the truck was driven across the bridge at a walking pace (speed < 5 miles per hour [mph]). Each load path was traversed twice to ensure repeatability of the measured bridge response. Additionally, the exact location of the truck front axle was recorded every 10.5 feet along the bridge when the truck travelled the bridge for each load path. For dynamic tests, the truck speed was increased to 30 mph to examine dynamic amplification effects.

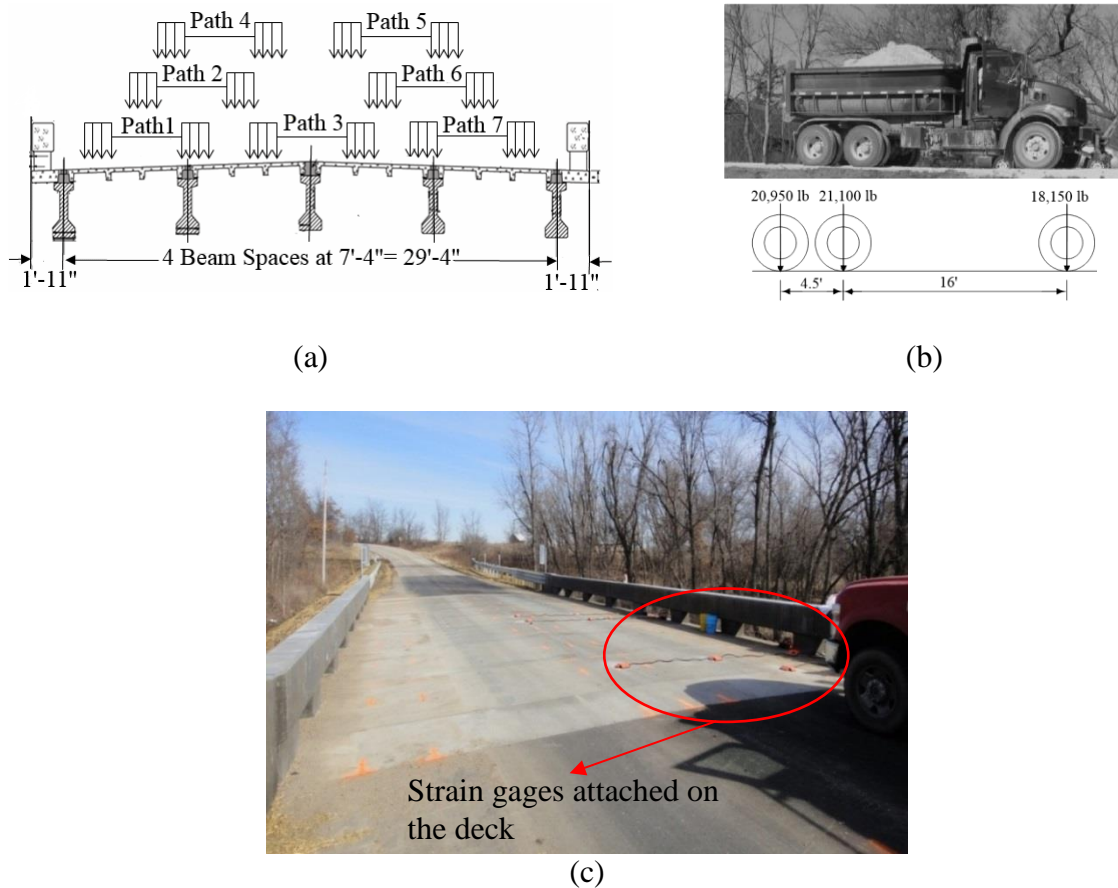


Figure 4.6. Loading: (a) Schematic layout of bridge loading paths; (b) Truck configuration and axle load; (c) Load paths marked on bridge deck

4.3 Results of Static Live Load Testing

The response of the bridge to a slowly moving truck load along the seven prescribed load paths is summarized, which includes maximum responses for the 14 truck passes executed (2 per load path to ensure repeatability). Because the load test captured only incremental live load deformations, the total strains presented were computed by superimposing the dead load strains estimated using the finite element model of the bridge with the measured live load strains from the load test. For the deck panels, the dead load strains typically comprised only a small portion of the total strains because the waffle slab panels are significantly lighter than a conventional cast-in-place concrete deck.

4.3.1 Maximum Strains of the Mid-Span Deck Panel

The maximum total strains observed for each load path at the mid-span panel are presented in Table 4.2 to Table 4.4. The maximum strains of the girders at mid-span are given in Table 4.5 to Table 4.6. It should be noted that the maximum strains for each load path occur at different

locations of the truck front axle along the bridge. All maximum strains for the UHPC waffle deck slab at the mid-span were less than the cracking strain for the UHPC ($\sim 250 \mu\epsilon$). This behavior implies that there was no cracking in this deck panel, and it was responding elastically to the applied truck load. Generally, the maximum transverse strains were higher than the maximum longitudinal strains for a given load path. The maximum transverse strain at the bottom of the panel occurred at gage MDTB2a4 with a value of 150.8 microstrain for load path 4 (see Table 4.2). The maximum longitudinal strain at the bottom of the panel occurred at gage MDLB1c5 with a value of 118.2 microstrain for load path 4 (see Table 4.4). Girder strains at mid-span were also small ($<106 \mu\epsilon$) and well within the elastic range. Note that the values tabulated in Table 4.3 confirm that gages MDTT35 and MDTT33 did not record significantly high tensile strains, which would have been due to opening of the interface between the precast panels and UHPC infill joints. In addition, the maximum registered transverse strains at the top of the panel were small ($<68 \mu\epsilon$) as shown in Table 4.3.

Table 4.2. Maximum Transverse Strains at the Bottom of Mid-Span Panel

	Load Path Number						
	1	2	3	4	5	6	7
Location	MDTB1b4	MDTB2a4	MDTB2a4	MDTB2a4	MDTB1b4	MDTB1b4	MDTB1b4
Live Load Strain ($\mu\epsilon$)	135.9	147.7	133.6	150.8	-10.2	-8.0	-7.2
Total Strain ($\mu\epsilon$)	137.8	149.6	138.7	156.9	-12.1	-9.9	-9.1

Table 4.3. Maximum Transverse Strains at the Top of Mid-Span Panel

	Load Path Number						
	1	2	3	4	5	6	7
Location	MDTT15	MDTT15	MDTT15	MDTT15	MDTT13	MDTT13	MDTT15
Live Load Strain ($\mu\epsilon$)	32.1	62.5	53.4	67.8	5.5	5.6	6.1
Total Strain ($\mu\epsilon$)	45.1	75.5	66.4	80.8	7.6	7.7	19.1

Table 4.4. Maximum Longitudinal Strains at the Bottom of Mid-Span Panel

	Load Path Number						
	1	2	3	4	5	6	7
Location	MDLB1c5	MDLB1c5	MDLB1c5	MDLB1c5	MDLB1c5	MDLB1c5	MDLB1c5
Live Load Strain ($\mu\epsilon$)	26.6	108.7	-5.4	118.2	-5.6	-3.4	-3.6
Total Strain ($\mu\epsilon$)	31.3	121.8	-18.5	131.3	7.5	-16.5	-16.7

Table 4.5. Maximum Girder Top Longitudinal Strain at Mid-Span

	Load Path Number						
	1	2	3	4	5	6	7
Location	MGLT25	MGLT25	MGLT25	MGLT25	MGLT35	MGLT35	MGLT35
Live Load Strain ($\mu\epsilon$)	-5.9	-6.6	-5.4	-6.1	-6.5	-6.0	-5.0
Total Strain ($\mu\epsilon$)	-23.9	24.6	-23.4	-24.1	-43.5	-43.0	-42.0

Table 4.6. Maximum Girder Bottom Longitudinal Strain at Mid-Span

	Load Path Number						
	1	2	3	4	5	6	7
Location	MGLB25	MGLB25	MGLB35	MGLB25	MGLB35	MGLB35	MGLB35
Live Load Strain ($\mu\epsilon$)	29.4	31.3	33.8	31.2	23.3	21.2	15.1
Total Strain ($\mu\epsilon$)	70.4	72.3	105.8	72.2	95.3	93.2	87.1

4.3.2 Maximum Strains of the Deck Panel Adjacent to Abutment

The maximum strains observed for each load path at the panel adjacent to the bridge abutment are presented in Table 4.7 to Table 4.10. The maximum strains of the girders near the abutment are given in Table 4.11 and Table 4.12. Unlike the mid-span panel, some hairline cracks were observed on the bottom of the ribs on the panel adjacent to the south abutment prior to loading. Consequently, relatively higher strains were observed at these locations (e.g., gages ADTB2a2 and ADLB1a2 in Table 4.7 and Table 4.9) during the live load test when compared to strains in the mid-span panel. These strains, however, are comparable to the expected cracking strain of UHPC ($\sim 250 \mu\epsilon$) and are smaller than the maximum strains observed in the laboratory panel tests as reported in Section 2.5. Because they are on the bottom of the deck and are not excessive in magnitude, small cracks at these locations are unlikely to pose a threat to the long-term performance of the panel. These relatively higher strains are examined and discussed more thoroughly later with the aid of the FEM in Section 4.4.

Table 4.7. Maximum Transverse Strains at the Bottom of the Panel near Abutment

	Load Path Number						
	1	2	3	4	5	6	7
Location	ADTB1b2	ADTB1b2	ADTB2a1	ADTB2a2	ADTB2a2	ADTB2a2	ADTB2a2
Live Load Strain ($\mu\epsilon$)	110.95	267.5	210.9	252.6	-10.3	-7.7	-3.2
Total Strain ($\mu\epsilon$)	115.4	276.2	219.6	261.3	-19.0	-16.4	-11.9

Table 4.8. Maximum Transverse Strains at the Top of the Panel near Abutment

	Load Path Number						
	1	2	3	4	5	6	7
Location	ADTT32	ADTT12	ADTT12	ADTT12	ADTT12	ADTT12	ADTT32
Live Load Strain ($\mu\epsilon$)	17.5	24.2	47.4	44.8	-5.3	-3.1	-2.1
Total Strain ($\mu\epsilon$)	18.2	25.5	48.7	46.1	-6.6	-4.4	-2.8

Table 4.9. Maximum Longitudinal Strains at the Bottom of the Panel near Abutment

	Load Path Number						
	1	2	3	4	5	6	7
Location	ADLB1a2	ADLB1a2	ADLB1c2	ADLB1c2	ADLB1a2	ADLB1a2	ADLB1c2
Live Load Strain ($\mu\epsilon$)	244.8	140.4	1.2	84.3	-2.5	-2.3	2.2
Total Strain ($\mu\epsilon$)	248.3	143.9	2.0	87.8	-6.0	-5.8	3.0

Table 4.10. Maximum Longitudinal Strains at the Top of the Panel near Abutment

	Load Path Number						
	1	2	3	4	5	6	7
Location	ADLT1c0	ADLT1c0	ADLT1c0	ADLT1c0	ADLT1c0	ADLT1c0	ADLT1c0
Live Load Strain ($\mu\epsilon$)	36.5	75	7.4	-81.2	-6.3	-5.7	-5.4
Total Strain ($\mu\epsilon$)	38.6	77.1	9.5	-83.3	-8.4	-7.8	-7.5

Table 4.11. Maximum Girder Top Longitudinal Strain near Abutment

	Load Path Number						
	1	2	3	4	5	6	7
Location	AGLT21	AGLT31	AGLT31	AGLT21	AGLT31	AGLT31	AGLT31
Live Load Strain ($\mu\epsilon$)	-9.5	-12.0	-1.4	-11.7	-0.8	-1.1	-1.3
Total Strain ($\mu\epsilon$)	-10.6	-13.8	-3.2	-12.8	-2.6	-2.9	-3.1

Table 4.12. Maximum Girder Bottom Longitudinal Strain near Abutment

	Load Path Number						
	1	2	3	4	5	6	7
Location	AGLB21	AGLB21	AGLB31	AGLB21	AGLB31	AGLB31	AGLB21
Live Load Strain ($\mu\epsilon$)	-2.2	-4.6	-14.8	-5.0	-8.3	-7.3	2.1
Total Strain ($\mu\epsilon$)	-12.8	-15.2	-28.3	-15.6	-21.8	-20.8	-8.5

4.3.3 Maximum Deflections at Mid-Span

The string potentiometers located at the mid-span recorded vertical deflections for different load paths for girders as well as the deck. Table 4.13 shows the maximum deflections registered for each load path.

Table 4.13. Maximum Live Load Girder and Deck Deflections (in.)

Location	MGLB15	MGLB25	MGLB35	MGLB45	MGLB55	MDLB1b5	MDLB2a5
Load Path 1	-0.040	-0.037	-0.005	-0.000	-0.001	-0.044	-0.025
Load Path 2	-0.032	-0.039	-0.014	-0.000	-0.001	-0.042	-0.036
Load Path 3	-0.007	-0.022	-0.031	-0.018	-0.002	-0.008	-0.037
Load Path 4	-0.028	-0.039	-0.019	-0.001	-0.003	-0.037	-0.038
Load Path 5	-0.001	-0.004	-0.016	-0.039	-0.020	-0.001	-0.008
Load Path 6	0.000	0.003	-0.013	-0.041	-0.024	-0.001	-0.006
Load Path 7	0.000	0.001	-0.006	-0.041	-0.037	-0.000	0.002

The maximum recorded girder vertical deflection (i.e., 0.040 inch) occurred at gage MGLB15 for load path 1. For the waffle deck panel, the maximum vertical deflection of 0.044 inch was registered at gage MDLB1b5 for load path 1.

In summary, the maximum strains and deflections experienced by the Dahlen Road Bridge during the static field test were well within expected performance parameters. No strains recorded on the top of the deck indicated a likelihood of cracking or opening of joint interfaces that might adversely affect durability. The only locations where strains approached the expected cracking threshold of the UHPC waffle deck were on the underside of the panel adjacent to the abutment. Cracking was indeed observed by visual inspection at these locations prior to commencing the load tests. These cracks were small in width, and the strains recorded during the test were less than those recorded on the laboratory test panels at service load levels. Whether these cracks were caused by vehicular loads or at some point during shipping or erection is not definitive. Further discussion on this topic is presented in Section 4.4 with the aid of an FEM.

4.3.4 Selected Data from the Static Live Load Test

To provide a broader view of the bridge's response to static loads, the live load strain data collected for load path 2 (for which many of the maximum strains were recorded) is provided in a graphic form. The strain data were recorded as a function of a time; nonetheless, the location of the truck front axle was recorded at discrete points every 10.5 feet along each load path as shown in Figure 4.7 for one of the transducers. The results from Figure 4.7 indicate that the strain can be higher than the strains corresponding to two consecutive truck locations, thus a continuous curve cannot be used to connect the strain for these discrete truck locations. Therefore, Figure 4.8 to Figure 4.16 exhibit the measured strain data points versus truck location.

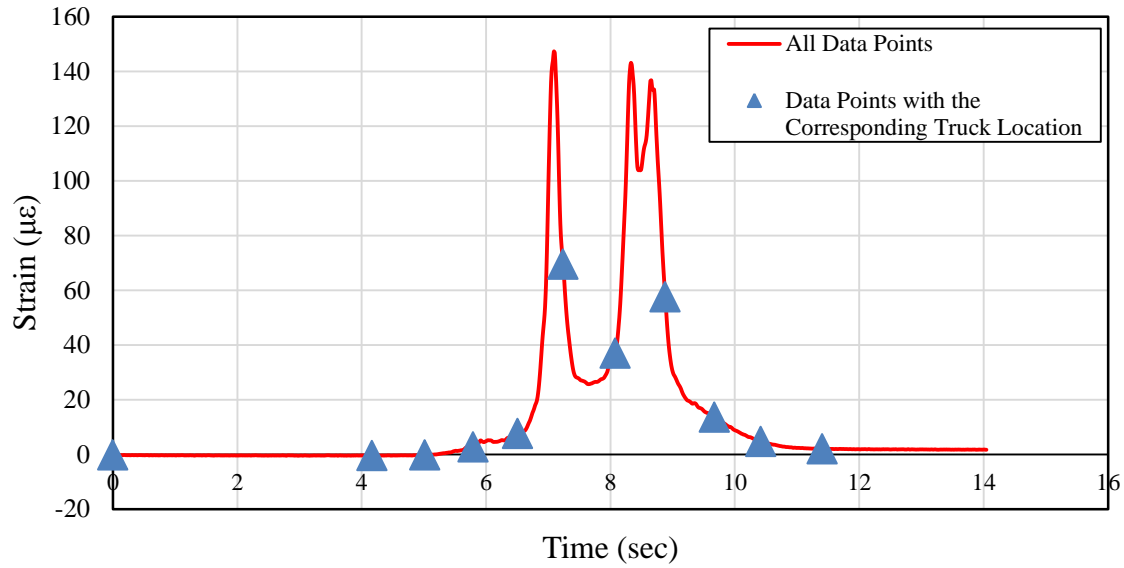


Figure 4.7. Measured transverse strains at the bottom of mid-span panel vs. time for MDTB1b5 transducer

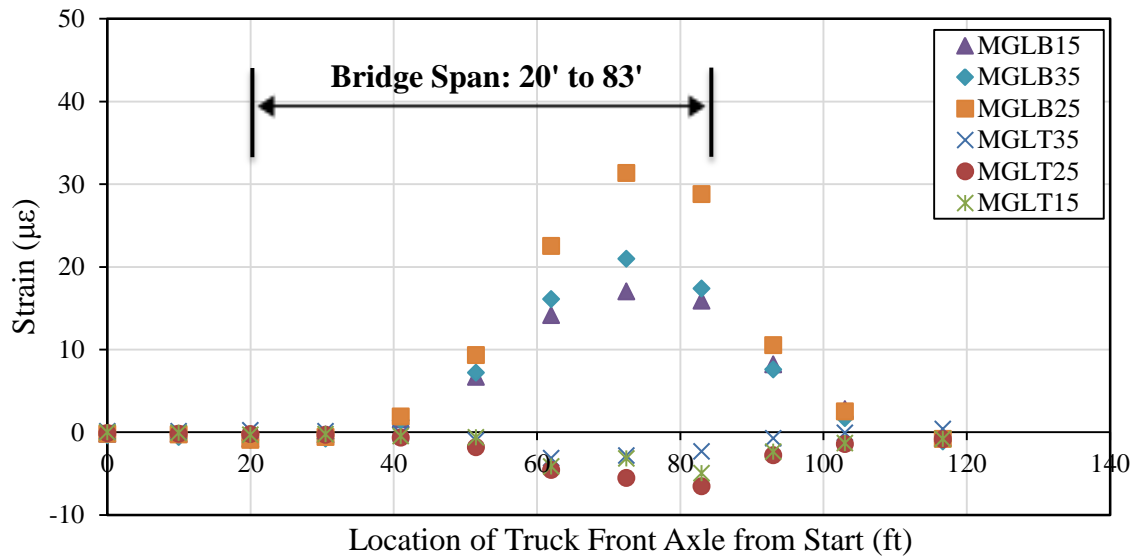


Figure 4.8. Girder top and bottom longitudinal strain at mid-span for load path 2

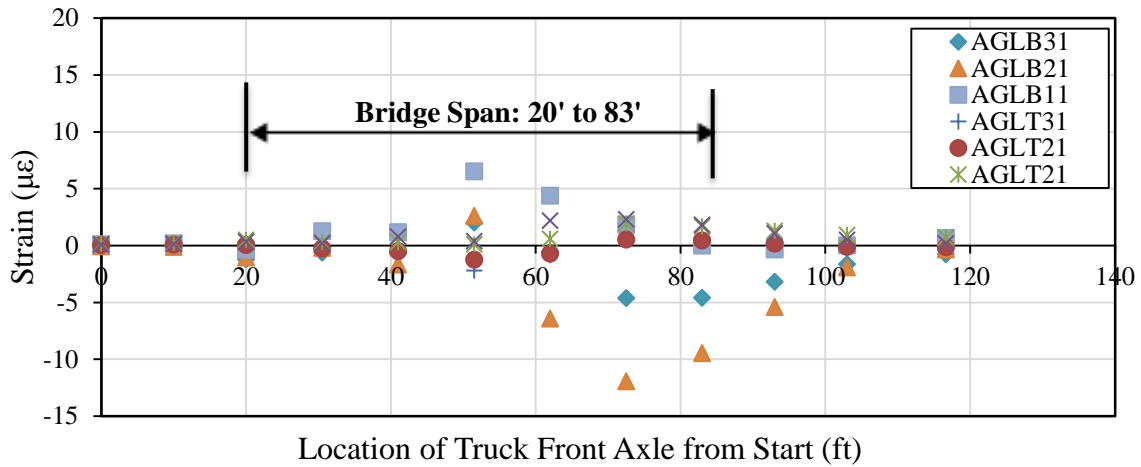


Figure 4.9. Girder top and bottom longitudinal strain near abutment for load path 2

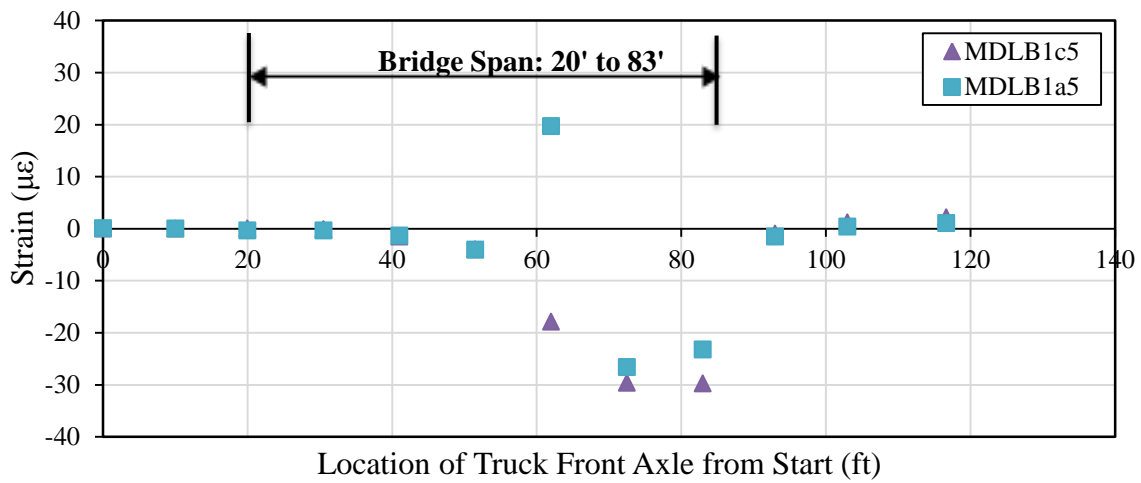


Figure 4.10. Longitudinal bottom strains at mid-span panel for load path 2

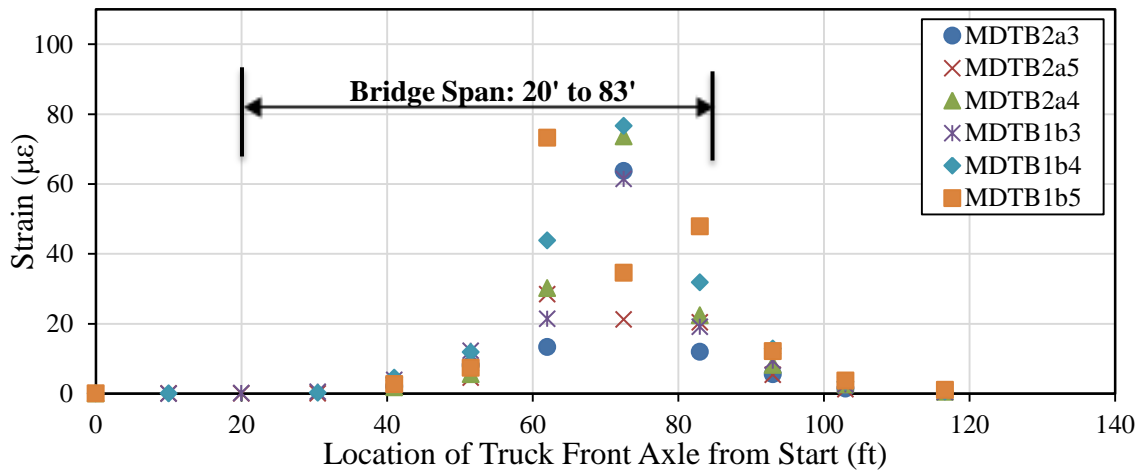


Figure 4.11. Transverse bottom strains at mid-span panel for load path 2

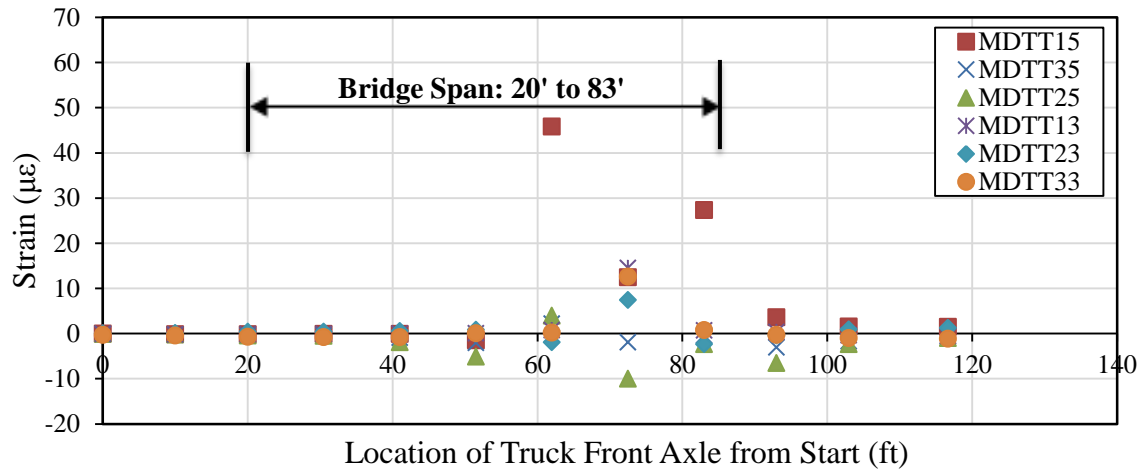


Figure 4.12. Transverse top strains at mid-span panel for load path 2

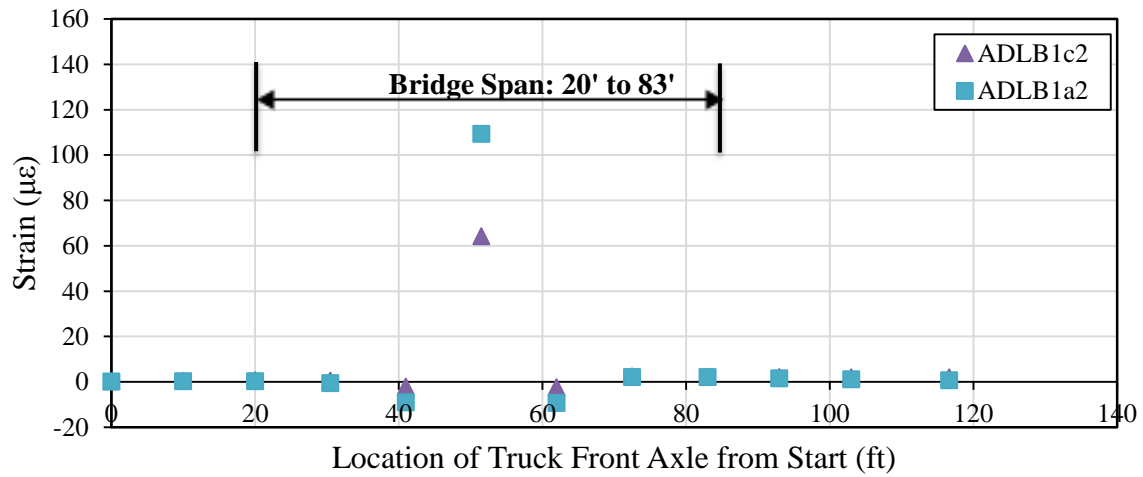


Figure 4.13. Longitudinal bottom strains at end panel for load path 2

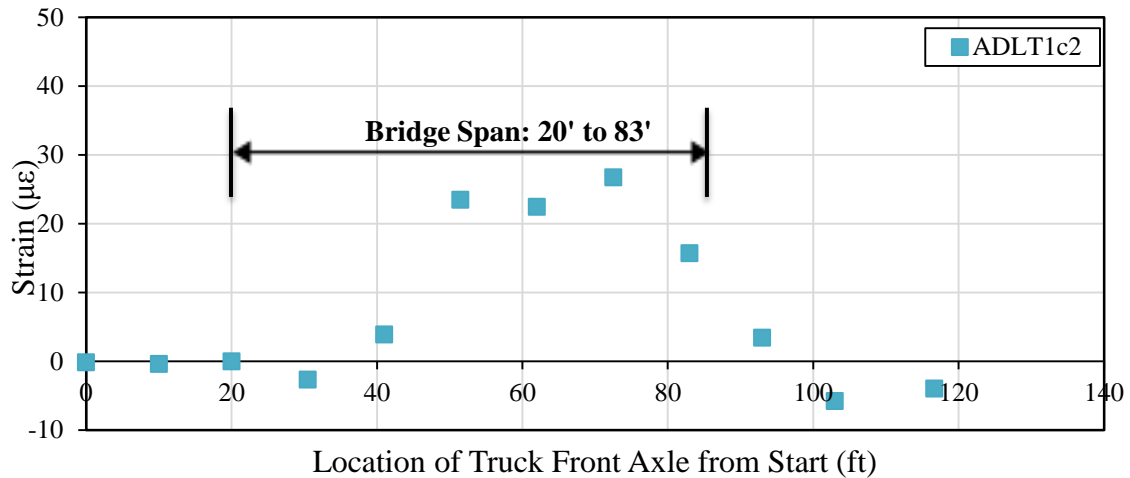


Figure 4.14. Longitudinal top strains at end panel for load path 2

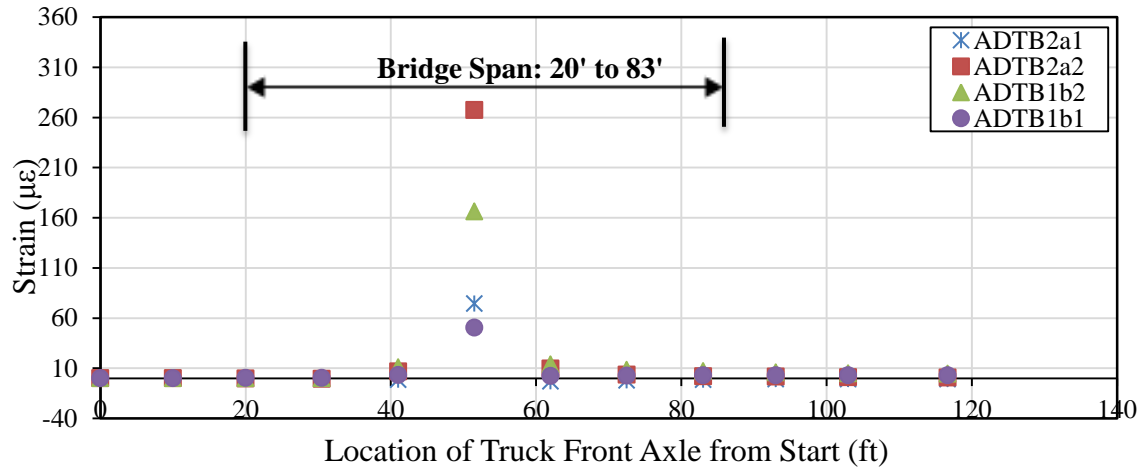


Figure 4.15. Transverse bottom strains at end panel for load path 2

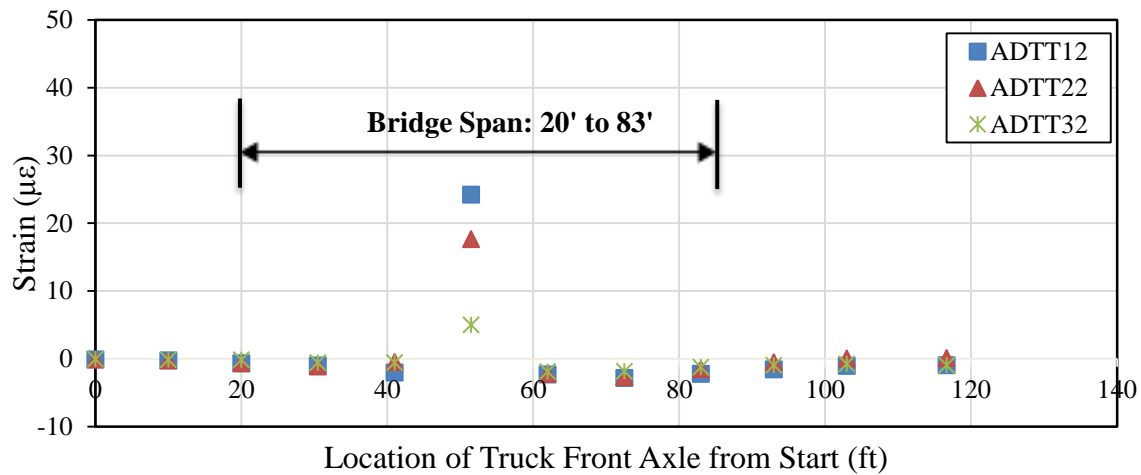


Figure 4.16. Transverse top strains at end panel for load path 2

4.4 Analytical Assessment

A nonlinear 3-D FEM using the commercial software package ABAQUS was developed to predict the bridge strains and deflections. In this section, selected results from the analytical model are presented for comparison with the experimental results. Similar to the described model in Section 2.6, linear elastic behavior was assumed for the prestressed girders, while inelastic behavior was assumed for the UHPC waffle deck slab to investigate any possible plastic strains. Concrete damaged plasticity based on compression and tension softening curves for UHPC was utilized to account for possible nonlinear behavior.

To assess the FEM's reliability in predicting the bridge's response to loads applied during the field test, predicted live load deflections and girder strains for load paths 2 and 3 were compared to the corresponding values measured during the test. For load path 2, the predicted deflection and strain values correspond to a critical truck location with the front axle of the truck placed at

52.5 feet and 31.5 feet from the south abutment face for the mid-span panel and the panel near the abutment, respectively. For load path 3, the predicted deflection and strain values correspond to a critical truck location with the front axle of the truck placed at 42 feet and 21 feet from the south abutment face for the mid-span panel and the panel near the abutment, respectively.

4.4.1 Global Bridge Behavior

Table 4.14 and Table 4.15 summarize the results for girder deflections and longitudinal strains to characterize the global response of the bridge to the applied live load.

Table 4.14. Maximum Live Load Girder Deflections

Location	MGLB15	MGLB25	MGLB35	MGLB45	MGLB55
Load Path 2					
Test Results (in.)	-0.0322	-0.0389	-0.0136	-0.0004	-0.0006
FEM (in.)	-0.0431	-0.0507	-0.0215	-0.009	-0.0027
Load Path 3					
Test Results (in.)	-0.0071	-0.0215	-0.0306	-0.0183	-0.0006
FEM (in.)	-0.008	-0.0388	-0.0532	-0.0374	-0.0001

From Table 4.14, it is clear that the FEM predicted the maximum live load deflections accurately for these two critical load paths for all of the girders. The slight over-prediction of deflection by the model is likely attributable to a small amount of rotational restraint supplied by the concrete diaphragms cast at the ends of the girders over the abutments. In most cases, the model captures actual live load deflection to within ± 0.01 inch.

Table 4.15. Girder Top and Bottom Longitudinal Strains at Mid-Span

Location	Bottom Strains			Top Strains		
	MGLB15	MGLB25	MGLB35	MGLT15	MGLT25	MGLT35
Load Path 2						
Test Results ($\mu\epsilon$)	17.0	31.3	21.0	-3.2	-5.5	-2.8
FEM ($\mu\epsilon$)	21	28.4	22.7	-3.3	-5.7	-3.4
Load Path 3						
Test Results ($\mu\epsilon$)	15.0	20.3	33.8	-3.1	-2.9	-4.7
FEM ($\mu\epsilon$)	8.3	21.7	38.4	-3.8	-6.7	-6.4

As may be seen in Table 4.15, the model is highly effective in predicting strain response for the girders supporting the instrumented panels, where the maximum discrepancy between the measured and predicted strain was 6.7 microstrain. Such accurate predictions of the global response of the bridge provide confidence when examining the more local response of the waffle slab deck panels during the static load test.

4.4.2 Comparison of Live Load Strains for the Mid-Span Deck Panel

For the live load strains of the mid-span panel (see Table 4.16 to Table 4.18), the FEM was also reasonably effective. The greatest discrepancies of up to 24 $\mu\epsilon$ (i.e., 34.5%) for gages MDTB2a3 and MDTB2a4 (see Table 4.17) could be attributed to slight variations of load placement as the truck was driven across the bridge.

Table 4.16. Live Load Longitudinal Strains at the Bottom of the Mid-Span Deck Panel

Location	MDLB1c5	MDLB1a5
Load Path 2		
Test Results ($\mu\epsilon$)	-29.6	-26.6
FEM ($\mu\epsilon$)	-30.9	-28.1
Load Path 3		
Test Results ($\mu\epsilon$)	-3.0	-2.9
FEM ($\mu\epsilon$)	-4.1	-3.5

Table 4.17. Live Load Transverse Strains at the Bottom of the Mid-Span Deck Panel

Location	MDTB2a3	MDTB2a5	MDTB2a4	MDTB1b3	MDTB1b4	MDTB1b5
Load Path 2						
Test Results ($\mu\epsilon$)	63.7	21.2	73.6	61.4	76.6	57.5
FEM ($\mu\epsilon$)	58.1	30.5	67.8	54.1	72.7	70.5
Load Path 3						
Test Results ($\mu\epsilon$)	67.8	20.4	68.9	-5.1	-9.1	-5.6
FEM ($\mu\epsilon$)	50	27	45	-3.1	-4.1	-2.1

Table 4.18. Live Load Transverse Strains at the Top of the Mid-Span Deck Panel

Location	MDTT15	MDTT35	MDTT25	MDTT13	MDTT23	MDTT33
Load Path 2						
Test Results ($\mu\epsilon$)	12.5	-2.0	-10.0	14.5	7.5	12.6
FEM ($\mu\epsilon$)	16.8	-1.4	-4.2	12	5.5	10.8
Load Path 3						
Test Results ($\mu\epsilon$)	-5.7	1.6	3.3	15.0	6.5	3.3
FEM ($\mu\epsilon$)	-4.4	2.6	1.7	10.5	7.1	2.7

4.4.3 Comparison of Live Load Strains of Deck Panel Adjacent to Abutment

Only at the deck panels adjacent to the abutment did the FEM predictions vary significantly from the measured live load strains (see Table 4.19, Table 4.20, and Table 4.21). This observation provides evidence that the cracking and thus the elevated strains in this region were most likely caused at some point during storage, shipping, or erection. Preexisting cracks in this location reduced the moment of inertia of the panel, causing the unexpectedly high strains recorded during the test. If the cracking was due to a large vehicular load, similar damage and strain response would be expected for the mid-span panel as well. If the connection and proximity of the end panel to the abutment were contributing to the elevated strains in this region, the strain recorded by gauge ADTB2a1 would also be expected to register similar strain levels, which was not the case.

Table 4.19. Live Load Longitudinal Strains at the Bottom of the Deck Panel Adjacent to the Abutment

Location	ADLB1c2	ADLB1a2
Load Path 2		
Test Results ($\mu\epsilon$)	64.2	109.3
FEM ($\mu\epsilon$)	4.7	8.6
Load Path 3		
Test Results ($\mu\epsilon$)	-0.9	-2.2
FEM ($\mu\epsilon$)	-2.1	-4

Table 4.20. Live Load Transverse Strains at the Bottom of the Deck Panel Adjacent to the Abutment

Location	ADTB2a1	ADTB2a2	ADTB1b2	ADTB1b1
Load Path 2				
Test Results ($\mu\epsilon$)	74.5	267.5	166.1	50.3
FEM ($\mu\epsilon$)	16.5	25	26.8	9.5
Load Path 3				
Test Results ($\mu\epsilon$)	136.7	120.5	-7.11	-3.5
FEM ($\mu\epsilon$)	60	30	-5.5	-4.2

Table 4.21. Live Load Transverse Strains at the Top of the Deck Panel Adjacent to the Abutment

Location	ADTT12	ADTT22	ADTT32
Load Path 2			
Test Results ($\mu\epsilon$)	24.2	17.6	5
FEM ($\mu\epsilon$)	18.1	14.8	4.2
Load Path 3			
Test Results ($\mu\epsilon$)	24.3	1.5	-1
FEM ($\mu\epsilon$)	17.5	2.5	-2.5

4.5 Girder Live Load Distribution Factor

A distribution factor (DF) is the fraction of the total load a girder must be designed to sustain when all lanes are loaded to create the maximum effects on the girder. The distribution factor can be calculated from the load fractions based on either strains or displacement. Load fraction is defined as the fraction of the total load supported by each individual girder for a given load path. Thus, the load fractions for paths 2 and 6 (i.e., when the truck is located at centerline of each respective lane) are calculated based on displacement as below. The results are summarized in Table 4.22.

$$LF_i = \frac{d_i}{\sum_{i=1}^n d_i} \quad (4-1)$$

where LF_i is load fraction of the i^{th} girder, d_i is deflection of the i^{th} girder, $\sum d_i$ is sum of all girder deflections, and n is number of girders.

So, the distribution factor for each girder can be computed as below:

$$DF_i = LF_{2i} + LF_{6i} \quad (4-2)$$

where DF_i is distribution factor of the i^{th} girder, LF_{2i} is load fraction from path 2 of the i^{th} girder, and LF_{6i} is load fraction from path 6 of the i^{th} girder.

Table 4.22. Live Load Distribution Factors for Bridge Girders

Location	MGLB15	MGLB25	MGLB35	MGLB45	MGLB55
LF for Load Path 2	0.38	0.45	0.16	0.01	0.01
LF for Load Path 6	0.01	0.03	0.17	0.50	0.29
DF	0.39	0.48	0.33	0.51	0.30

The maximum calculated distribution factors were 0.51 and 0.39 for the interior and the exterior girders, respectively, as shown in Table 4.22. Also, DFs for interior and exterior girders are computed according to 2010 AASHTO LRFD Bridge Design Specification (AASHTO 2010). Case (k) from AASHTO Table 4.6.2.2.1-1, precast concrete I section with precast concrete deck, is the most similar to the Dahlen Road Bridge system. Table 4.23 shows the results from AASHTO DF equations as well as average distribution factors from Table 4.22 for interior and exterior girders.

Table 4.23. Live Load Distribution Factors

Beam	DF AASHTO	DF Displacement
Interior Beams	0.63	0.44±0.10
Exterior Beams	0.52	0.34±0.06

It is observed that AASHTO equations overpredict DFs for both interior and exterior girders; in other words, the UHPC waffle deck is behaving in a stiffer manner than what is assumed in AASHTO LRFD 2010 Bridge Design Specification.

4.6 Dynamic Amplification Effects

The dynamic test was performed for load paths 2, 3, and 6. The truck was driven at a speed of approximately 30 mph along the bridge to quantify dynamic amplification. The dynamic load allowance, also known as dynamic amplification (DA), accounts for hammering effects due to irregularities in the bridge deck and resonant excitation as a result of similar frequencies of vibration between bridge and roadway (Interim AASHTO 2008). The 2008 Interim AASHTO LRFD DAF design value is 1.33. Dynamic amplification can be computed experimentally as follows:

$$DA = \frac{\varepsilon_{dyn} - \varepsilon_{stat}}{\varepsilon_{stat}} \quad (4-3)$$

where ε_{dyn} is the maximum strain caused by the vehicle traveling at normal speed at a given location and ε_{stat} is the maximum strain caused by the vehicle traveling at crawl speeds at the corresponding location.

The dynamic amplification factor (DAF) is then given by:

$$DAF = 1 + DA \quad (4-4)$$

Figure 4.17 to Figure 4.19 show the dynamic live load strains experienced by the girders at mid-span for three load paths.

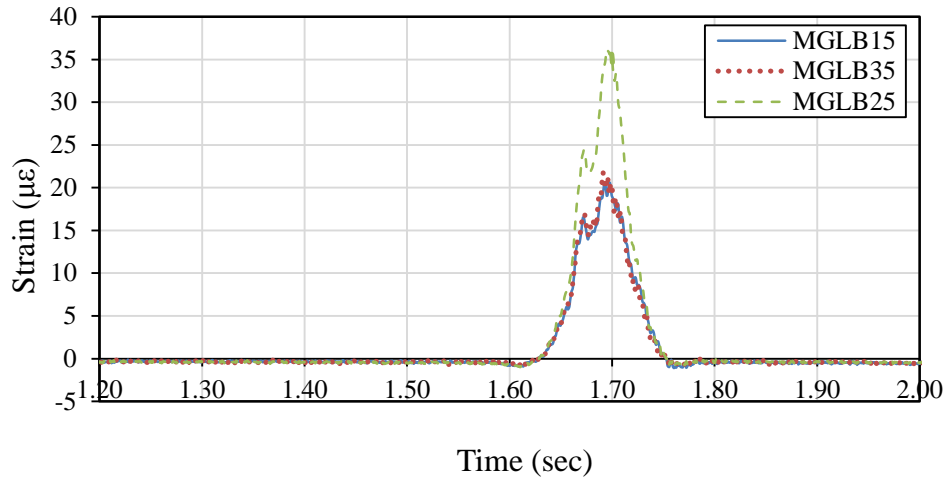


Figure 4.17. Dynamic live load longitudinal strain at mid-span for load path 2

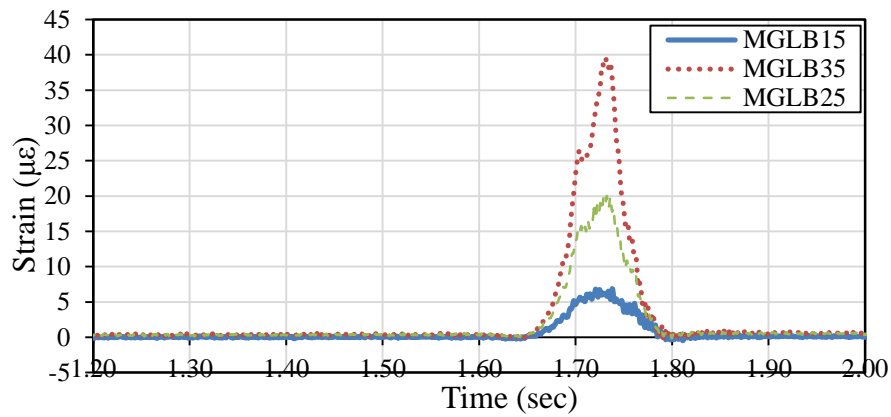


Figure 4.18. Dynamic live load longitudinal strain at mid-span for load path 3

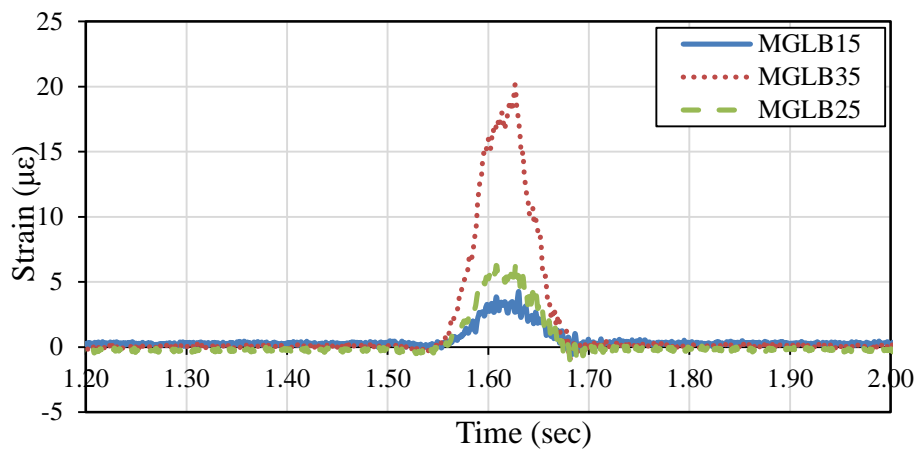


Figure 4.19. Dynamic live load longitudinal strain at mid-span for load path 6

Table 4.24 and Table 4.25 below summarize the results for static and dynamic live load strains at the bottom of the girders for three load paths at mid-span. Consequently, the DAF may be

computed as shown in Table 4.26. The maximum DA computed for the bridge girders is 1.41, slightly greater than the 1.33 recommended by AASHTO for design. This result is attributable to the relatively light waffle deck as opposed to a solid concrete deck. Also, investigation of DA effect for gauges on the top of the deck revealed that some gauges recorded relatively high DAFs, but none of the dynamic strains approached the assumed cracking strain for UHPC. Gauges on the bottom of the waffle deck panels also revealed some mild DA effects, but in all cases the dynamic strains were well below those recorded in laboratory tests.

Table 4.24. Summary of Static Live Load Strain ($\mu\epsilon$) for Bottom of Girders at Mid-Span

Load Path	MGLB15	MGLB25	MGLB35
Load Path 2	17.5	31.3	20.9
Load Path 3	6.88	19.15	33.8
Load Path 6	3.06	7.22	21.2

Table 4.25. Summary of Dynamic Live Load Strain ($\mu\epsilon$) for Bottom of Girders at Mid-Span

Load Path	MGLB15	MGLB25	MGLB35
Load Path 2	20.6	36.2	21.8
Load Path 3	6.9	20	39.4
Load Path 6	4.3	6.6	20.1

Table 4.26. Dynamic Amplification Factors

Load Path	MGLB15	MGLB25	MGLB35
Load Path 2	1.18	1.16	1.04
Load Path 3	1.00	1.04	1.17
Load Path 6	1.41	0.91	0.95

5. CONCLUSIONS AND RECOMMENDATIONS

A full-depth precast UHPC waffle deck panel with ribs in the longitudinal and transverse directions and a set of simple connections suitable for field implementation of waffle deck panels were developed. Following a successful laboratory validation of the full-scale bridge deck system consisting of two panels connected to two precast girders and recommended connections, the waffle deck was installed successfully on a replacement bridge in Wapello County, Iowa. A subsequent load testing confirmed the desirable performance of the UHPC waffle deck bridge.

5.1 Conclusions

Based on the laboratory testing of the UHPC waffle deck system under service, overload, ultimate, and fatigue load conditions, the following conclusions have been drawn for the prototype bridge system:

- Overall system behavior of the UHPC waffle deck bridge system would be satisfactory.
- Neither the UHPC waffle panel nor the UHPC joints are expected to experience any fatigue damage under service loads.
- Displacements of the bridge deck under service conditions will be much smaller than the AASHTO-specified allowable limits.
- The provided reinforcement and the use of field cast UHPC infill for the joints will be satisfactory, but the bar sizes could be reduced.
- Expect hairline cracks to form in the prototype bridge on the underside of the deck under service conditions.
- Crack widths will be negligibly small and are not expected to widen because of repeated loading under the most critical service conditions.
- Larger cracks may form if the boundary conditions of the deck are altered from what was used for the test setup (e.g., by providing rigid connections between the deck and abutments).
- Dowel bars attached to the sides of the panels to form a positive connection with an interior girder experienced stresses in the order of only 3 to 8 ksi, and these bars should be included but smaller bar sizes would be adequate in the prototype bridge.

Based on the field testing of the prototype Dahlonga Road Bridge under static and dynamic truck loads, the following conclusions have been drawn about the local and global behavior of the bridge:

- No cracking is expected in the bridge deck panels, because none of the gauges placed on the top of the deck registered strains that could indicate cracking during live load testing.
- Preexisting flexural cracks on the bottom ribs of the UHPC waffle slab panel adjacent to the abutment were observed prior to live load testing. Finite element analysis indicated that these cracks were likely caused during storage, shipping, or erection rather than due to vehicular loads.
- Only two strain gauges on the deck panels adjacent to the abutment registered strains greater than the expected cracking strain of the UHPC. Because these strains were not excessive (i.e.,

less than those measured at service load levels during laboratory testing) and were located on the underside of the deck, no negative impacts to the performance and durability are expected for the waffle deck panels.

- None of the strain gauges spanning the interface between prefabricated deck panels and their adjacent UHPC infill joints indicated opening of the interface.
- The maximum live load distribution factor for the interior girder was computed to be 0.51, which is lower than the AASHTO-recommended value of 0.63.
- The maximum dynamic amplification factor for the bridge girders was computed to be nearly 1.4, which is close to the AASHTO-recommended value of 1.33.

5.2 Recommendations for Future Research

1. In this completed prototype bridge, the UHPC waffle deck panel was used in a single span, straight simply supported bridge. For broader implementation of this concept, the applicability of current concept and the connection details for curved and skewed bridges need to be investigated.
2. The performance of connections and deck panels at the pier location in a continuous bridge needs to be investigated. Appropriate modifications need to be developed.
3. Given the low strain demand, it may be possible to optimize the rib spacing to make the waffle deck system more economical.
4. Develop and characterize the performance of a hybrid bridge deck panel by combining the UHPC as an overlay on normal concrete to minimize the cost of current UHPC deck panel and improve the durability of traditional concrete decks.

REFERENCES

- ABAQUS. 2008. *ABAQUS User's Manual, Version 6.8*. Dassault Systèmes Simulia Corp., Velizy-Villacoublay, France.
- American Association of State Highway Transportation Officials (AASHTO). 2007. *AASHTO LRFD Bridge Design Specifications*. American Association of State Highway and Transportation Officials, Washington, D.C.
- American Association of State Highway Transportation Officials (AASHTO). 2008. *AASHTO LRFD Bridge Design Specifications*. American Association of State Highway and Transportation Officials, Washington, D.C.
- AFGC (AFGC). 2002. Association Française de Génie Civil Interim Recommendations for Ultra High Performance Fibre-Reinforced Concretes. SETRA (Service d'études techniques des routes et autoroutes). (Bétons Fibrés à Ultra-Hautes Performances – Recommandations Provisoires), France.
- Bhide, S. 2001. *Material Usage and Condition of Existing Bridges in the US*. PCA, Skokie, Illinois.
- Federal Highway Administration (FHWA). 2007. Analysis of an ultra-high performance concrete two-way ribbed bridge deck slab. *TECHBRIEF*, FHWA-HRT-07-055, McLean, Virginia.
- Harris, D. K. and C. L. Wollmann. 2005. *Characterization of the Punching Shear Capacity of Thin Ultra-High Performance Concrete Slabs*. VTRC 05-CR26 final report, Virginia Department of Transportation.
- Keierleber, B., B. Phares, D. Bierwagen, I. Couture, and F. Fanous. 2007. Design of Buchanan County, Iowa, bridge using ultra high performance concrete and PI girders. In *Proceedings of the 2007 Mid-Continent Transportation Research Symposium*, Ames, Iowa.
- K. Stantill-McMcillan and C. A. Hatfield. 1994. Performance of steel, concrete, prestressed concrete, and timber bridges. In *Developments in Short and Medium Span Bridge Engineering '94: Proceedings of 4th International Conference on Short and Medium Span Bridges*, Halifax, Nova Scotia, Canada. Montreal, P.Q., August 8–11. The Canadian Society for Civil Engineering, Canada. Pp. 341–354.
- Perry, V., P. Scalzo, and G. Weiss. 2007. Innovative precast deck panels and field-cast UHPC joints for bridge superstructures. In *Proceedings of the PCI National Bridge Conference, 53rd PCI Annual Convention*, Phoenix, Arizona.
- TRRL (1969). Instructions for Using the Portable Skid Resistance Tester. Road Note 27, Transport and Road Research Laboratory HMSO.
- Sritharan, S. 2009. Use of UHPC for sustainable bridges in seismic regions. In *Proceedings of the 2009 US-Korea Conference on Science, Technology and Entrepreneurship; Main Theme: Creative Minds for Global Sustainability*, Raleigh, North Carolina.
- Vande Voort, T., S. Sritharan, and M. T. Suleiman. 2007. A precast UHPC pile for sub structural applications. In *Proceedings of the PCI National Bridge Conference, 53rd PCI Annual Convention*, Phoenix, Arizona.
- Vande Voort, T., M. T. Suleiman, and S. Sritharan. 2008. *Design and Performance Verification of Ultra-High Performance Concrete Piles for Deep Foundations*. IHRB Project TR-558 Report, Iowa Department of Transportation.
- Zell Comp Inc. 2011. *Infrastructure in Crisis*, www.zellcomp.com/infrastructure_crisis.html (July 4, 2014)